THE UNIVERSITY *of* EDINBURGH

The Origin of the Circular Silverpit Structure, UK North Sea: Meteorite Impact or Salt Withdrawal?

Zana Kate Conway

PhD
The University of Edinburgh
2006

For Grandma,

as you always predicted, I got there in the end.

Acknowledgements

A seemingly endless number of people made the path to completing this thesis possible. Thanks first to Stuart Haszeldine and Malcolm Rider for all their help and support throughout, for their sense of humour, patience and allowing me the freedom to drive the PhD in many different directions. The project would not have existed without Phil Allen and Simon Stewart's discovery of the Silverpit structure and their guidance particularly at the start of the project was invaluable. Phil Allen is also thanked for teaching me to interpret seismic, although I never imagined I would end up doing quite so much of it. John Underhill is recognised for assistance with the regional mapping. Tony Fallick made the stable isotope work possible and is thanked for all of his patience with the endless drafts of the paper. Mark Wilkinson and Alex Whittaker are acknowledged for their valuable input.

The success of this PhD has relied on the generosity of a number of bodies for three vital elements: funding, data and software. NERC are recognised for the provision of the NERC PhD grant NER/S/A/2003/11233. Production Geoscience Limited provided not only CASE sponsorship, but training, data, software, guidance and many laughs along the way, for which I am indebted. Landmark and Terrasciences kindly donated the use of software. Data were provided by PGS, the DTI, RWE UK, and CDA.

Completing my PhD would not have been possible without the amazing support from my friends and family. Thanks to Mum for the funding, endless taxi service and the gentle persuasion that I would get there in the end. To Clare for everything, the laughs, the tears, the chats and moans, but mostly for the dancing and to all my other friends who made my time in Edinburgh fly faster than I could have imagined.

There are so many people not mentioned above that made my PhD possible and although not mentioned I really appreciate everything they have done to help me get to this point.

Abstract

The origin of the Silverpit structure, UK North Sea has been contested since its discovery on seismic data in 2002. The Silverpit structure consists of a 3 – 4km central zone of deformation, which includes a conical uplift. This is surrounded by a series of ring faults up to a maximum diameter of 20km. Meteorite impact, evaporite withdrawal, pull-apart basin tectonics and halokinesis tectonics have all been suggested as possible origins. This thesis uses a multi-discipline approach to test these hypotheses and determine with certainty the origin of the Silverpit structure.

Seismic interpretation of the Silverpit structure has highlighted that deformation in the central deformation zone and beneath the structure is comparable with other meteorite craters. However, the ring faults are comparable with other structures formed by regional evaporite dissolution and movement. Seismic interpretation on a regional, 3500km^2 scale proved that the structure is unique and that salt movement was taking place at the same time as the Silverpit structure was created.

Unusual diagenesis in the chalk beneath the Silverpit structure was identified as a result of the presence of both unusual geophysical and geochemical signatures. An anomalous sonic log response is attributed to a significantly decreased porosity at the base of the chalk unit. Anomalously negative stable oxygen isotopes were also found in the chalk beneath the structure. Unusually elevated heat flow is the likely cause of these irregularities.

The evidence presented in this thesis leads to the conclusion that the origin of the Silverpit structure is in fact two-phase. Meteorite impact has lead to the formation of the central zone of deformation and conical uplift. It has also influenced the diagenesis of the chalk beneath the crater and created a more brittle chalk unit. Regional salt withdrawal is responsible for the formation of the ring faults, which have only formed in the meteorite impact induced brittle chalk. In simple terms, a meteorite impact formed the 3km crater and then salt withdrawal produced the circular rings during several million years after the impact.

Contents

Chapter 1

1 Introduction

1.1 Thesis Objectives

This thesis sets out to investigate the origin of the 20-km-diameter, circular, Silverpit structure, UK southern North Sea. It uses a multi-discipline approach to examine a series of features associated with the Silverpit structure. It then systematically and rigorously tests whether these features could have formed from the range of geologic processes that have been suggested as possible origins for the Silverpit structure. Finally, a carefully considered hypothesis of origin for the Silverpit structure is outlined.

1.2 Thesis Format

This thesis combines traditional thesis chapters with a set of four papers that are in various stages of the publication submission process. As a result of this format some repetition is inevitable particularly at the beginning of each of the papers. Zana Conway is the first author of each of the four papers and has been responsible for generating the majority of the ideas presented, as well as carrying out all of the technical work and composing the bulk of the text and figures in the papers. The co-authors are listed at the beginning of each paper. The contents of each chapter and a more detailed description of the contribution of each author to the paper based chapter is detailed below:

Chapter 2: Background. In this chapter the background and rationale of the study are discussed. It includes the various hypotheses that have been suggested as possible origins of the Silverpit Structure.

Chapter 3: The first paper included in this thesis, entitled: "Is Stratigraphy Key to Identifying the Origin of the Silverpit Structure, UK North Sea?". This paper uses seismic and well log interpretation to examine in detail the relationship that the Silverpit structure has with its surrounding stratigraphy. It also determines the age of the Silverpit structure. Zana Conway developed most of the ideas, carried out all of the seismic and well log interpretation, wrote all of the text and created all of the images. Stuart Haszeldine and Malcolm Rider corrected text, developed some ideas and helped to organise paper structure.

Chapter 4: The second paper included in this thesis, entitled: "The Silverpit Structure, North Sea UK: Seismic Evidence For A Unique Structure". This paper uses seismic interpretation to prove that the Silverpit Structure is unique within a 3500km^2 study area. Zana Conway developed most of the ideas, carried out all of the seismic and well log interpretation, wrote all of the text and created all of the images. Stuart Haszeldine and Malcolm Rider corrected text, developed some ideas and helped to organise paper structure.

Chapter 5: The third paper included in this thesis, entitled: "Regional Salt Mobility in the Southern North Sea and its Influence on the Formation of the Silverpit Structure". This paper uses seismic interpretation to understand the detailed timing of salt movement throughout the study area and link this to the formation of the Silverpit structure. Zana Conway developed most of the ideas, carried out all of the seismic and well log interpretation and wrote the majority of the text. John Underhill wrote some of the text, corrected text, developed some ideas and helped to organise paper structure.

Chapter 6: The fourth paper included in this thesis, entitled: "Geophysical and Geochemical Evidence for Anomalous Chalk Diagenesis Associated with the

Circular Silverpit Structure, UK North Sea". This paper uses sonic well log data and stable isotope data to examine the nature of the chalk beneath the Silverpit structure. It recognises that unusual diagenesis has taken place beneath the Silverpit structure. Zana Conway developed most of the ideas, carried out all of the well log interpretation, acquired and prepared chalk samples for stable isotope analysis, wrote all of the text and created all of the images. Tony Fallick carried out the stable isotope analysis and helped with interpretation of results, Stuart Haszeldine and Malcolm Rider corrected text, developed some ideas and helped to organise paper structure.

Chapter 7: This chapter presents the UK fieldwork and onshore core analysis that has been carried out.

Chapter 8: This chapter provides a discussion of the research results presented within this thesis and proposes a two-phase formation process for the Silverpit structure.

Chapter 9: This chapter summarises the main conclusions from the research presented in this thesis.

References cited in the papers and other chapters can be found compiled into one bibliography towards the end of this thesis.

Chapter 2

2 Background

2.1 Introduction to the Silverpit Structure

2.1.1 Discovery

The Silverpit structure was first identified by Stewart and Allen in 2002. It was discovered as a result of routine hydrocarbon exploration on the high resolution Trent three-dimensional (3D) seismic reflection survey of the Trent gas field, in the UK southern North Sea, 130km from the East coast UK (1° 51' E, 54° 14' N). The initial interpretation of the structure highlighted a 3 – 4km diameter centrally deformed region, including a conical uplift (central peak), surrounded by a series of concentric normal faults forming rings to a maximum of 20km diameter (Figure 2.1 and 2.2). The deformation associated with the centrally deformed zone and ring faults is most prominent on the top Cretaceous Chalk horizon and Stewart and Allen (2002) suggest that the conical uplift affects the Cretaceous chalk and Jurassic shales.

2.1.2 Rival Hypotheses

The identification of the structure sparked significant controversy about its likely origin. Stewart and Allen (2002) published an interpretation of the structure as a multi-ringed impact crater formed as a result of a meteorite impact. Stewart and Allen (2002) dismiss the possibility that the structure formed as a result of the intrusion of igneous material, such as ring dykes, cone sheets, a caldera or phreatic explosion above a dyke, because gravity and aeromagnetic surveys over the area highlight no anomalies. By contrast the Blyth Tertiary basaltic dyke complex in the southern North Sea basin produce distinct linear trends on the aeromagnetic map

(Figure 2.3). However, only the morphology of the structure was considered when the meteorite impact crater hypothesis was published. Underhill (2004) highlighted the structural setting of Silverpit in the centre of a salt induced syncline (Figure 2.4) and proposed that Silverpit is a salt withdrawal structure. Smith (2004) looked even deeper than the salt horizon for a possible origin for Silverpit.

He suggested that the structure formed as a result of pull-apart tectonics in the basement, combined with a shale diapir as an explanation for the presence of the conical uplift (Figure 2.5). Smith has later played down the possibility that pull-apart basin tectonics are the likely cause of the formation of Silverpit (Thompson et al 2005), but suggests that a more mundane explanation for the origin of the structure should still be considered. Thomson (2004) examines the faulting seen on the ridges of halokinetically produced anticlines in the Silverpit region. He compares this with the Silverpit structure to suggest that this keystone subsidence along anticline axes is also what has caused the formation of the Silverpit structure (Figure 2.6).

In summary, the following hypotheses have been suggested to explain the origin of the Silverpit structure:

1) Meteorite impact (Stewart and Allen 2002).
2) Salt withdrawal tectonics (Underhill 2004).
3) Pull-apart basement tectonics combined with shale diapirism (Smith 2004 and Thomson et al 2005)
4) Overburden deformation associated with halokinesis (Thomson 2004)

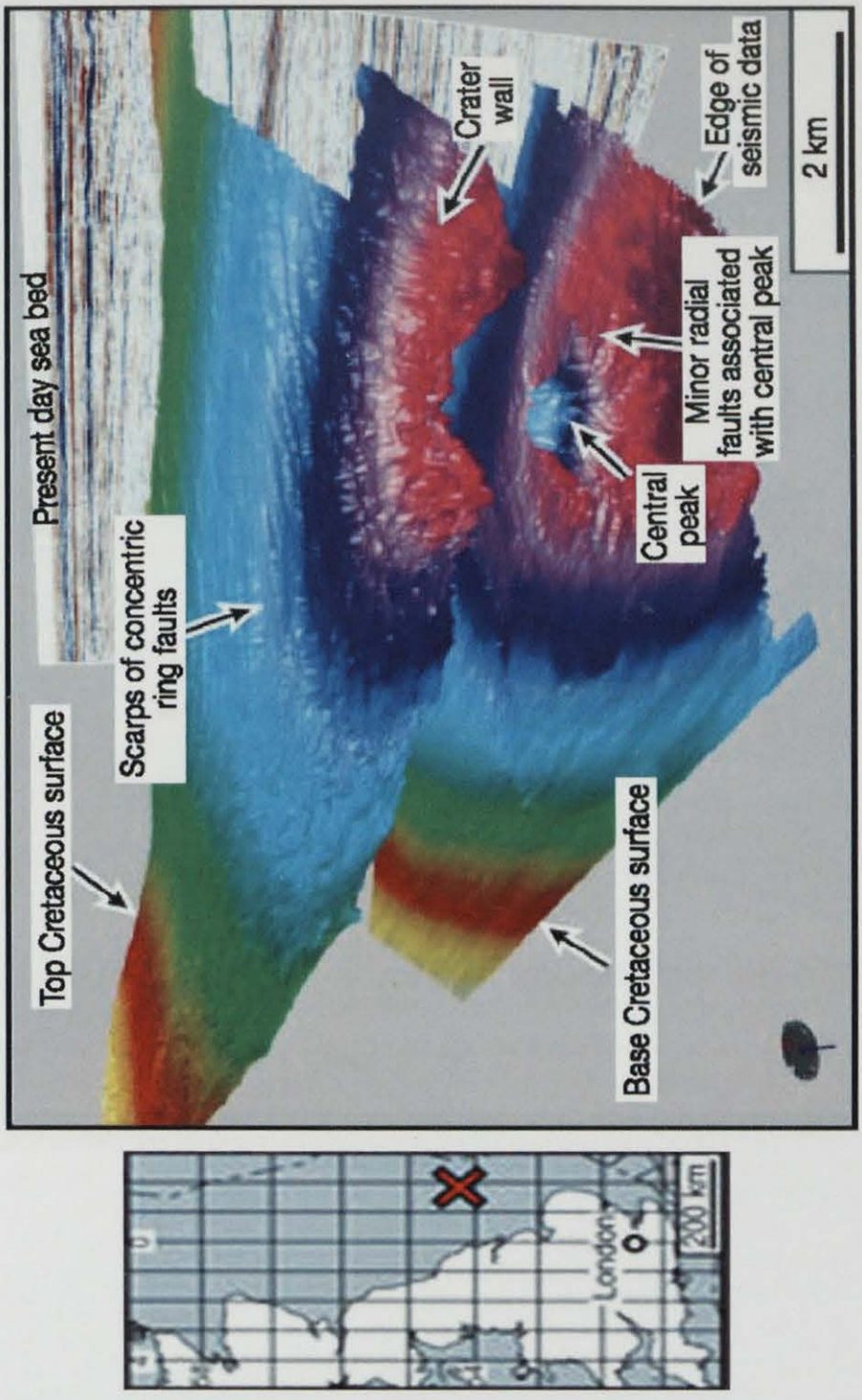

Figure 2.1: Features associated with the Silverpit structure and its location. Based on this morphology Stewart and Allen (2002) suggest that the structure formed as a result of meteorite impact. Picture from Stewart and Allen (2002).

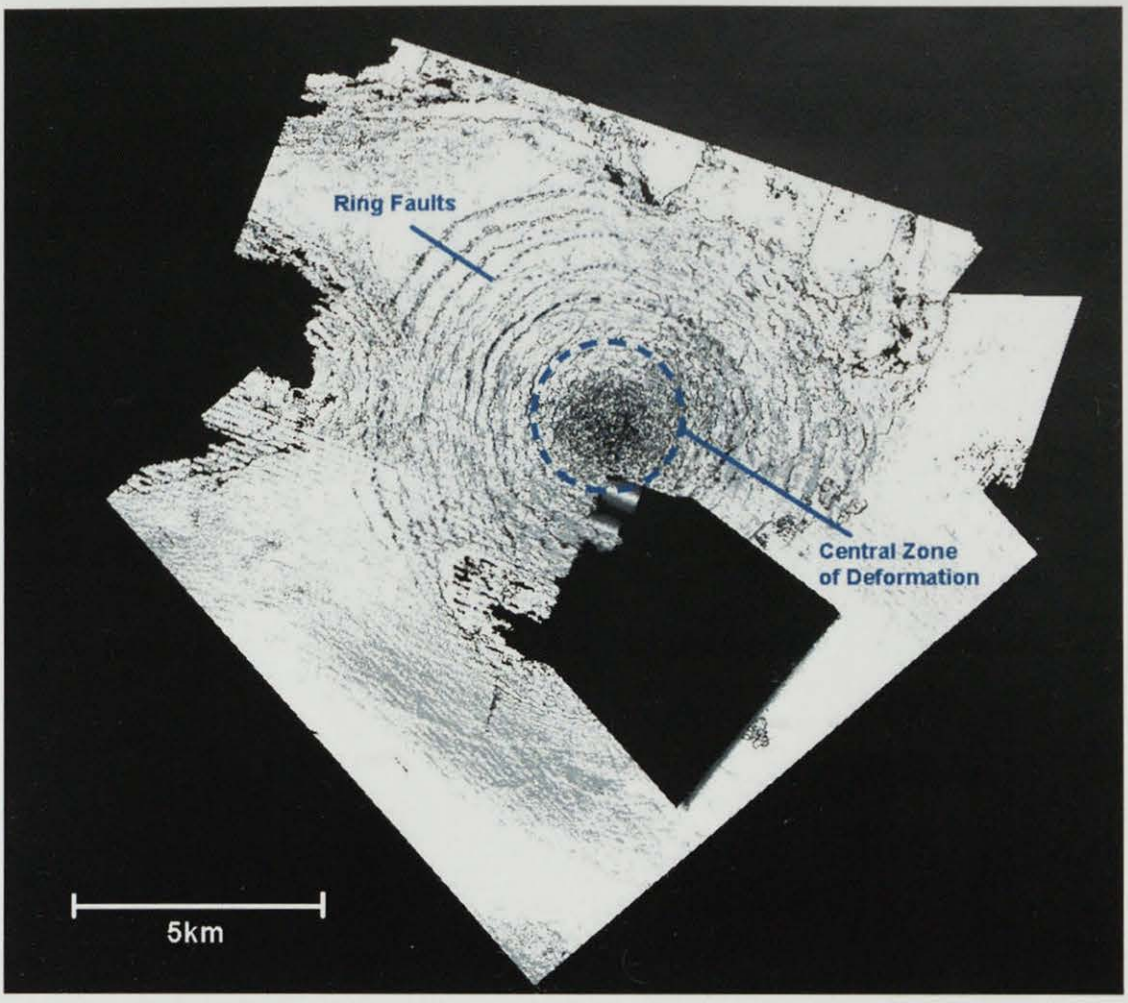

Figure 2.2: Seismic interpretation generated edge detection map of the Top Cretaceous Chalk horizon, showing the "aerial" view of the Silverpit structure. The central zone of deformation and ring faults are clear on this horizon

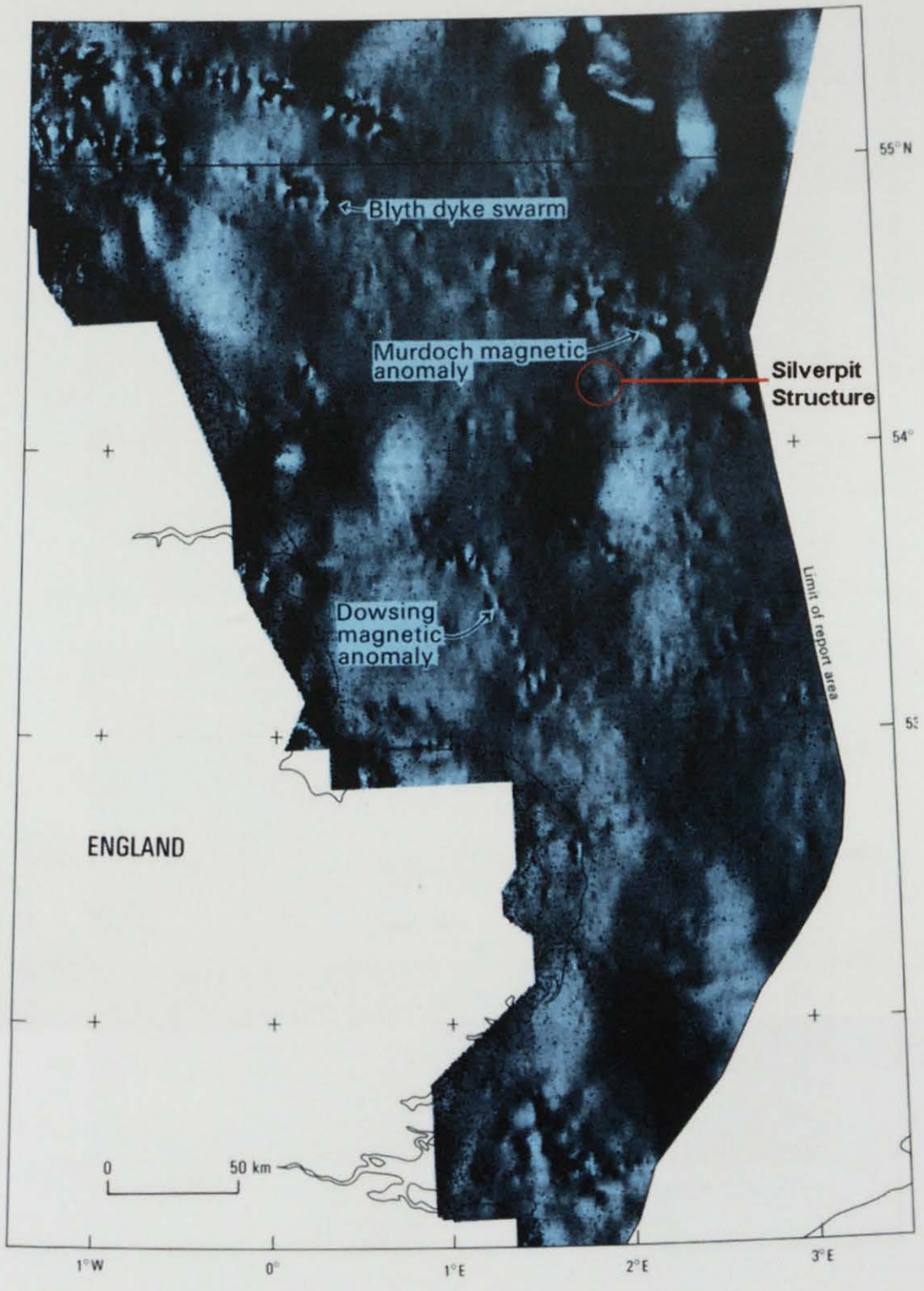

Figure 2.3: Pseudorelief aeromagnetic anomaly map of the southern North Sea, highlighting the linear trends of the Blythe Dyke swarm. Note that the Silverpit structure cannot be seen. From Cameron et al (1992).

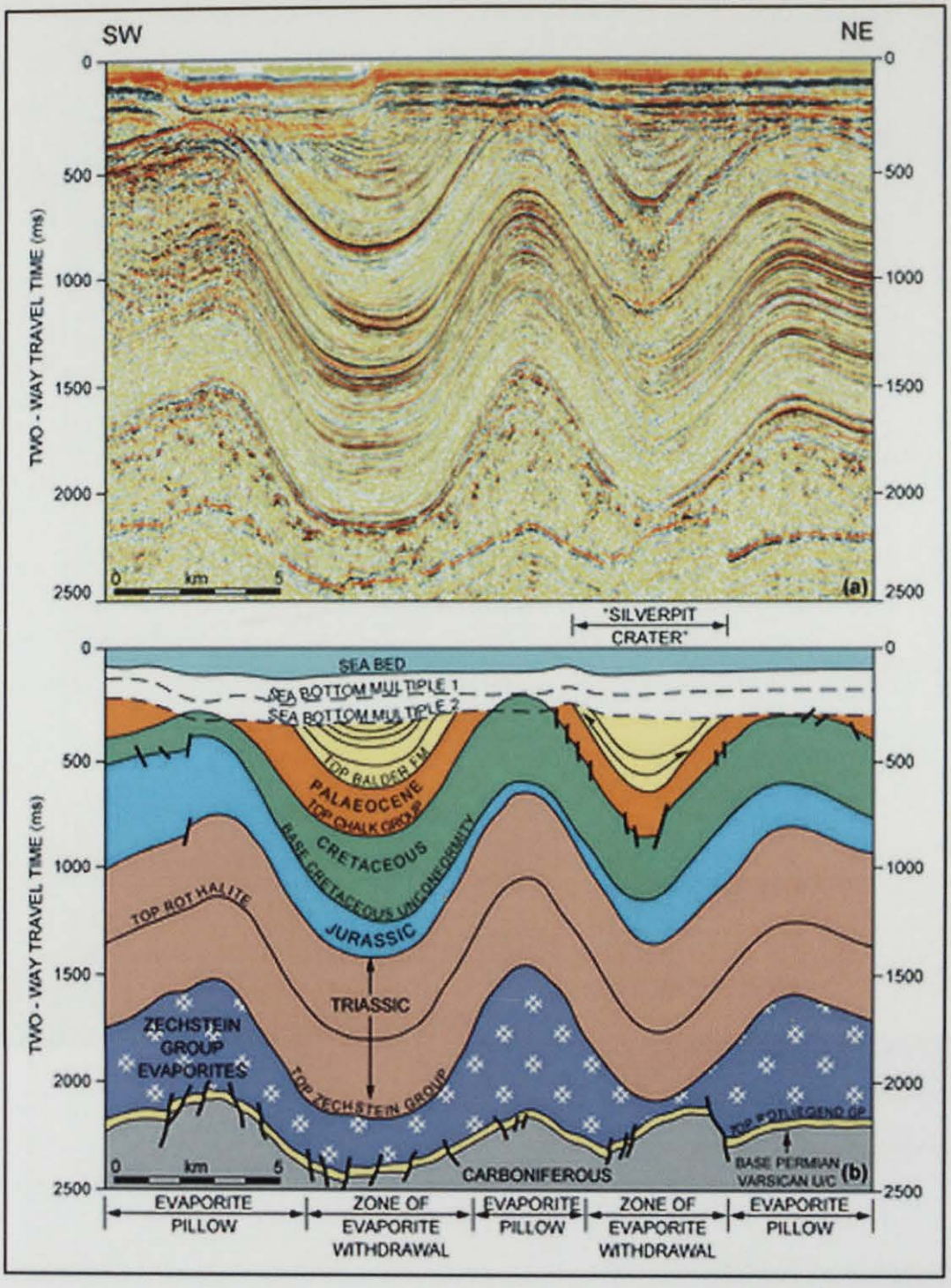

Figure 2.4: The salt withdrawal hypothesis of Underhill (2004), which compares the Silverpit structure with a neighbouring synclinal structure, suggesting that Silverpit formed only as a result of evaporite withdrawal. Picture from Underhill (2004).

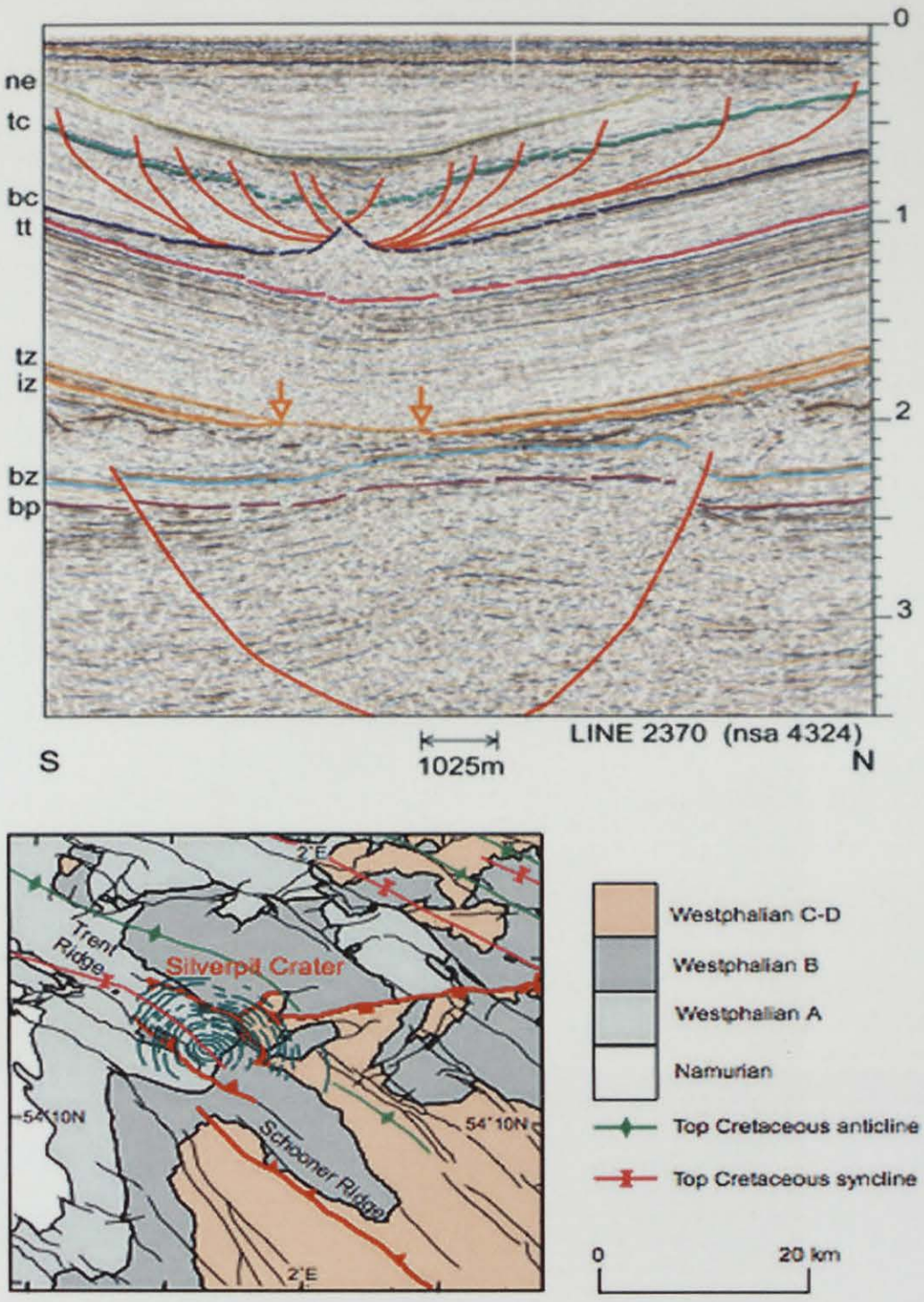

Figure 2.5: Pull-apart basin and shale diapir hypothesis of Smith (2004). The seismic section highlights the basement faults and faulting through the Silverpit structure. The map shows the large-scale structures of the southern North Sea basin and the relationship that Silverpit has with these. Picture from Smith (2004). Here ne = Neogene, tc = top Cretaceous, bc = base Cretaceous, tt = top Triassic, tz = top Zechstein, iz = intra-Zechstein, bz = base Zechstein and bp = base Permian.

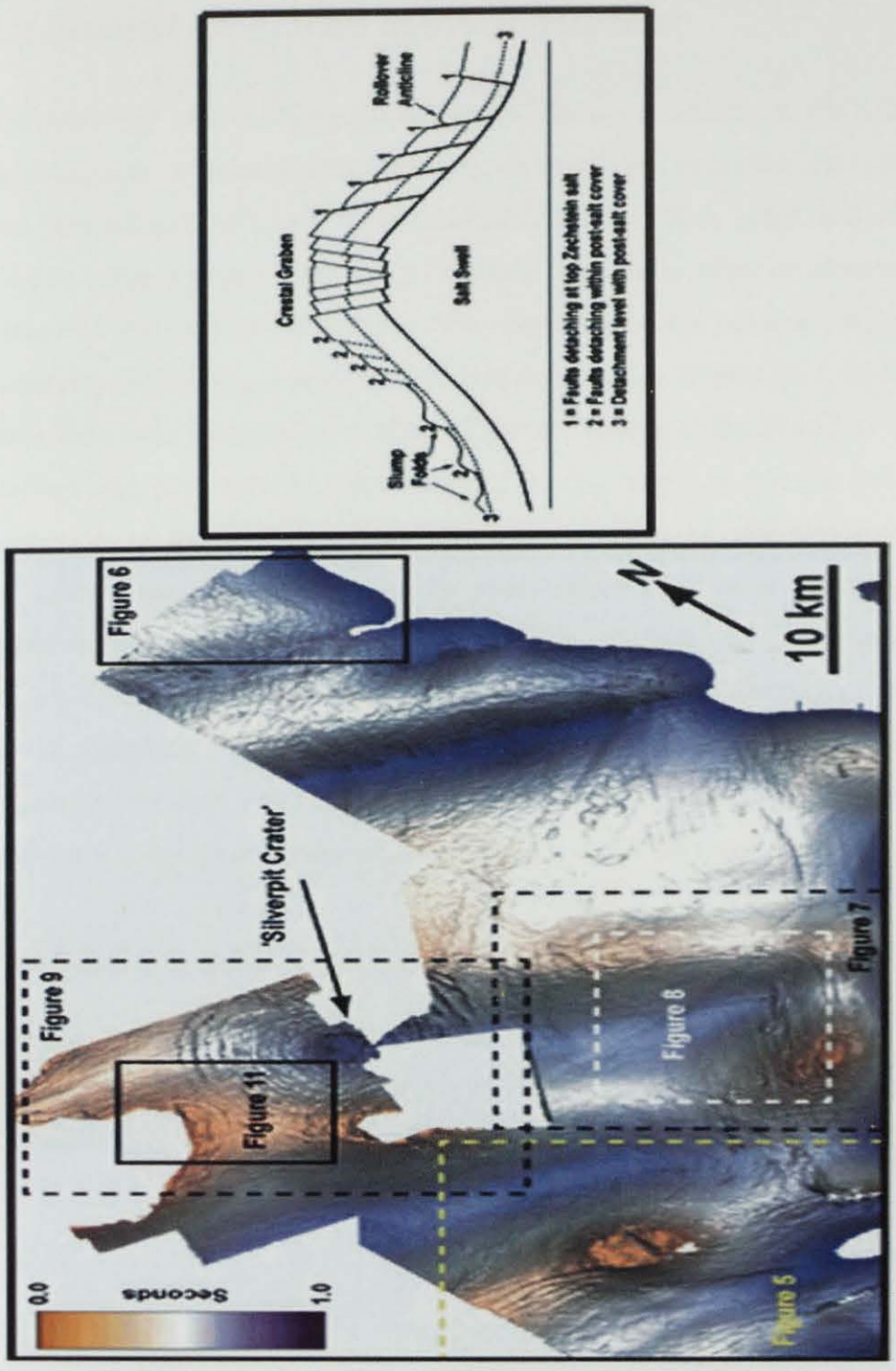

Figure 2.6: Crestal graben collapse hypothesis of Thomson (2004). Plate A highlights the different structures seen on the top Cretaceous Chalk which Thomson (2004) suggests formed in the same way as Silverpit. Plate B highlights how the crestal graben faults form. Pictures from Thomson (2004).

2.2 Circular Structures in the Subsurface

The challenge of identifying the origins of circular structures in the subsurface has become more prominent with the evolution of seismic reflection data surveys, from two-dimensional (2D), to three-dimensional (3D). With more and more of the Earth's surface being surveyed it is likely that the number of circular structures identified will increase. Stewart (1999) comments on the possible origin of circular structures identifying at least ten different possibilities (Figure 2.7). These processes have then been categorised to allow different features to be related to the different settings and processes. In some cases, it is clear that one process has lead to the formation of the structure, but there are a number of ubiquitous features that complicate the discrimination of the likely origin of circular structures. Table 1, taken from Stewart (1999) highlights the characteristic features associated with a variety of circular structures. Although the identification of meteorite craters initially seems straightforward, without rock samples from the crater, conclusive "proof" is extremely difficult to establish. A lack of reliable rock material from the crater horizon is a significant problem in the example of the Silverpit structure.

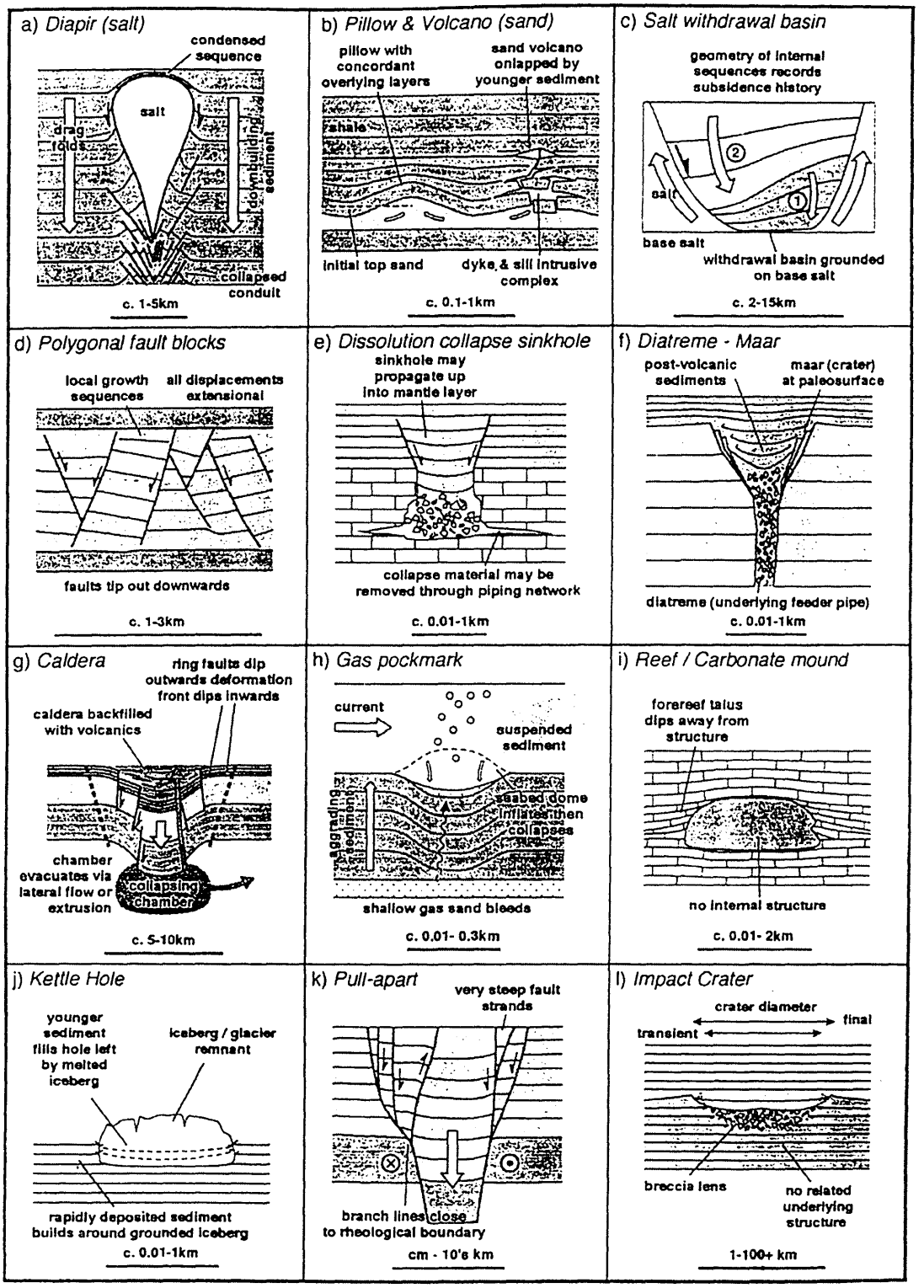

Figure 2.7: The mechanisms of formation of circular structures and the scale and geometric features that may be seen at each setting. Picture from Stewart (1999).

	Geometrical characteristics					Geological relationships				
	Scale: typical diameter (km)	Shape: typical max/min diameter ratio	Shape: typical depth/ width aspect ratio	Coherent internal structure/fill?	Genetic requirement to form linked arrays?	Related to regional trends?	Characterize specific sedimentary environment?	Related structure in underlying strata?	Restricted stratigraphic occurrence?	Reference
Diapirs (salt, shale)	1–5	1	1–5	N	N	~	N	Y	N	Price & Cosgrove (1990)
Pillows (salt, sand, shale)	1–5	1+	0.01–1	N	~	~	Y	N	N	Stewart & Coward (1996)
Withdrawal basin (salt)	2–15	1+	0.5–1	Y	Y	~	N	N	N	Jackson & Vendeville (1995)
Polygonal faults	0.3–2	1	0.5–3	Y	Y	~	Y	N	N	Cartwright & Dewhurst (1998)
Dissolution collapse	0.01–1	1	0–1	~	~	~	Y	N	N	Waltham *et al.* (1997)
Diatreme/maar	0.01–3	1	2+	~	N	~	N	~	N	Lorenz (1986)
Calderas	2–50	1	0.1–1	N	~	~	N	Y	N	Branney (1995)
Volcanoes (igneous)	1–50	1+	0.1–0.5	~	~	~	N	Y	N	Francis (1993)
Gas pockmarks	0.01–0.3	1	0.01–0.2	Y	~	~	Y	N	N	Hovland & Judd (1988)
Reefs/carbonate mounds	0.01–2	1+	0.1–0.5	N	N	~	Y	N	Y	James & Bourque (1992)
Kettle holes	0.01–1	1+	0.01–0.1	Y	N	N	Y	N	Y	Solheim *et al.* (1991)
Pull-aparts	0–40	2–5	0–1	Y	N	Y	N	Y	N	Aydin & Nur (1982)
Impact craters	1–100+	1	0.1–0.2	Y	N	N	N	N	N	Melosh (1989)

~ equivocal

Table 2.1: The geological and geometrical criteria that might be used to identify circular features encountered on 3D seismic data. From Stewart (1999).

2.3 Regional Geology

The Silverpit structure is located in the southern North Sea, a region well studied as a result of its actual and potential hydrocarbon presence. Little is known of the Devonian and older units, however, the Carboniferous through to Tertiary rocks have been studied in depth and detail. This has been achieved with the aid of onshore data (in particular field studies and borehole data) and offshore data e.g. seismic surveys, well logs, cores gravity surveys and aeromagnetic surveys (Cameron et al 1992). The southern North Sea basin geology is unusual as a result of the Permian Zechstein evaporite deposits. Mobile salt has played a significant role in the development of the diapir, fault and fold structures seen throughout the region as a result of halokinesis (Stewart and Coward 1999).

The Cretaceous chalk horizon, where the deformation of the Silverpit structure can be seen most prominently, is a particularly good unit on which to study any effects associated with the Silverpit structure. The homogenous nature of the chalk in the North Sea (Mallon and Swarbrick 2004) means that any anomalies associated with the Silverpit structure should be easily recognised.

2.3.1 Summary of the Post Devonian Geology of the Southern North Sea

This account is based on Cameron et al 1992: Carboniferous fluviodeltaic, coal measures and redbed sequences were gently folded and faulted during the Variscan orogeny and are buried beneath up to 4000m of Permian, Mesozoic and Cenozoic sediments.

Throughout Permian and Triassic times, most of the southern North Sea lay within a gently subsiding Variscan foreland basin extending from eastern England through northern Germany into Poland. During the early Permian a series of aeolian, fluvial and desert-lake sediments accumulated between the London-Brabant Massif and the Mid North Sea High. Five, short-lived, marine transgressions across the basin produced a complex series of marine and evaporite deposits during the late Permian.

Locally, these deposits are up to 1000m thick. Since the middle Triassic, the Late Permian evaporites have intermittently deformed by halokinesis, leading to widespread growth of salt diapirs and salt pillows across the central offshore area. The Triassic sediments were deposited in a range of playa-lake, floodplain, fluvial and quasimarine environments and are dominated by a series of reddish brown mudstones with subsidiary sandstones and evaporites up to 1650m thick.

In the late Triassic, fully marine conditions extended across the southern North Sea and have continued to do so intermittently until the present day. During the Jurassic the Sole Pit Trough and the Cleveland Basin were the principal depocentres, accumulating up to 1000m of marine mudstones with subsidiary sandstones and limestones. Erosion occurred at the end of the Jurassic period, followed by localised post Jurassic inversion along specific fault trends. The Lower Cretaceous sediments are dominantly argillaceous. Upper Cretaceous sediments, which are locally up to 1000m thick, are pelagic carbonates deposited in a Chalk Sea. These carbonates experience widespread uplift (locally up to 400m (Glennie 1998)) and regression during the Danian, which was followed by the deposition of mainly argillaceous marine sediments up to 800m thick during the Palaeogene. Neogene sediments are generally absent as a result of erosion and or no deposition. During the early Quaternary, a northwestward expansion of peripheral delta systems dominated the southern North Sea and is now represented by up to 600m of sediment. Glacial erosion and deposition dominated in the Later Pleistocene until the development of the present day, strongly tidal, marine environment between 7000 and 10000 years ago.

Post Devonian basinal subsidence in the southern North Sea has been punctuated by regional episodes of deformation during Late Carboniferous, Late Jurassic, Late Cretaceous and mid-Tertiary times. The regional structure of the southern North Sea will not be discussed as it is beyond the scope of this report. Instead, a more localised structural style will be discussed centred on the Silverpit structure region.

In most of the offshore area north of 53°20'N (which includes the Silverpit structure region), Mesozoic and early Tertiary sediments have been gently-to-tightly folded over Permian salt swells and pillows. Many of the halokinetic structures are several hundred metres in amplitude. This halokinetic motion was triggered as a result of Upper Permian salt remaining metastable, and in a mobile state after deposition as a result of its density not changing with burial in comparison to the overlying sediments, where density increases with burial. Changes in the regional stress regime are likely to have triggered the motion. More detail regarding the timing of salt movement and its triggers are discussed in Chapter 5.

2.4 The Terrestrial Crater Record

Meteorite craters have played a significant role in the in the Earth's history with large impacts being related to mass extinctions and significant environmental change (Alvarez 1987). Following the late heavy bombardment <3.2Ga, the flux of impacts has remained constant (Shoemaker 1998). In August 2006 the total number of discovered and confirmed impact craters on Earth was 174 (Earth Impact Database 2006). Many other crater shapes have also been discovered but no conclusive supporting evidence has yet been discovered to confirm their meteorite impact origin.

In order for a structure to be positively identified as a meteorite impact crater, supporting evidence must be found at the impact site in the form of shatter cones, shocked metamorphic material (principally shocked quartz), or a geochemical anomaly (such as an iridium or other platinum group element anomaly) (Koeberl 2002). This means that many buried candidate craters imaged on seismic data, but which are not drilled remain unclassified (Stewart 2003). As a result, the impact crater record tends to be biased towards continental localities, with only four submarine craters identified (Figure 2.8): Chicxulub - Mexico, Chesapeake Bay - USA, Montagnais - Canada and Mjølnir – Norway (Earth Impact Database 2006).

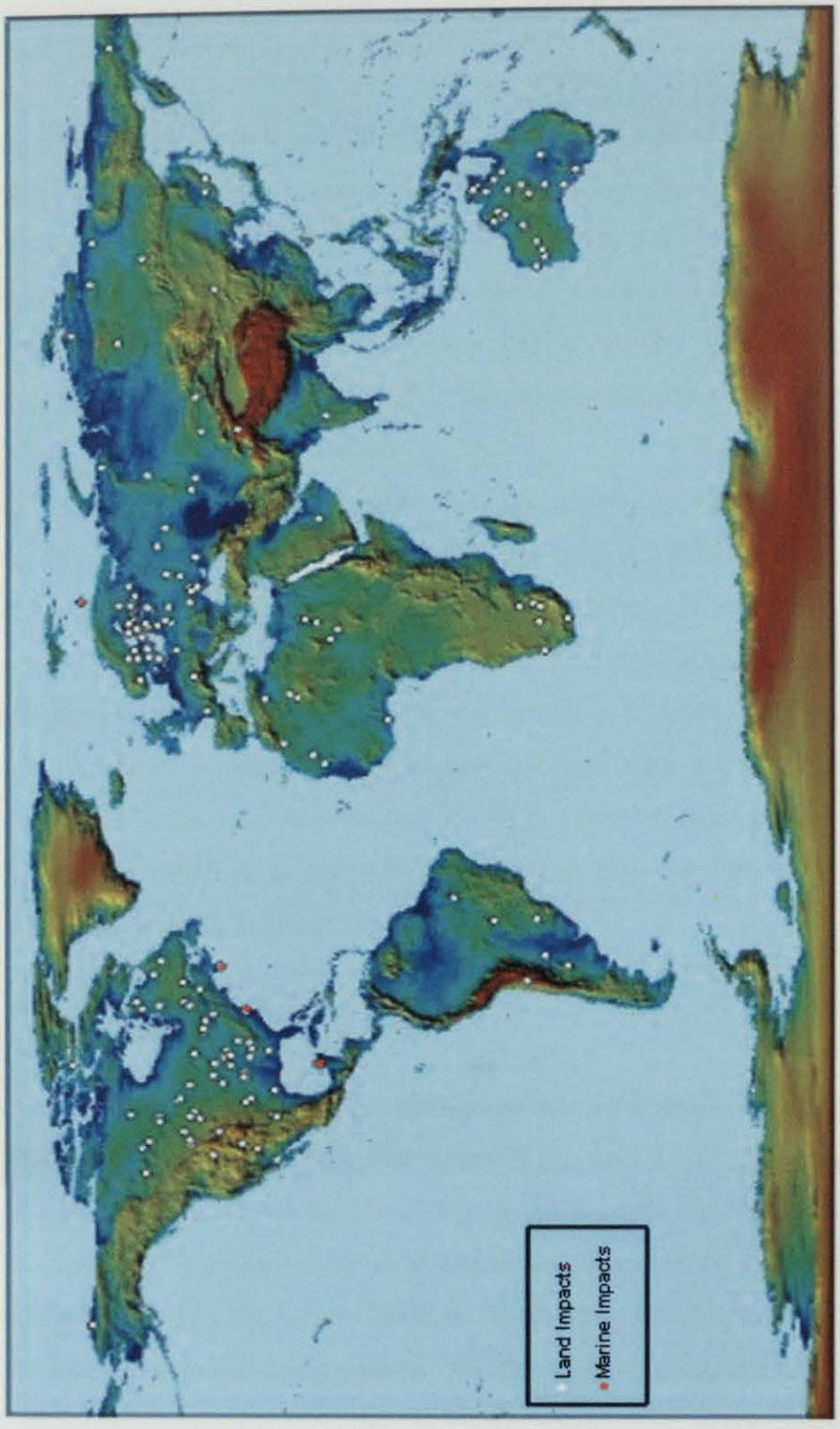

Figure 2.8: The terrestrial crater record highlighting the locations of all of the confirmed meteorite impact craters. Picture from Earth Impact Database www.unb.ca/passc/impactdatabase/index.html

2.4.1 The crater record in the UK

The United Kingdom currently has no confirmed meteorite craters, Walkden et al. (2002) have identified a layer of impact ejecta, including spherules and shocked quartz, in the late Triassic of southwestern Britain. However, no crater has been found in the UK. Instead these ejecta material which have been dated to be 214 ± 2.5 million years old have been associated with either the Manicougan impact crater, Canada or the Rochechouart impact crater, France (Walkden et al. 2002).

The advent of sub surface imaging has significantly increased the surface area that can be mapped. The UK is in the relatively unique position of having much of its offshore North Sea subsurface seismically mapped. If we consider the area of exposed land combined with area of subsurface stratigraphic horizons imaged by seismic reflection data in the UK and compare it to other countries throughout the world, it is not implausible that a meteorite impact crater be found. For example, five impact structures have been identified on the present day land surface in Sweden (Figure 2.8) which is in fact a smaller surface area than the UK land surface and seismically mapped area combined.

2.5 Meteorite Impact Craters

A meteorite is defined as any extraterrestrial solid mass that reaches the Earth's surface (Farris Lapidus 1990). The term strictly extends from the nano scale e.g. dust particles, through to the macro scale e.g. 100s of metres in diameter (Zanda and Rotaru 2001). However, the term meteorite is generally reserved for the larger particles that reach the Earth's surface. Four types of meteorite have been identified, iron, stony, stony-iron and carbonaceous chondrites (Zanda and Rotaru 2001).

A meteorite crater is the expression left on the Earth's surface following the impact of a meteorite. The formation of a meteorite impact crater can be divided into three main stages: 1) contact and compression, 2) excavation and 3) modification (Kenkman 2002). Impact craters are categorised into three different types: simple, complex and multiring basins, which are generated following the collapse of an

unstable transient or initial crater in the modification stage of development (Melosh 1989). In general it is the diameter of the crater that determines its morphology, but there are some environmental factors that can also be of influence e.g. if the impact is sub-aerial or sub-marine. If the impact occurs in deep water (deeper than 1km) then the craters tend to be concentric and often lack melt sheets and rim walls but have deposits and radial gulleys formed by resurge of the sea (Ormö and Lindström 2000). The size of the crater is intimately related to the size, speed and angle at which the meteorite collides with the Earth (Melosh 1989).

Collins et al (2005) have suggested that if the Silverpit structure were formed as a result of a meteorite impact then the meteorite would have been approximately 120m diameter, travelling at between 20 – 50 Kms^{-1} and weighing approximately 2.0 x 10^9kg (assuming a stony meteorite).

The three morphological types of impact crater have been categorised below:

2.5.1 Simple Craters

Simple craters (Figure 2.9) are the smallest of the three crater types and range from 0 – 20km in diameter. They are characterised by a simple bowl shape similar to that of the transient crater suggesting minor gravitational collapse following impact. Simple craters generally have depth / diameter ratios of between 1/5 (0.2) and 1/3 (0.33) (Melosh 1989). One example of a simple crater is the Barringer Crater, Arizona, which is 1.186km in diameter today.

2.5.2 Complex Craters

The formation of complex craters (Figure 2.9) arises as a result of large-scale gravitational collapse of the transient crater (O'Keefe and Ahrens 1999). Consequently, complex craters are commonly larger than simple craters. The transition from simple to complex craters on Earth can occur in craters as small as 5km in diameter (Kenkman 2002). Complex craters are characterised by the presence of such features as central peaks,

terraced walls and flat floors (Melosh 1989). The most complicated complex crater structure is a peak ring crater (Figure 2.10) whereby a series of rings develop within the original crater rim. This occurs in the larger complex craters where the central peak collapses and creates a peak ring before the motion stops (Melosh 1989).

The morphological study of complex craters from eroded remnants exposed at the surface suggests that their formation is just an extension of the simple crater formation. However, geologic investigation of the central peak highlights that they are composed of deformed and fractured rocks, which originally underlay the transient crater (Melosh 1989). Structural studies of terrestrial craters suggest that the modification from the bowl-shaped transient crater to the complex form occurs as a result of complete gravity driven collapse of an initially deep transient crater. The collapse is achieved principally by uplift of the rocks underlying the crater's centre as a result of the release of a pressure overburden, with the rock units near the rim slumping downwards and inwards (Melosh 1989).

2.5.3 Multiring Basins

Multiring basins are large circular structures with not just one rim but an additional concentric raised ring or rings and a system of radial furrows. In order to be classified as a multiring basin and not a peak ring crater the basin must posses at least two asymmetric scarped rings, one of which may be the crater rim (Melosh 1989). Multiring basins are much larger structures (100s to 1000s km in diameter) than either simple or complex craters. At present no multiring basins have been formally recognised on Earth and as such the study of multiring basins is based principally on examples seen on the Moon, Callisto and Ganymede (Figure 2.11) (Melosh 1989).

The formation of multiring basins is more complicated than just gravitational collapse and a number of different hypotheses have been developed in explanation. These hypotheses include; the volcanic modification hypothesis (Hartmann and Yale 1968), the megaterrace hypothesis (Head 1974) and the nested crater hypothesis

(Hodges and Wilhelms 1978). However, it is the ring tectonic theory (Melosh and McKinnon 1978) that is the widely accepted hypothesis. The ring tectonic theory suggests that in layered media in which the strength decreases with increasing depth, one or more ring fractures arise outside the rim of the original crater (Figure 2.12) (Melosh and McKinnon 1978). This suggests that for the formation of multiring basins to occur, there must be a high brittle-ductile thickness ratio in the impacted material i.e. where thick crust exists over a deeper ductile layer (Allemand and Thomas 1999).

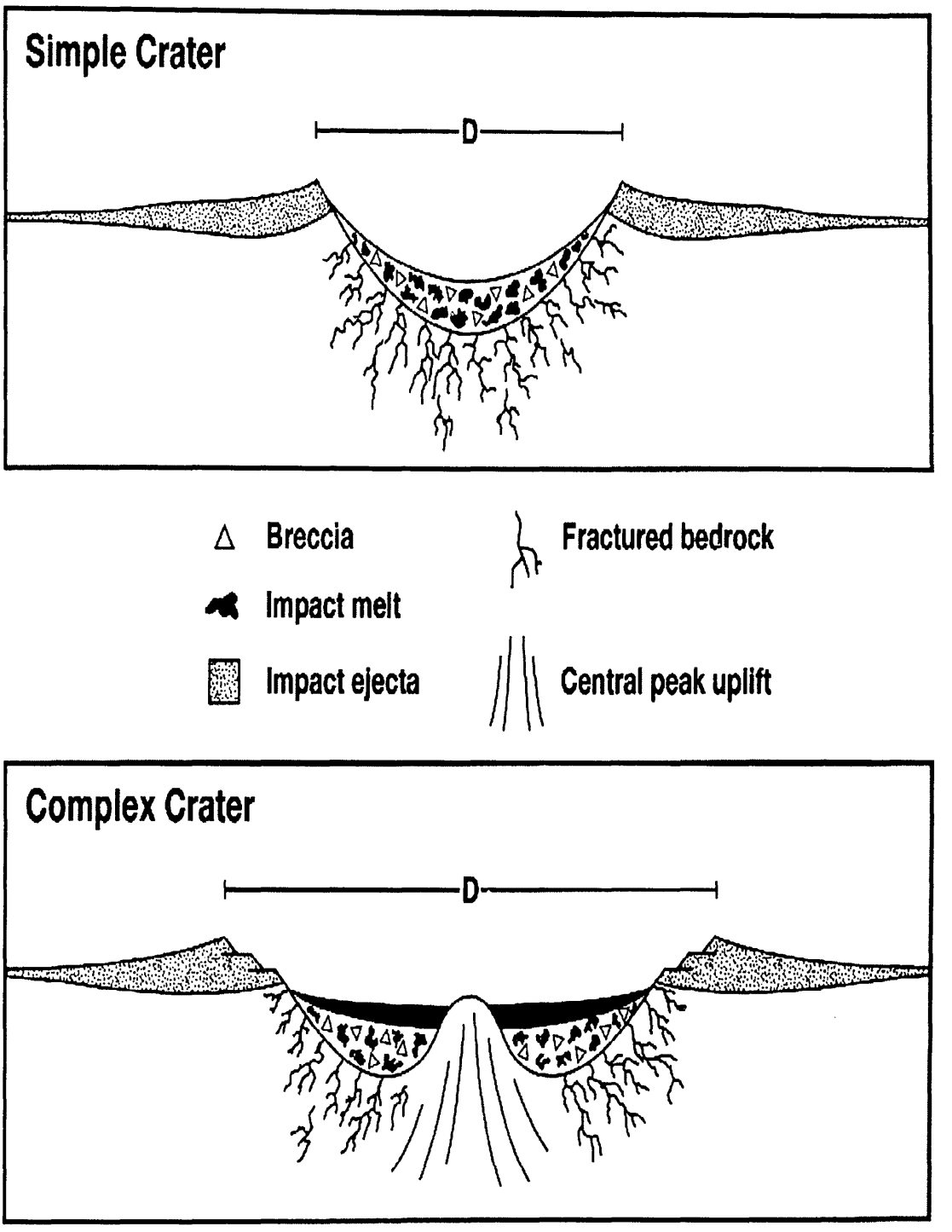

Figure 2.9: Diagram to show the differences in formation of a simple crater and a complex crater. The central peak of the complex crater is formed as a result of uplift of material stratigraphically beneath the crater, which rebounds in response to compression caused by the impact. From Melosh (1989).

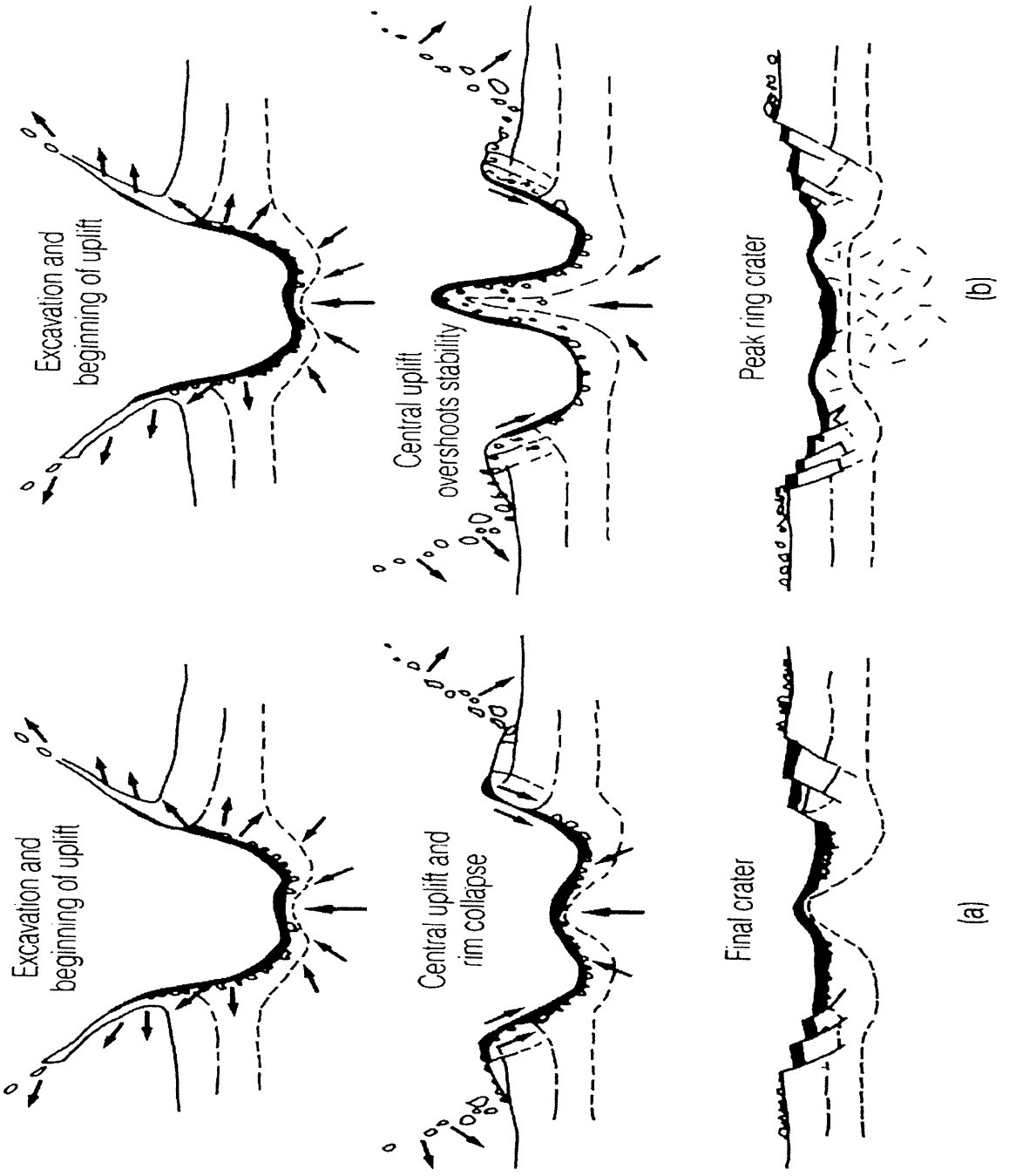

Figure 2.10: Diagram to show the formation of complex and peak ring craters. Peak ring craters are the more complex form and occur as larger (greater than 50km) complex craters. From Melosh (1989)

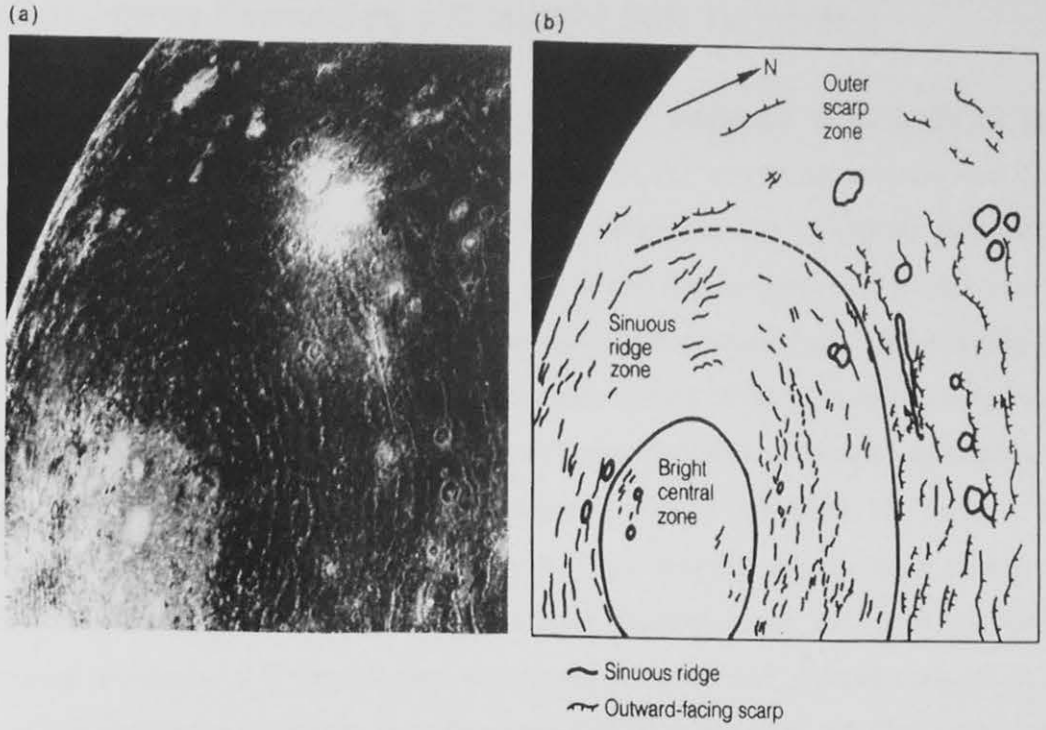

Figure 2.11: The Valhalla basin on Callisto an example of a multiring basin with an internal deformed region and a number of outward facing concentric ring scarps. From Melosh (1989).

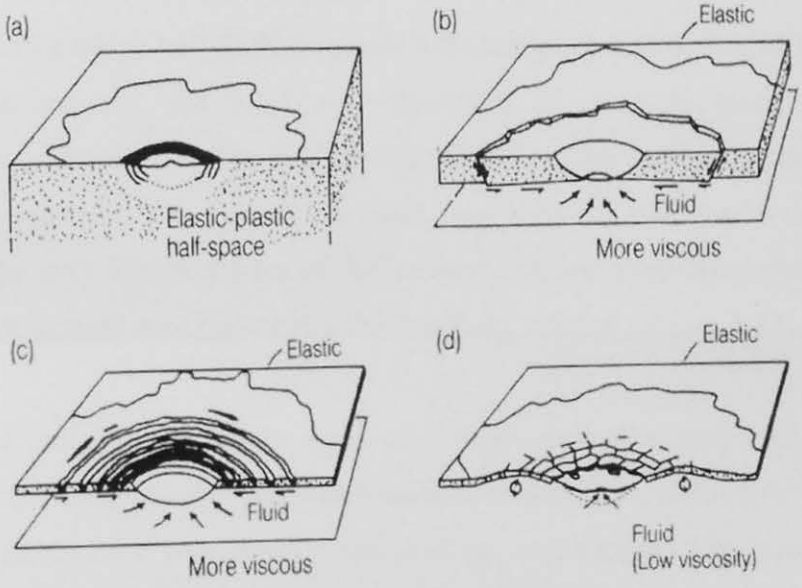

Figure 2.12: The widely accepted ring tectonic theory of multiring basin formation. Drawings (a) through to (d) illustrate the effect of decreasing lithosphere thickness. From Melosh (1989).

2.6 Structures Formed as a Result of Salt Tectonics

The presence of evaporite rocks in a stratigraphic sequence often leads to the formation of a series of unique structures in both the evaporite horizon and the overburden stratigraphy (Davison et al 1996). Many of the evaporite provinces throughout the world have been studied in detail and the formation of features such as diapirs, pillows, walls and withdrawal basins have been examined. Deformation in the overburden stratigraphy is common. The deformation of the post salt cover of the southern North Sea has been studied in detail (Jenyon 1988 and Stewart and Coward 2005). The formation of salt swells requires the overburden to expand to accommodate the increased volume of salt. This usually occurs as a result of extensional faulting and crestal grabens form frequently at the crest of these structures (Figure 2.6). If the salt then withdraws, these crestal grabens collapse. It is one of these collapse structures that Thomson (2004) suggests is the likely origin of the Silverpit structure.

Evaporite withdrawal basins form as a result of two different processes: 1) a local withdrawal of a diapir and 2) the regional withdrawal or dissolution of the evaporite. In the first process, the localised withdrawal of a diapir leads to extensive deformation in the overburden. Collapse structures including extensional faulting and folding are common. The East Texas basin example of Maione and Pickford (2001) is one of the very few examples of this process that has been documented in detail, where the deformation of the overburden has been imaged (Figure 2.13).

The second process occurs as a result of a more regional withdrawal of evaporite either through dissolution or the withdrawal to feed diapirs, pillows or walls. In this case, the salt has not previously penetrated the overburden. The formation of the withdrawal structures takes place in the overburden with extensional faults forming in order to accommodate the space creation. These withdrawal basins come in all different shapes and sizes (Cartwright et al 2001), but can be circular. In the Eastern Mediterranean example (Bertoni and Cartwright 2005), dissolution of the Messinian evaporite sequence has lead to the formation of a number of circular structures, ranging from 0.5 – 2km, in the stratigraphy above the evaporites. Some of these

include a series of concentric ring faults surrounding an undeformed central region (Figure 2.14). It is this process that Underhill (2004) proposes is the likely cause for the formation of Silverpit.

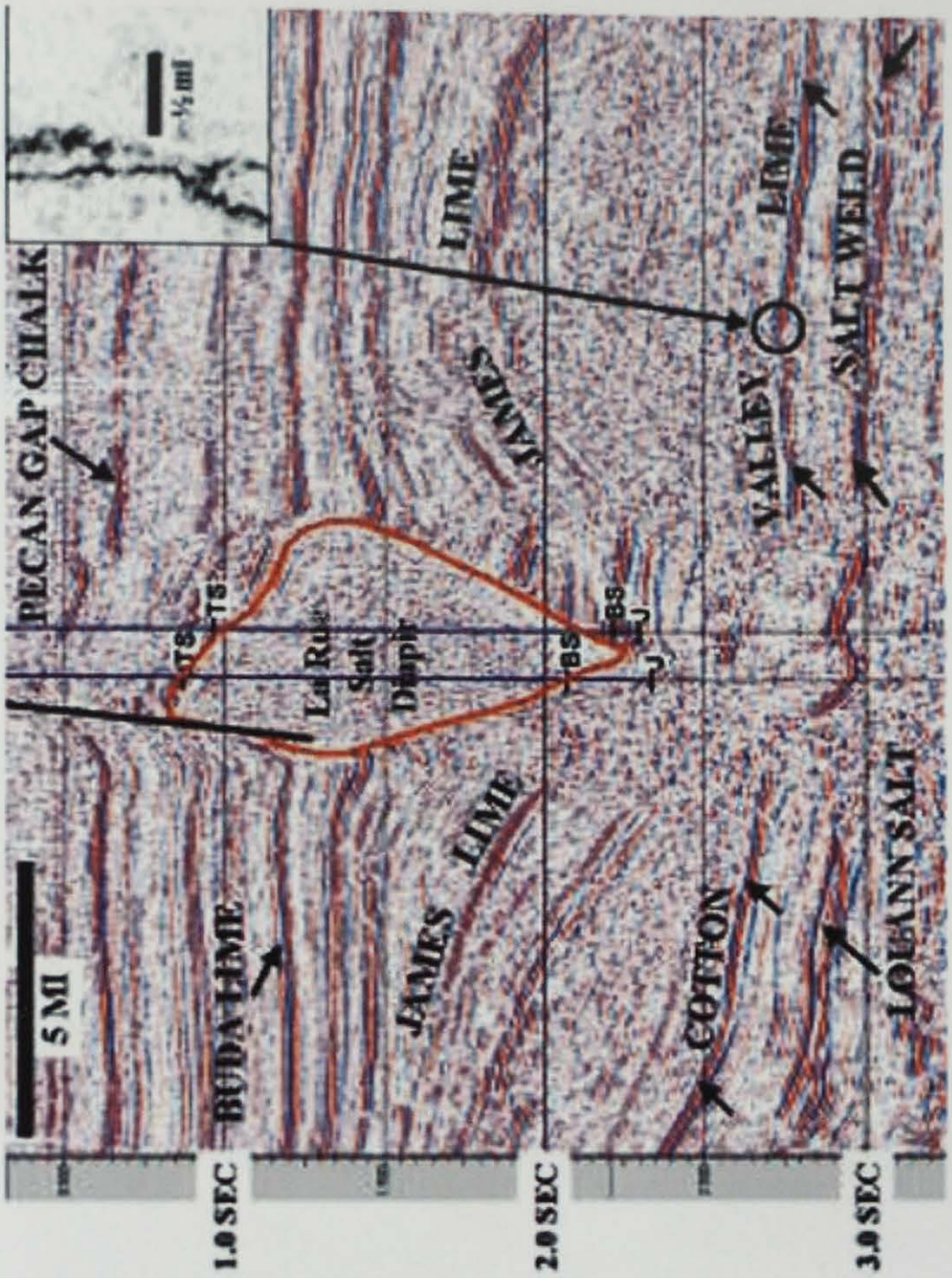

Figure 2.13: The deformation seen with the withdrawal of a salt diapir, in the East Texas Basin, USA. Note the extreme deformation of the overburden both above and below the diapir. From Maione and Pickford (2001).

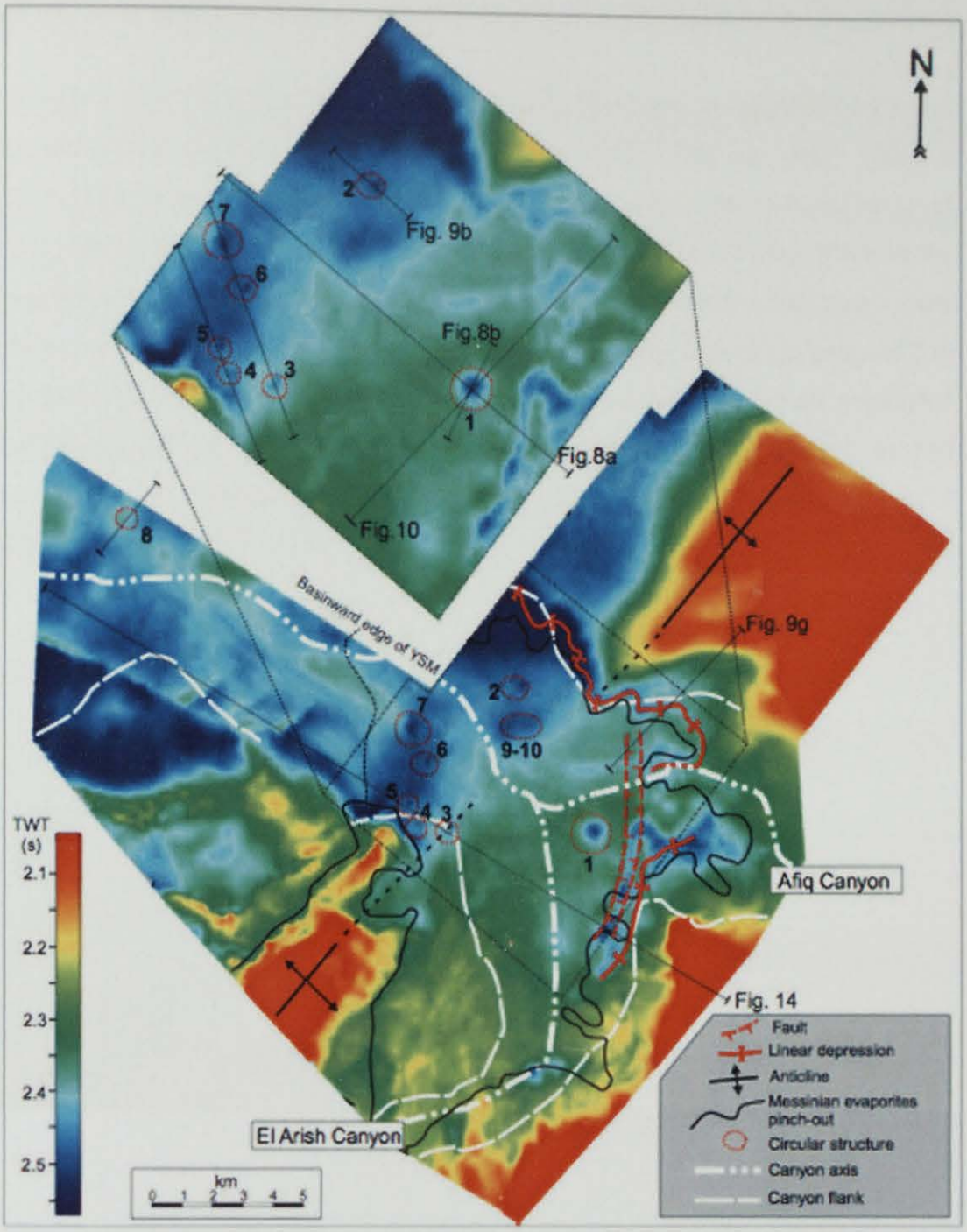

Figure 2.14: Regional salt withdrawal of the Eastern Mediterranean. Note the presence of ten circular structures formed as the Messinian salt is dissolved beneath. From Bertoni and Cartwright (2005).

2.7 Pull Apart Basins

Pull apart basins form in settings where strike-slip faults are accompanied by space creation during the fault displacement (Sylvester 1988). This can occur where a strike-slip fault bends, or where the fault dies out and displacement transfers to an offset, sub-parallel strand (Stewart 1999). Often the displacement takes place in the basement structure and the pull-apart basin forms in the overburden. The plan – view aspect ratio of pull-apart basins throughout the world usually falls in the range of 2 to 5 (Aydin and Nur 1982). Flower structures, both negative and positive are associated with pull-apart basins (Figure 2.15). It is a pull-apart basin with ring faulting, formed as a result of the basement tectonics that Smith (2004) suggests is the likely origin of the Silverpit structure.

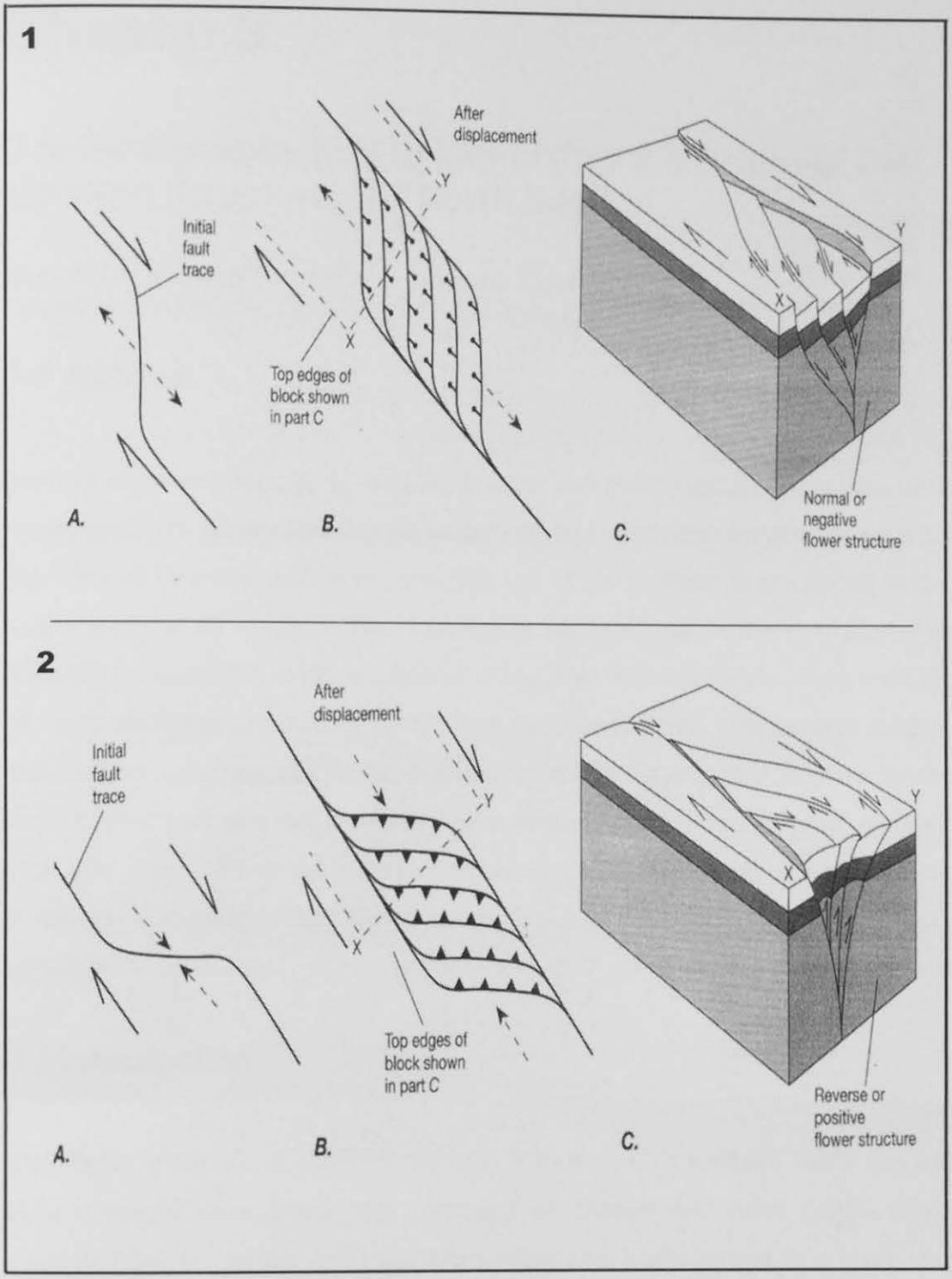

Figure 2.15: How flower structures are formed in pull-apart basins. 1 highlights the formation of normal or negative flower structures. 2 highlights the formation of reverse or positive flower structures. From Twiss and Moores (1992).

Chapter 3

3 Is Stratigraphy Key to Identifying the Origin of the Silverpit Structure, UK North Sea?

Zana Conway, Stuart Haszeldine & Malcolm Rider
School of Geosciences, University of Edinburgh, Edinburgh, EH9 3JW

3.1 Abstract

Seismic sequence stratigraphy, well log analysis and biostratigraphy have been used to determine the relationship that the underlying and overlying stratigraphy has with the Silverpit structure, UK North Sea. The age of the structure is bracketing to the Lower Eocene, 49 – 53Ma. The deformation patterns seen in the stratigraphy at Silverpit are compared to deformation resulting from other candidate origin settings. We have attempted to match all the Silverpit structure features, with the assemblages and features occurring in circular features, which do not originate from meteorite impact. That indicates that downward penetrating deformation is similar to other meteorite craters. However, younger circular faults are similar to salt withdrawal structures. Formation of the Silverpit structure is a combination of impact, followed by salt withdrawal.

3.2 Introduction

The origin of the 20 km diameter Silverpit Structure, UK, southern North Sea has been contested since it was first identified by Stewart and Allen (2002). They suggested that the central uplift and surrounding ring faults formed as a result of a meteorite impact crater. Rival hypotheses were rapidly proposed and include salt withdrawal subsidence (Underhill 2004) and pull – apart basin with Jurassic shale diapir (Smith 2004). These are each based on selected structural attributes of the Silverpit structure. However, these hypotheses have not carefully considered the full compendium of relationships that the structure has with the underlying, overlying and lateral surrounding stratigraphy. We have completed a full analysis of

deformation patterns within and surrounding the Silverpit structure, and then compared the stratigraphic implications of this deformation to each of the candidate origins

3.3 Data

3.3.1 Seismic and Well Log Data Sets

The 3D seismic data used in this study (Figure 3.1) is the same data set used by Stewart and Allen (2005). It comprises three survey areas, the Trent gas field, the Cavendish gas field and a small part of the Southern North Sea Mega Merge Survey. The total area for this study covers over 400km^2. The use of the databases was donated by two oil companies (BP and Shell) and a specialist geophysical company (Petroleum Geo-Services).

The study also used over sixty geophysical well logs acquired from the online Common Data Access (CDA) database in order to examine the stratigraphy (Figure 3.1). The CDA database contains all of the data from wells drilled and logged in the UK offshore sector and Edinburgh University has access to the publicly released data. This database is updated when the government release wells, approximately four years after the well has been logged. In order to identify the stratigraphy in the Silverpit area, four main logs were used, the caliper, the sonic, the gamma and the density (Figure 3.2).

The caliper log is a measure of the borehole size and shape and is usually measured in inches, either as the actual size of the hole or the differential size from the drill bit size (Rider 2002). The caliper is used to quickly identify permeable and impermeable layers, most commonly sand and shale horizons.

The sonic log is a measure of a formation's interval transit time (Δt), i.e. a measure of the formation's capacity to transmit sound waves and is the reciprocal of velocity. Geologically, the sonic varies with lithology and rock texture, in particular porosity

(Rider 2002). Low sonic (slow transit time) is taken to represent more cemented rock.

The gamma log is a measure the radioactive energy emitted from a formation and is measured in American Petroleum Institute (API) units. It measures the combined radiation flux emitted from naturally occurring uranium, thorium and potassium. Formations containing a high percentage of clay minerals tend to be the most radioactive because of their high uranium, thorium and potassium content (Rider 2002). The gamma log is most commonly used to identify shale units, however many other lithologies also emit similar radioactivity so other logs are used for confirmation. In general, shales and mudrocks have high APIs whereas sandstones have low APIs.

The density log measures, as its name suggests, the bulk density of the formation. This includes the solid matrix and the fluids enclosed in the pores. It is measured in grams per cubic centimetres ($g.cm^{-3}$). This tool operates by means of emitting gamma rays and measuring their attenuation between the tool source and detectors. The attenuation is a function of the electron density of the formation, which is closely linked to the density of the formation. Geologically, bulk density is the combination of the density of the minerals forming the rock (the matrix) and the volume of the free fluids it encloses (the porosity) (Rider 2002).

Accurate identification of the different lithologies is only possible using the suite of well logs available. When the boreholes are drilled a composite log is also created which includes as public information, a combination of the different well logs available, a bio-chronological stratigraphy, a lithological stratigraphy, a lithological log and the mud loggers comments. The composite logs were used for each of the wells examined, in particular for the identification of the age and formation of different horizons on the seismic data. Once the horizon has been identified on the composite log, the depth (usually in feet) is converted to two-way-travel time in milliseconds (ms) using a calibrated velocity log, another of the logs run for each of

the different wells. The calibrated velocity log includes depths in feet as well as two-way-travel time in milliseconds.

The data sets available have been completely controlled by the requirements of the hydrocarbon companies. As such, a 100km^2 section of the study area has not been imaged by either two or three-dimensional seismic methods. The majority of the well logs run through the boreholes, do not start until the Cretaceous or Jurassic sediments. Thus part of the ring complex of the Silverpit structure has not been imaged and much of the Palaeocene and younger sediment is impossible to determine.

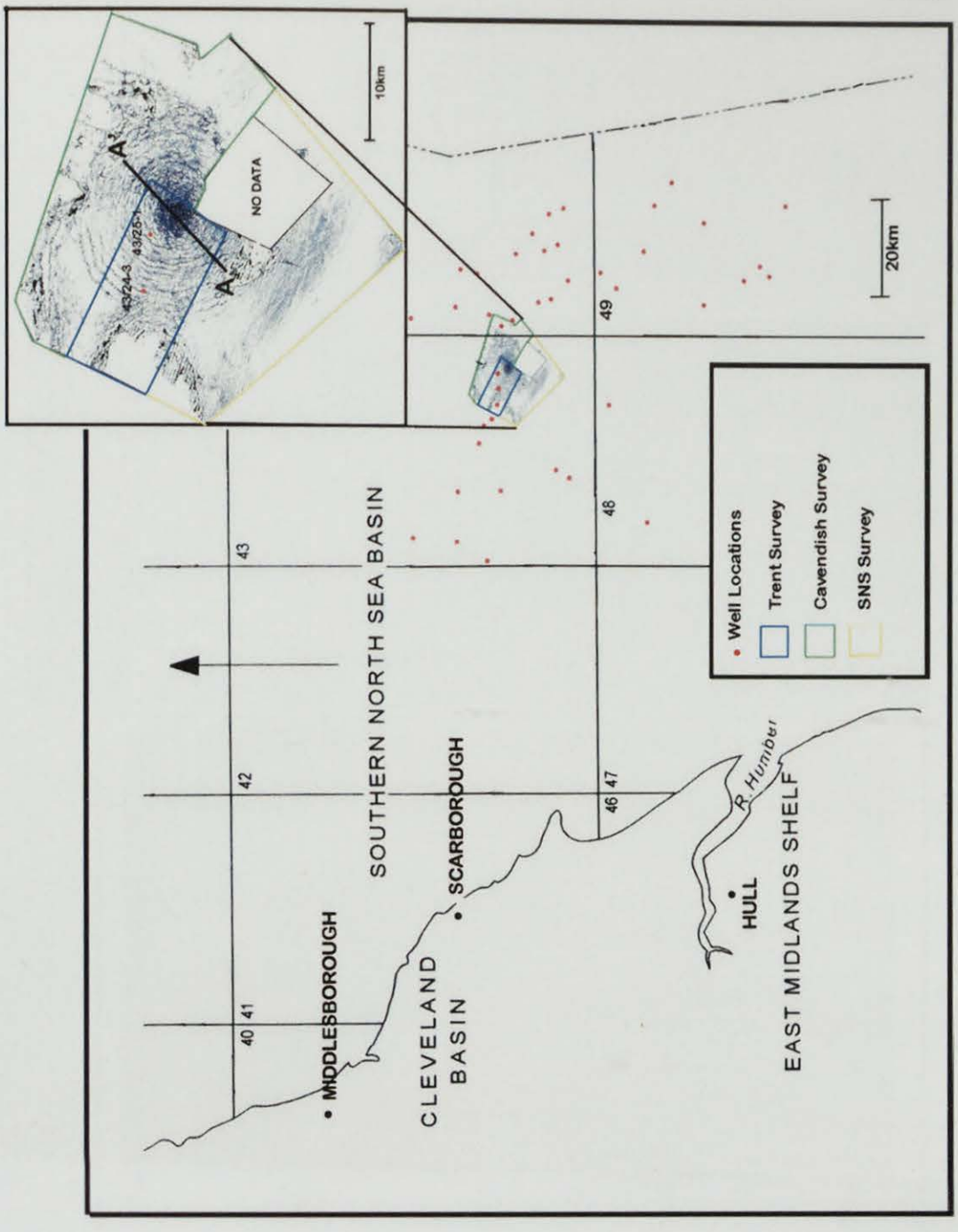

Figure 3.1: Location of the Silverpit structure, well locations and the extent of the 3D seismic surveys used. No seismic coverage of the Silverpit structure is available in the area of no data seen on the inset of the structure.

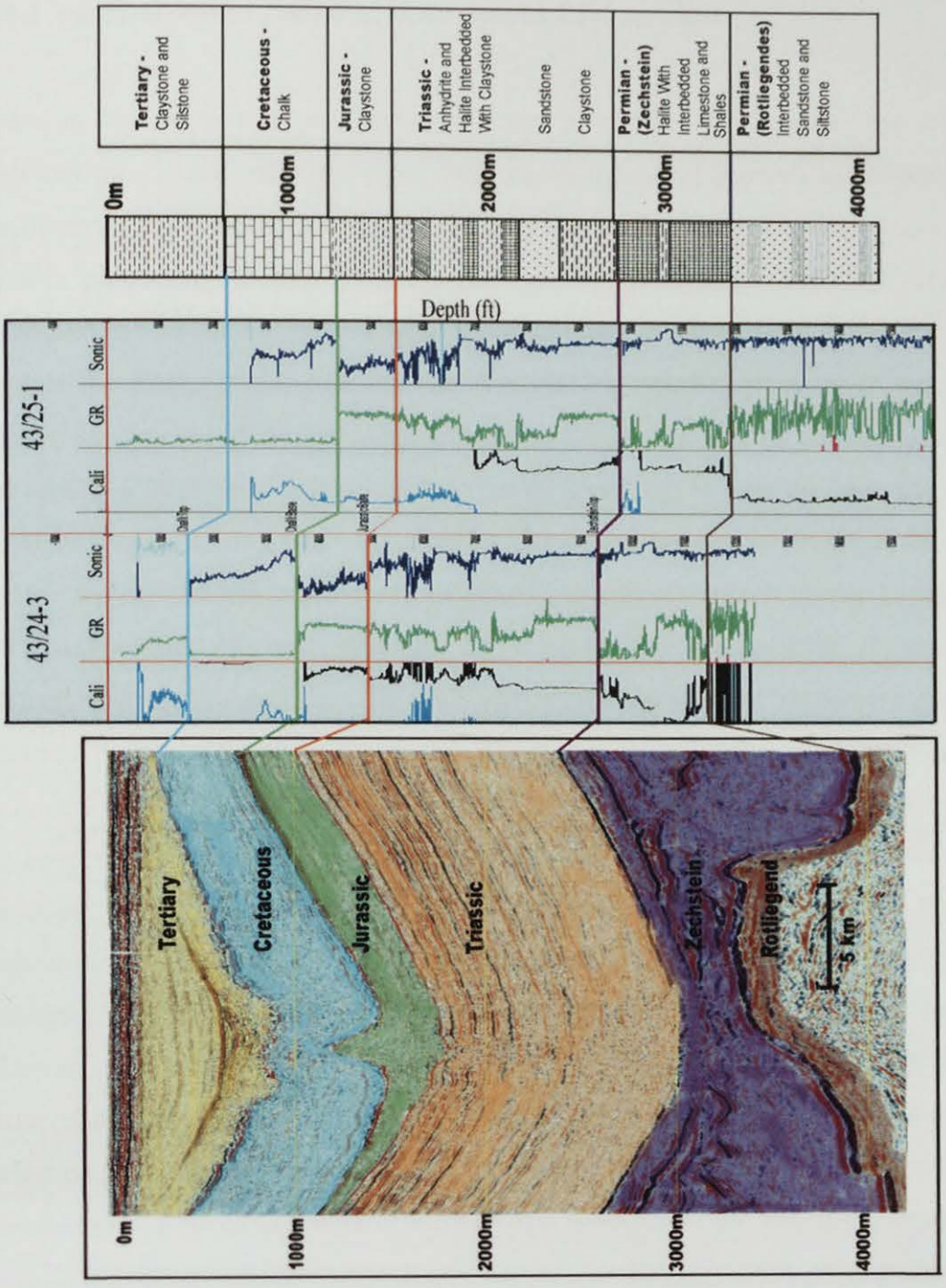

Figure 3.2: Seismic section A-A' with stratigraphic age of horizons highlighted, a well log panel highlighting the log response of the caliper, gamma and sonic geophysical logs from the two wells that penetrate the Silverpit structure and a stratigraphic column indicating the lithologies of the stratigraphy seen in the area surrounding the Silverpit structure.

3.3.2 Verification of Seismic Data Depth Conversion

Previous studies have all used data converted to depth, by processing the original two-way-travel-time reflection data. Because of the novel features associated with the Silverpit structure, queries have been raised about artefacts potentially introduced by this processing. Details of the depth conversion carried out on the data are published in Stewart and Allen (2005). In order to be certain that the features that are seen at the Silverpit structure are real features and not just artefacts of the depth conversion process as suggested by Thompson (2004), the current authors examined the principal features of the structure on the three surveys in both the time and depth domains. Figure 3.3 is a panel highlighting this examination. It is clear that the depth conversion has not led to the development of any artefacts which may have affected the study of the Silverpit structure. By contrast, depth conversion expands the vertical scale and so enhances the study as the true geometry of the structure can be studied.

A zone of disturbance is visible affecting the reflectors beneath the Silverpit structure, which if the structure were a meteorite crater, may reflect a zone of deformation created as a result of the impact. However, the disturbance is continuous through the Permian Zechstein evaporite unit which acts as a decollement horizon (Stewart and Coward 1995) and would have acted as a barrier, stopping the impact induced deformation affecting the underlying Rotliegend and older sequence. The deformation is therefore attributed to a processing artefact and is not considered as a possible indication of the origin of the Silverpit structure.

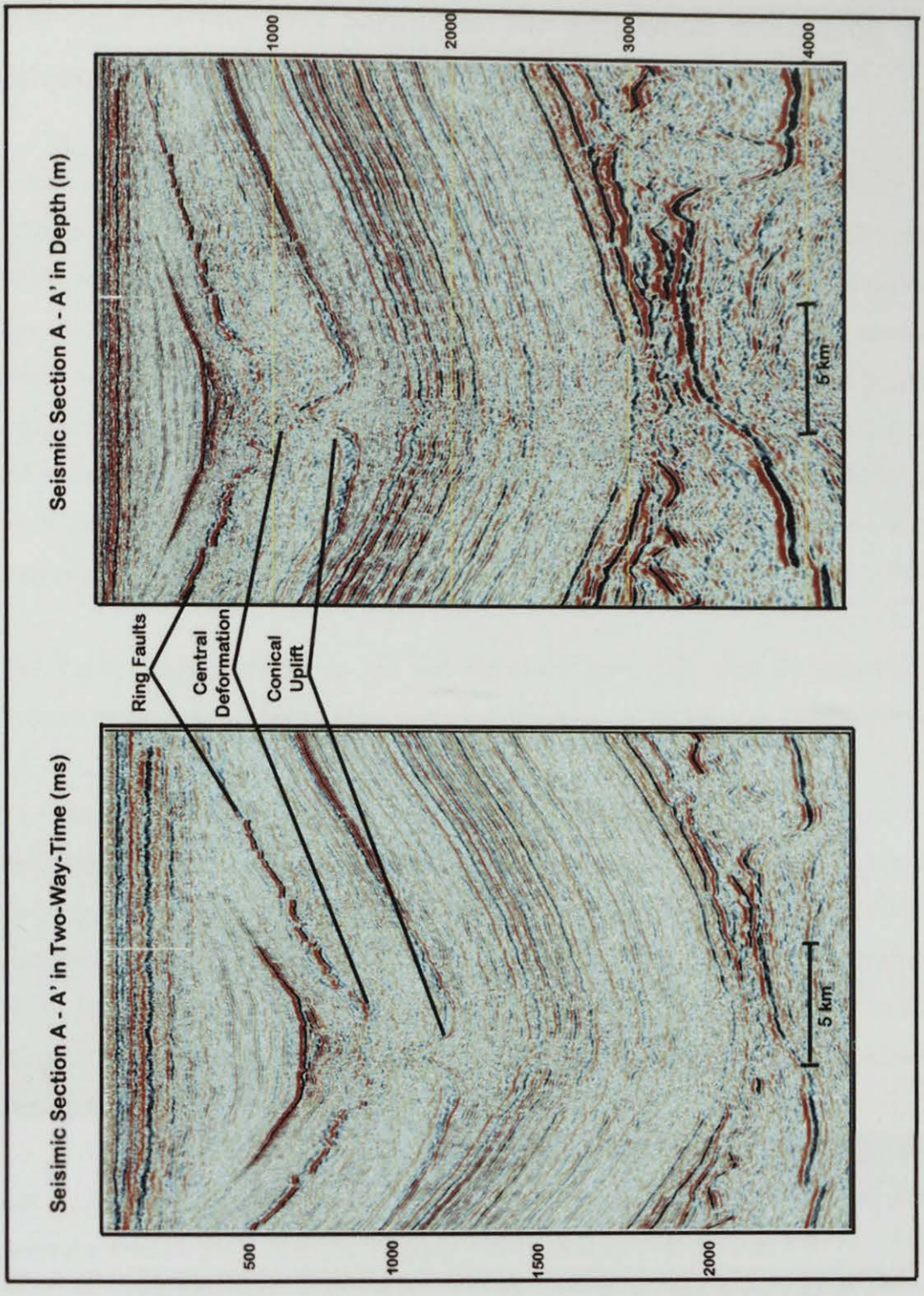

Figure 3.3: A-A' seismic section in two-way-travel-time and A-A' seismic section following depth conversion. Note that all features associated with the Silverpit structure are seen on both seismic sections.

3.4 Determining the Stratigraphic Sequence Bounding the Silverpit Structure

It has not been possible to study the processes leading to the formation of the Silverpit structure without first determining the nature of the post Devonian stratigraphy within the area surrounding the Silverpit structure. We also consider if this post Devonian stratigraphy is similar to that seen in the rest of the southern North Sea basin. Using the seismic reflection data surveys, geophysical well logs and composite logs available, a stratigraphic column has been developed to understand the variety of lithologies and combined with the seismic data their relationships have been studied. Figure 3.2, integrates the different data and the stratigraphic column produced.

The Carboniferous sediments are not discussed here. The data donated by the hydrocarbons companies has been restricted and does not include the Carboniferous.

The oldest units studied are the lower Permian Rotliegend sands, which have been deformed as a result of basement (pre-Variscan unconformity) structural development (Glennie 1998). Above the Rotliegend, lies the Permian Zechstein evaporite sequence, which varies significantly in thickness throughout the southern North Sea. Beneath the Silverpit structure the Zechstein is approximately 400m thick (Figure 3.2). Where the Zechstein is rich in evaporites, remobilisation has occurred during burial. This forms salt walls, diapirs and subsidence synclines. Locally the Zechstein reaches thicknesses of over 3000m, usually in the form of salt diapirs or salt walls. The influence of the Zechstein mobility on subsequent depositional trends from the Triassic through to the Tertiary is discussed more in Section 3.8.

Specific surfaces have been interpreted using the seismic data to examine the main stratigraphic intervals, the Permian Zechstein, Triassic, Jurassic, Cretaceous and Tertiary. Figure 3.4, highlights the surfaces mapped as well as the 3D structural relationship that the principal horizons have. The surfaces mapped have been chosen because they are the oldest or youngest surface in a stratigraphic interval and are: the

Top Cretaceous, the Base Cretaceous, the Top Triassic and the Top Zechstein. Each of the post Zechstein stratigraphic intervals and surfaces are discussed in turn below.

The Lower Triassic is dominated by a series of mudstones, known as the Bunter shales, overlain by sandstone, known as the Bunter sands (Cameron 1992), which together are locally up to 350m thick. The Middle Triassic consists of intermittent mudstone and halite up to 500m thick. The Upper Triassic includes mudstones with intermittent anhydrite up to 320m thick.

The Jurassic sediments are entirely mudstones with minor inter-bedded limestone. The Jurassic thickness varies significantly within the southern North Sea basin ranging from no Jurassic being present up to a thickness of 1000m in known depocentres (Cameron et al 1992). Figure 3.2 indicates that the thickness of the Jurassic is clearly variable across this 10km section ranging from 400m to 10m thick. The Jurassic to Cretaceous unconformity, caused by end Jurassic uplift and erosion, has been well documented (Glennie 1998) and can be clearly seen on the seismic data beneath Silverpit with Jurassic horizons offlapping the oldest Cretaceous horizon (Figure 3.2).

The Cretaceous is dominated by a chalk sequence, locally up to 800m thick. Beneath the Silverpit structure the chalk is thin and shallow (base chalk 1500m deep). The two wells that penetrate the outer ring faults of the Silverpit structure, 43-25-1 and 43/24-3 contain a very thin (less than 60m) section of the Cromer Knoll Group, in 43/25-1 this is dominated by the Red Chalk Formation. There is also an extremely thin layer of the Speeton Clay Formation (less than 9m). In 43/24-3, 10m of the Red Chalk Formation sits on top of 30m of the Speeton Clay Formation. This is important as it the base of the Chalk that has been mapped in this study to represent the base Cretaceous surface. The base of the Cretaceous chalk provides a continuous and recognisable horizon to map on the seismic data. The Cretaceous stratigraphy beneath the base of the Chalk is thin and extremely variable and would not provide a suitable horizon to map.

The Tertiary lithology has been established from the Mud Logger's comments on the composite logs, as no well logs were run throughout the any of the Tertiary. The sediments consist of interbedded sand and shale units that vary quite significantly in thickness (as seen on Figure 3.2) from 600m thick in the centre of the syncline to less than 10m on the top of the anticlinal structures.

Comparison of the lithologies seen in the 400km^2 area surrounding the Silverpit structure with the rest of the southern North Sea basin suggest that they are unremarkable and are the same as are seen in the rest of the basin (Glennie 1998).

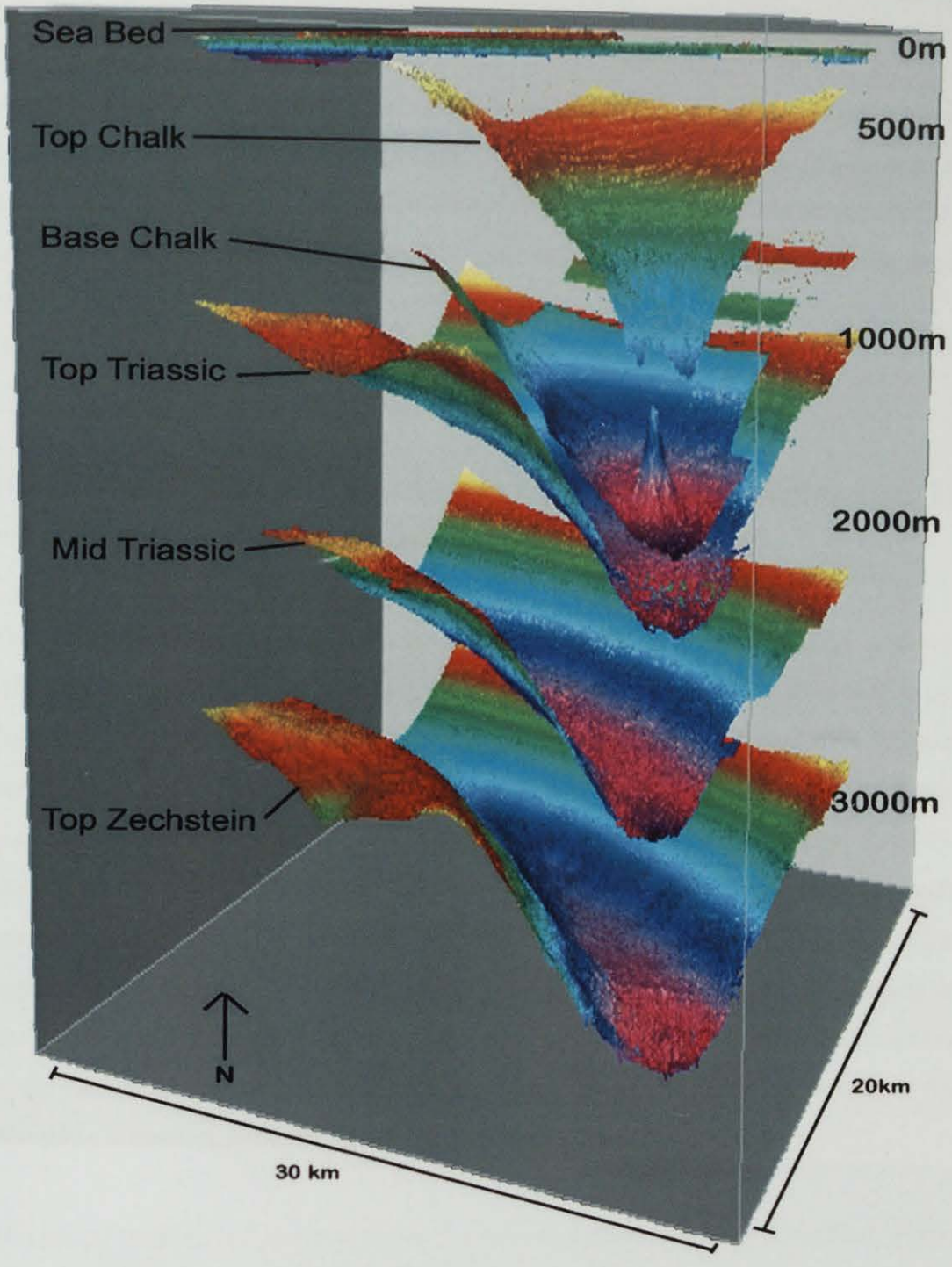

Figure 3.4: Three-dimensional view of the key horizons and their structural relationship derived from the maps produced by hand picking the different seismic horizons.

3.5 The Age of the Structure

In order to establish the origin of the Silverpit structure it has been necessary to determine it's age. Two methods will be outlined, which enable the structure to be dated: 1) Seismic surface age identification directly above the Silverpit structure by reference to a regional framework; 2) Direct new biostratigraphy on cuttings from near-by boreholes.

3.5.1 Seismic Stratigraphic Age

This study used seismic reflection data stratigraphic analysis combined with well log and biostratigraphic data in an attempt to date the Silverpit structure.

The deformation associated with the Silverpit structure is most clearly observed affecting the top Chalk horizon (Figure 3.5). However, the deformation is younger than this and can be seen affecting Tertiary stratigraphy (Figure 3.5). Detailed examination of the Silverpit structure indicates that the ring faults have formed after the central deformation. Figure 3.5, highlights that an undisturbed horizon identified above the central deformation is offset by the ring faults as it is traced from the centre to the edge of the structure. The ring faulting associated with the structure appears to be instantaneous with no evidence of growth faulting or reactivation of the faults. Therefore the ring faults must have occurred at some stage after the formation of the central deformation zone. As such, it is the age of the central deformation that this study considers to be the age of the Silverpit structure.

The oldest undisturbed horizon above the central deformation was identified (Figure 3.5). The chosen horizon was then mapped and identified at each of the two well locations within the Silverpit structure, 43/25-1 and 43/23-3 (Figure 3.1). The depth of the horizon was determined by acquiring the depth in two-way-time in milliseconds (ms) at the two wells from the seismic section. This depth was then converted to feet using the calibrated velocity well log (a standard well log acquired when the well is drilled) from each of the two wells. The depths were then correlated with independent biostratigraphic zones. The Varol (1998) zonation scheme indicates

that the depths acquired are equivalent to the nanoplankton zones NP10 – NP14. Using this method the structure has been bracketed in to the Ypresian, Lower Eocene, 53 – 49Ma (Cameron et al 1992). Figure 3.6 displays the Tertiary stratigraphy and links together the nanoplankton zones and relative and absolute ages.

It is important to consider that this age represents the age of a horizon that is in fact younger than the central deformation zone. The horizons immediately above the top Cretaceous Chalk are deformed, faulted and undrilled, so cannot be tied to boreholes at shallower depths, hence the exact age of the central deformation cannot be established. The central deformation of the Silverpit structure is slightly older than the age suggested.

The ring faults associated with the Silverpit structure cannot be dated using this method because the calibrated velocity logs used to establish the depth of the horizon from the boreholes has not been run at such shallow depths.

3.5.2 Nanofossil Age

Bidgood et al (in prep) used cuttings taken from 43/25-1 and 43/24-3, the two wells that penetrate the outer rings of the structure and carried out biostratigraphic analysis of the samples collected from the Lower Oligocene through to the Mid Cretaceous. This analysis indicates the age of the structure to be equivalent to the nanoplankton zones NP4 to NP13, which have also been determined from the Varol scheme (1998). This suggests that the age of the structure is post Seelandian to pre / intra Ypresian, middle Palaeocene – Early Eocene, 63 – 50Ma

As no core material is available from within the structure (it has not been drilled) any of the dating techniques have certain resolution problems. The seismic sequence stratigraphy method is subject to the vertical resolution of the seismic data that is no more than 20m and can only date the horizon above the structure. This means that the age is approximate rather than an absolute age. The biostratigraphic method

adopted by Bidgood et al (in prep) is confined to the availability and resolution of the cuttings. These have been sampled every 8m in well 43/24-3 and every 16m in well 43/25-1. The cuttings are a mix of material from between the two sampled intervals and so it is difficult to gauge exactly where each sample is from, thus only an estimate of the age is possible.

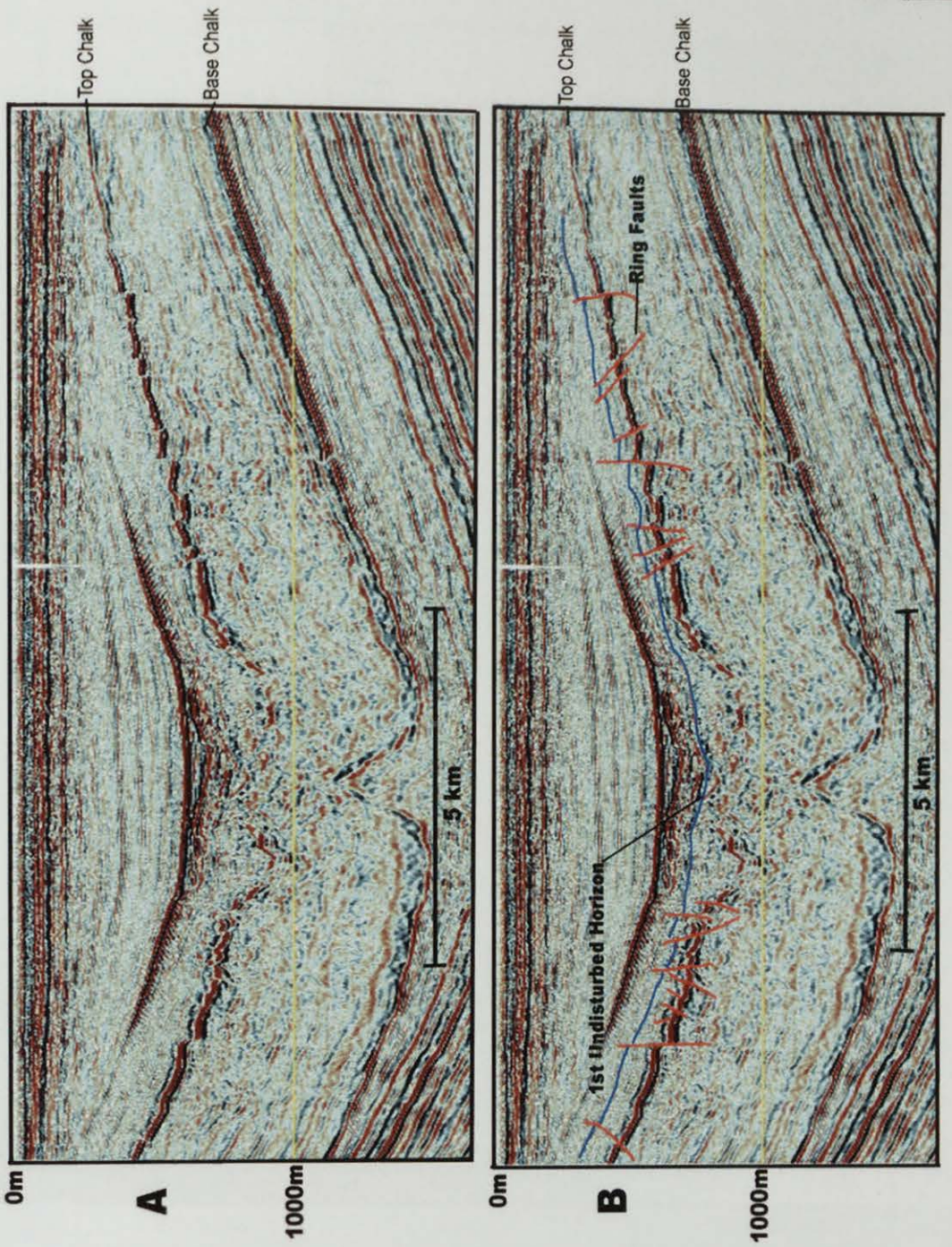

Figure 3.5: The seismic section used to determine the age of the Silverpit structure. The Blue horizon is the first undisturbed horizon above the central deformation. Note that the blue horizon is offset by the ring faults.

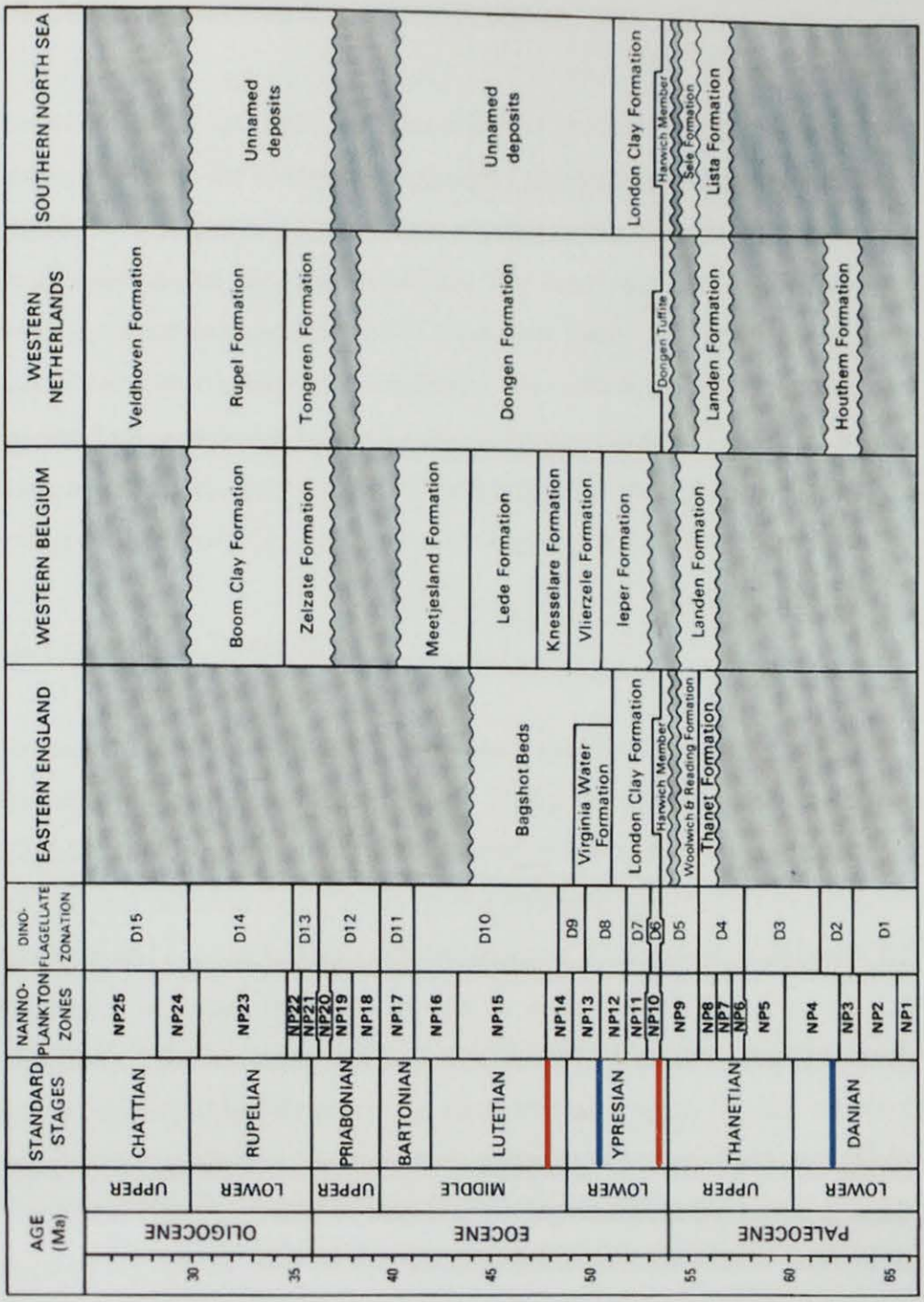

Figure 3.6: A panel highlighting the age of Tertiary stratigraphy using chronostratigraphy, lithostratigraphy and biostratigraphy. From Cameron et al (1992). The red lines bracket the seismic stratigraphy derived age and the blue line the nannofossil derived age.

3.6 Deformation in the Structure

The deformation associated with the Silverpit structure and the relationship that the structure has with the overlying stratigraphy plays a key role in understanding how it formed. In this section we examine the deformation and relationships seen with the stratigraphy at the Silverpit structure. We then examine deformation styles for examples of the proposed method of formation: meteorite impact crater, regional salt withdrawal and localised salt withdrawal. By comparing these structural styles, we can conclude a probable origin for the Silverpit structure. Figure 3.7 highlights the deformation styles and specific features seen at the Silverpit structure and the analogue structures suggested as possible origins for the Silverpit structure.

3.6.1 Evaporite Dissolution

Bertoni and Cartwright (2005) investigate the 3D circular evaporite dissolution structures of the Eastern Mediterranean. This study provides a good example of the deformation associated with the dissolution of salt on a regional scale leading to the collapse and deformation of the overlying stratigraphy with the formation of circular structures and concentric ring fault development. If the Silverpit structure were a salt withdrawal structure then this would be a likely analogue for the method of formation of the structure. As such it is useful to examine the deformation seen associated with these structures in comparison to what is seen at the Silverpit structure. In the Eastern Mediterranean example, a series of sub vertical faults and extensional faults surround an undeformed depression in the centre of the structure (Figure 3.7). In the case of the Silverpit structure, the central zone is extremely deformed with no horizon being traceable all the way through the centre. Also, the ring faults associated with Silverpit are penetrate only the early Eocene through to the late Cretaceous and do not continue deep beneath the structure. Thus although the ring faults seen at the Silverpit structure could have formed as a result of regional evaporite dissolution, the other features cannot be explained by this method.

3.6.2 Diapir Withdrawal

The East Texas basin study (Maione and Pickford 2001) is an example of where the La Rue salt diapir, has intruded the overlying sediment. Subsequently the salt began to withdraw locally and reduce in vertical size. This has led to significant deformation in the in the stratigraphy with faulting and folding present. The deformation is continuous from the deep Louann salt through to the shallower Pecan Gap Chalk, the shallowest stratigraphy the salt diapir reached (Figure 3.7). Comparison of the deformation seen in this example with that seen at Silverpit highlights that the there are few if any similar features apart from the fact that the deformation associated with each structure sits in the centre of a salt withdrawal induced syncline and one set of ring faults are present.

3.6.3 Meteorite Impact

The Mjølnir crater, Barents Sea is a 40 km diameter confirmed buried impact structure (Tsikalas et al 2002). The structure was initially identified in a similar way to Silverpit, with seismic reflection data. Unlike Silverpit, Mjølnir has been drilled, cored and confirmed to be an impact crater with the presence of both shocked quartz and a geochemical iridium anomaly (Dypvik and Ferrell 1998; Dypvik and Attrep 1999). Shocked grains of quartz and geochemical iridium peak are two of the key criteria used to confirm the presence of an impact structure (Koeberl 2002). Analysis of the seismic sections through the structure show that the structure consists of an eroded conical peak (the central uplift) surrounded by a zone of deformation with many small-scale faults (throws of <15 milliseconds). The structure is then bound by a series of curved to circular faults up to 70 milliseconds throw (Figure 3.7). The deformation that is seen at this confirmed meteorite impact crater is very similar to that seen at the Silverpit structure. The characteristic central uplift is clear on the base Cretaceous Chalk horizon at the Silverpit structure, but is not as clear on the top Cretaceous Chalk horizon. At the Silverpit structure this is likely to be as a result of erosion and compaction. The two structures also have the small scale faulting and deformation in the centre of the structure in common. The curved faulting on the

outer parts of the Mjølnir crater is not the same as the ring faulting seen at Silverpit. The curved faults at Mjølnir are inside the crater created when the impact occurred which makes the Mjølnir crater a peak ring complex crater. The ring faults associated with Silverpit are outside the central crater section.

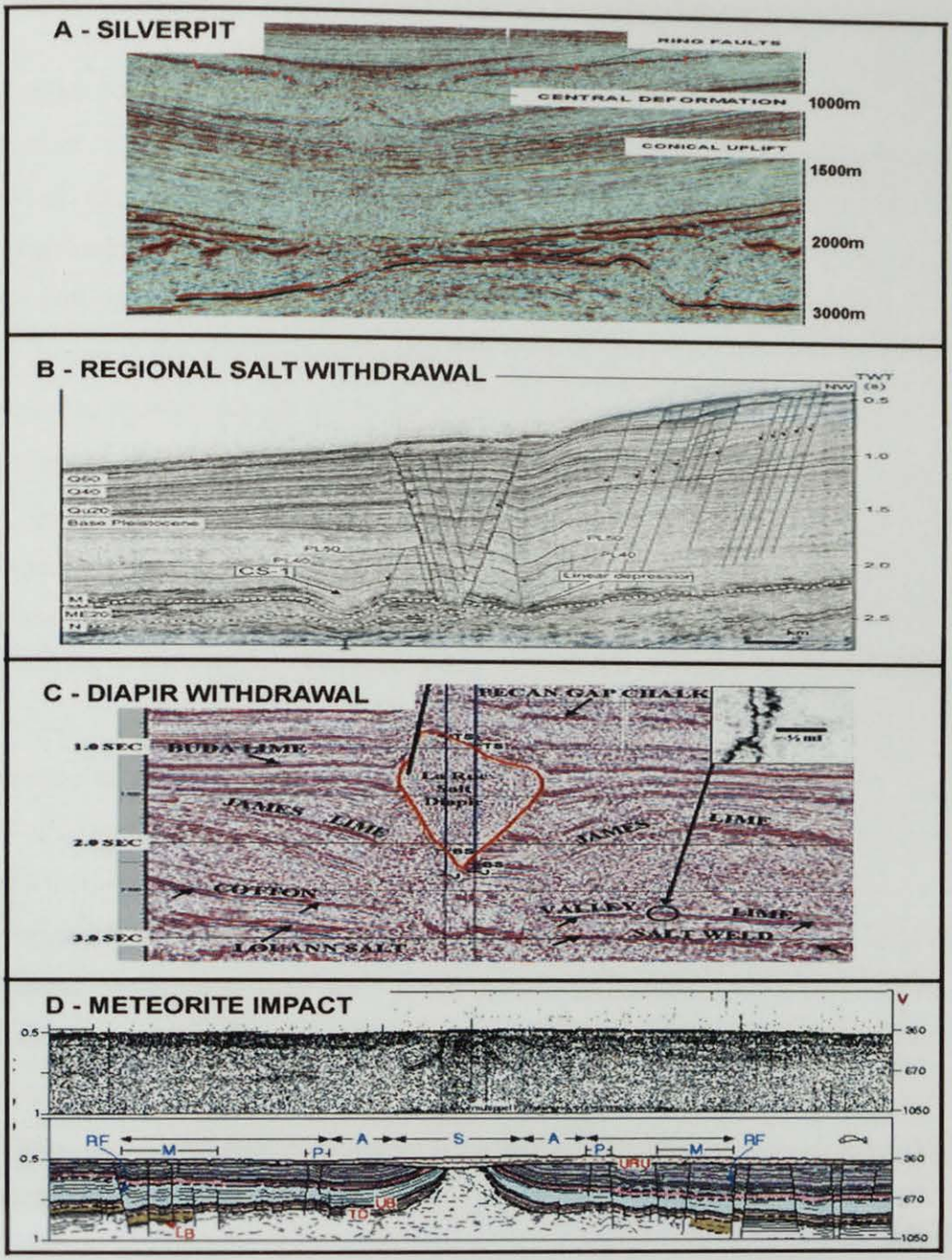

Figure 3.7: The seismic architecture of the Silverpit structure (A) and analogue structures suggested as the possible origin of the structure. B – Regional evaporite dissolution in the Eastern Mediterranean example, from Bertoni and Cartwright (2005). C – Salt diapir withdrawal from the East Texas Basin example, from Maione and Pickford (2001). D – The Mjølnir meteorite impact crater, Barents Sea, from Tsikalas et al (2002).

3.7 Deformation in the Underlying Stratigraphy

In order to understand the processes involved in the formation of the Silverpit structure, it is also important to examine the deformation patterns in the stratigraphy beneath the structure. Maione (2003) examines the salt withdrawal basins of the East Texas basin, USA, where a salt diapir has intruded the overlying stratigraphy but has then withdrawn leaving a series of ring faults in the Early Cretaceous stratigraphy. In this example the stratigraphy beneath the ring faults has been deformed as the salt diapir has moved through it. Offsets of the horizons are seen on the seismic data and in some cases the horizons are so deformed where the diapir has passed through, they are no longer traceable using the seismic data. If the Silverpit structure is a salt withdrawal feature a downward increase in deformation would be expected in the centre of the structure. Conversely, if a meteorite impact were responsible for the formation of the Silverpit structure, a decrease in the deformation would be expected, moving from younger to older stratigraphy. This is because of the downward decrease of impact energy.

Two methods have been used in order to test the deformation seen in the stratigraphy beneath the Silverpit structure. Firstly the seismic sections of the East Texas basin example were compared with those from the Silverpit structure looking for disturbances in the horizons such as faults, folds or minor offsets. Figure 3.8, examines the seismic data beneath the Silverpit structure. At the resolution of the seismic data there appear to be no disturbances similar to those seen in the East Texas Basin salt withdrawal basins, with the horizons remaining coherent and traceable.

Secondly, the seismic data set was used to construct maps of four stratigraphic horizons, the top Cretaceous Chalk, the base Cretaceous Chalk, the top Triassic, and the top Zechstein, representing the principal horizons in the study area. An edge detection process was then applied and edge detection maps created. The edge detection process identifies significant steps in depth (or milliseconds on non depth converted data) where an "edge" in the stratigraphy exists. Where lots of edges exist there are strong signals on the map and any structure can be clearly identified. This

method provides a way of identifying large-scale deformation on one horizon and a good way to compare a number of horizons. Stewart and Allen (2005) used the same method but on different horizons beneath the structure.

Figure 3.8, highlights that deformation associated with the structure is most prominent on the top Chalk horizon and that the deformation decreases with increasing depth.

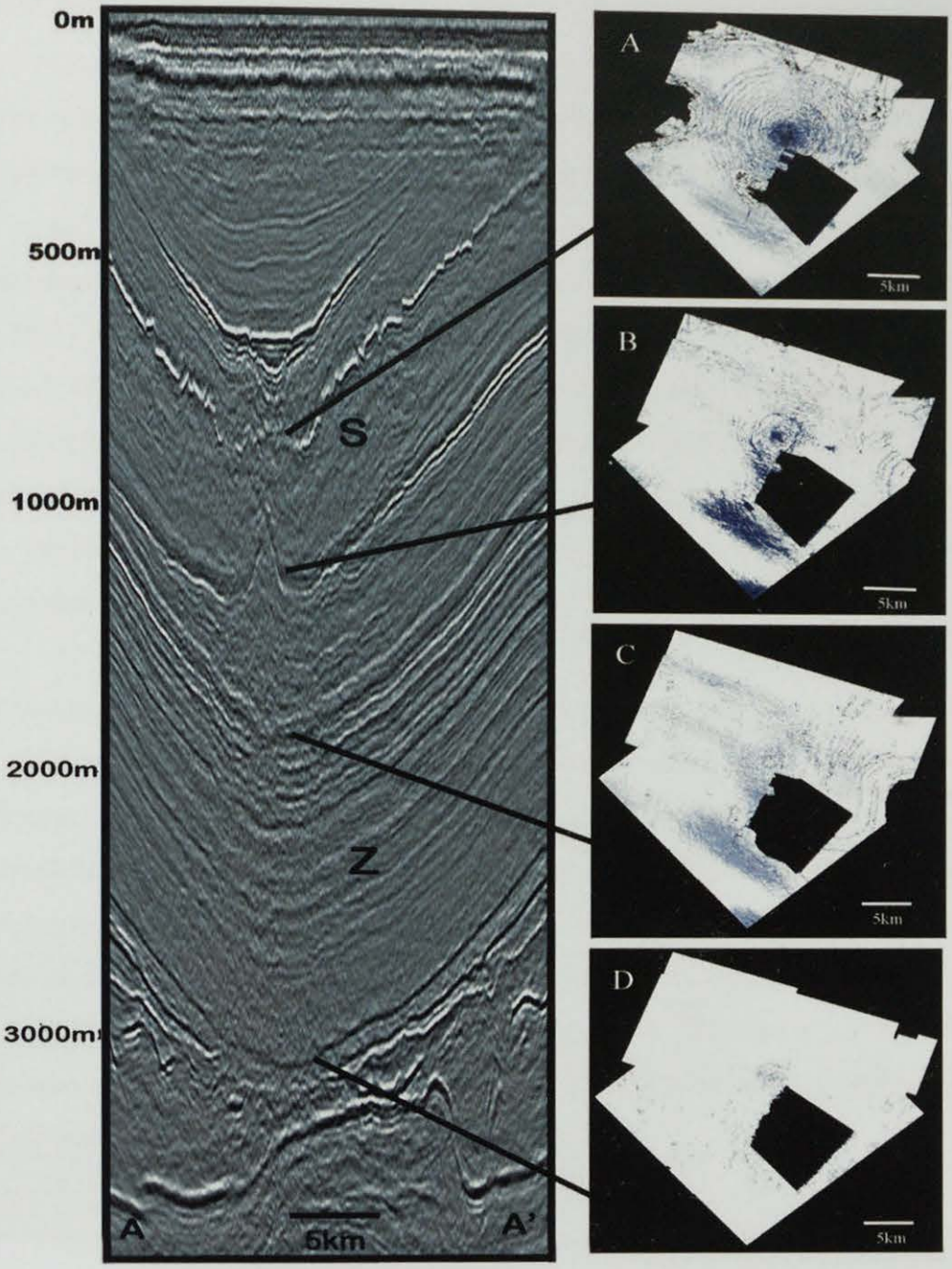

Figure 3.8: Seismic section A-A' and edge detection maps highlighting decreasing deformation with depth associated with the Silverpit structure. The edge detection maps are of the surfaces: A – Top Cretaceous Chalk, B – Base Cretaceous Chalk, C – Top Triassic, D – Top Upper Permian Zechstein. Point S highlights the Silverpit structure. Point Z indicates that coherent and traceable horizons are present beneath the Silverpit structure.

3.8 The Role of Salt Movement

The role of salt tectonics in the southern North Sea and the influence it has on the structures formed in the post Zechstein stratigraphy, is reported by Stewart and Coward (1995). As already discussed, the Silverpit structure is located in what is at the present day a region of dominant salt movement. Underhill (2004) and Thomson (2004) suggest that the Silverpit rings and depression structure have formed as a result of this salt movement. However, they each invoke by different methods. In particular there is the coincidence that the structure today occurs in the centre of a halokinetically-induced syncline (Figure 3.4). Consideration thus needs to be given to the exact timing of salt movement in this region, in order to determine whether the salt was moving at the time of formation of the Silverpit structure.

The history of salt movement and in particular the locations of previous salt highs and lows, can be established by looking at thickness variations through different time frames. During time periods of salt withdrawal and diapirism, then accommodation space is being created above locations of salt withdrawal. This allows sediment to accumulate and hence a thick succession of sediment to develop. Where salt highs are developing by diapirs or walls, the salt needs space to move into and consequently little deposition of sediment takes place. The most extreme of this case is where a salt diapir breaks through to the sea floor surface and there is no new sediment deposited above the salt.

In order to examine these thickness variations isopachs were developed from the seismically mapped horizons. The isopachs were developed by subtracting a shallower horizon, from a deeper horizon, for example, in order to generate the Triassic isopach, the Top Triassic horizon (Figure 3.4) was subtracted from the Top Zechstein horizon (Figure 3.4). This gives the thickness of all the Triassic aged sediment. Five isopachs were generated for this study (Figure 3.9), which examine the depositional variations in five time periods: the Tertiary, the Cretaceous, the Jurassic, the Triassic and the Zechstein (Upper Permian). This series of isopachs developed from seismic interpretation of significant horizons above and below the

Silverpit structure, will give some indication of when predominant salt movement was taking place. Axes of subsidence were due to salt withdrawal. Locations of thin sediments were due to salt injection.

Figure 3.9 documents the changes in locations of salt lows and highs through time. It is clear that a major change takes place between the Jurassic and Tertiary, with the location of the thinnest Jurassic sediment being the location of the thickest Tertiary sediment. The salt movement of the southern North Sea is discussed in significantly more detail in Chapter 5.

It can be seen that movement of the Zechstein salt had commenced many tens of million years before the formation of the Silverpit structure. The axes of subsidence were not influenced by the Silverpit structure. After the formation of the Silverpit structure, salt subsidence axis located through Silverpit. It is unclear if this is consequential.

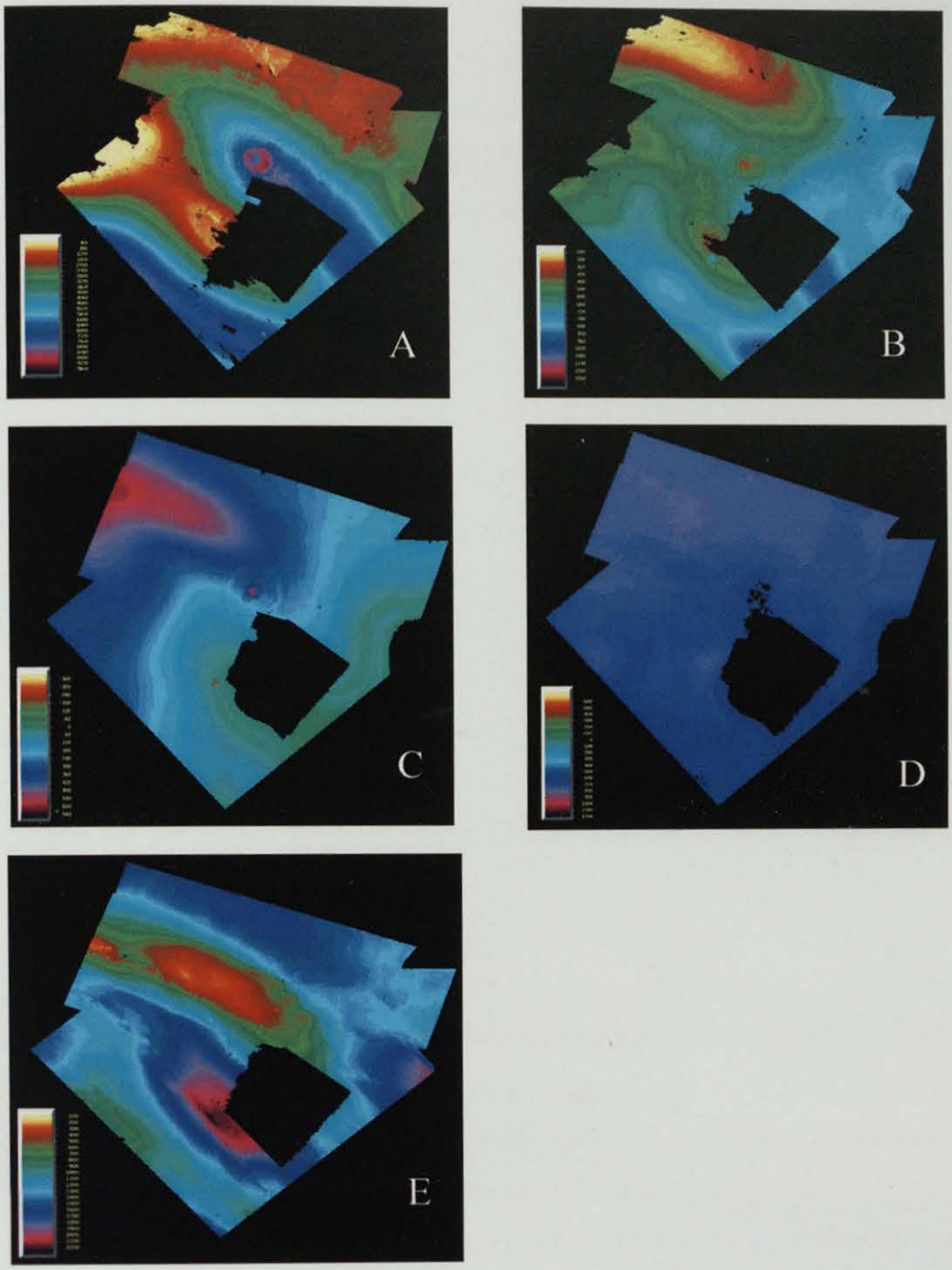

Figure 3.9: A series of isopachs through the post Rotliegendes stratigraphy. The Silverpit structure can be seen as the series of rings located to the NW of the missing data area on isopach A and B. The isopachs represent: A – Tertiary, B – Cretaceous Chalk, C – Jurassic, D – Triassic, E – Zechstein.

3.9 Discussion

This study sets out to examine the relationship that the Silverpit structure has with the surrounding stratigraphy. The nature of the lithologies seen in the study area is unremarkable, in comparison to the rest of the southern North Sea. This suggests that the Silverpit structure is unlikely to have formed as a result of unusual depositional events. Unusual depositional events would create several similar structures in other areas of the southern North Sea basin.

Understanding the timing of formation of the different elements of the structure has been a crucial part of establishing the age of the Silverpit structure. The identification of undisturbed horizons above the central deformed zone that have been faulted suggests that either the ring faults have formed after the main deformation stage or that the faults have been reactivated after the initial event. However, because the faults are not growth faults it is less likely that reactivated faults are the explanation and more likely that the ring faults are in fact later stage. This means that when we consider the age of the structure we are in fact considering the age of the central deformation and conical uplift formation.

Determining the exact age of the structure has proven to be extremely difficult. The data currently available significantly limits the methods that can be used to date the structure. The date suggested from the method used in this study can be considered to be a fair estimate of the age of the structure given the resolution of the data. The age range covers virtually the same time span as the age range acquired from the biostratigraphy method of Bidgood et al (in prep). It is likely that these age ranges developed will be the most accurate assessment of the age of the Silverpit structure unless it is drilled and cored.

By comparing the patterns of deformation seen in settings that are considered as candidates for the origin of the Silverpit structure with that seen in this study area, it is clear that not one of these settings can clearly be considered as the cause of formation of the Silverpit structure. Of the case studies examined the least likely

origin of the Silverpit structure is that of withdrawal of a salt diapir, as in the East Texas Basin example (Maione and Pickford 2001). There is virtually no deformation on the horizons beneath the structure suggesting that no diapir large enough to form the 20km diameter Silverpit structure has passed through the stratigraphy. The deformation at the top of the structure is completely different to the ring faults, central deformation region and conical uplift seen at the Silverpit structure and can therefore be considered redundant as the likely origin of the Silverpit structure.

The Eastern Mediterranean example, that sees the formation of multiple circular structures formed as a result of regional salt withdrawal, could be used to explain the origin of the ring faults seen at Silverpit. In particular the isopach maps created highlight the fact that salt movement has played a significant role in the trends seen in the stratigraphy throughout this area of the southern North Sea and that there was an episode of salt movement during the Tertiary. However, this does not explain the presence of the central zone of deformation or the conical uplift seen on the base Cretaceous horizon. Also, one might expect to see a number of different structures throughout the southern North Sea basin if this were the likely cause of formation of Silverpit. This is examined rigorously in Chapter 4.

The Mjølnir crater, an example of a buried meteorite impact crater shares the most significant features with the Silverpit structure. The two structures have a central zone of deformation, which includes a central peak (conical uplift). Deformation associated with structures also decreases as you move down through the stratigraphy beneath the structures. The major difference between the two structures is the fact that the curved to circular faulting seen at Mjølnir are within the rim of the crater created when the meteorite impacted the surface. However, the ring faults seen at Silverpit are outside of the central deformation zone, which if Silverpit were an impact crater would be the rim of the crater created by the impacting body.

The complex nature of the deformation seen at Silverpit suggests that the origin of the structure may not be a simple case of salt withdrawal or meteorite impact. None of the examples studied fit the patterns seen exactly. The Mjølnir meteorite impact

crater shares a number of the features of the internal zone of deformation but not the exterior ring faults. The Eastern Mediterranean examples fit the ring faults but not the internal zone of deformation. So what is the origin of the structure? This study focuses on only the seismic and well log data available which are unlikely to be enough to solve the question of origin of the structure. Future work needs to focus on answering three main questions:

1) Is the Silverpit structure unique and unlike the structures seen in the Eastern Mediterranean example, but the same as the Mjølnir crater example?
2) What is the exact timing of the salt movement seen in the southern North Sea basin and does this correspond to the timing of the movement of the ring faults at Silverpit?
3) Can other independent methods be used to look for the standard meteorite crater identification features such as shocked quartz or geochemical anomalies be identified?

3.10 Conclusions

1) The age of the central deformation zone and conical uplift of the Silverpit structure has been determined to be Ypresian, Early Eocene.
2) The ring faults at Silverpit formed after the central deformation and conical uplift.
3) Deformation associated with the structure decreases with increasing depth suggesting that the deformation occurred from the top down rather than the bottom up. No disturbance of the horizons beneath the structure exists.
4) Zechstein salt movement has played the dominant role in the deposition of the post Triassic sediment and has continued to move into the Tertiary, with a significant change in direction of movement of the salt at some stage between the Jurassic and late Tertiary.
5) Deformation of the central section of the Silverpit structure and the overlying stratigraphy is comparable with that seen in other meteorite impact craters,

but the ring faults are comparable with that seen in regional salt withdrawal settings.

ACKNOWLEDGEMENTS

We are pleased to thank NERC for PhD grant NER/S/A/2003/11233. CASE sponsorship and seismic interpretation facilities were provided by Production Geoscience Limited (Banchory) and P Allen. The local data sets around Silverpit were courtesy of S Stewart and BP Plc. Use of the Mega Merge Survey is thanks to PGS and J Underhill.

Chapter 4

4 The Silverpit Structure, North Sea UK: Seismic Evidence for An Unique Structure?

Zana Conway, Stuart Haszeldine & Malcolm Rider
School of Geosciences, University of Edinburgh, Edinburgh, EH9 3JW

4.1 Abstract

The origin of the 20km diameter circular Silverpit structure, UK southern North Sea basin, has been contested since its discovery in 2002. Although its shape and central uplift suggest a meteorite crater, no definitive evidence is available to confirm the origin of the structure. Without direct drilling of the structure, there is a lack of rock material to use for mineralogical and geochemical analyses to confirm the origin. Consequently other methods are being developed which, although not conclusive, may converge on an explanation for this structure. Rival hypotheses include salt withdrawal and mud diapirism. Salt withdrawal, or mud diapirism, would be anticipated to produce several analogous structures in the region. A 3D seismic reflection data set has been used in an attempt to test the uniqueness of the structure. Three regionally extensive surfaces were mapped and a series of criteria developed to search for similar structures throughout the 3500km^2 area. Silverpit is the only structure, which fulfils all of the criteria, and as such can now be considered as a unique structure in the southern North Sea basin. This makes a unique origin, such as meteorite impact, more probable.

4.2 Introduction

The origin of the Silverpit structure, 130km offshore of eastern England (Figure 4.1), has been contested since its discovery in 2002. Stewart and Allen (2002) suggested that the structure is a meteorite crater, based on its circular geometry and central uplift. However, meteorite craters are rare and particularly difficult to confirm in offshore locations (Becker et al., 2004). A clear demonstration is obviously important, because many types of circular structural features can exist in the subsurface (Stewart, 1999) and these usually have uniformitarian origins rather than being catastrophically caused. Because of this ambiguity, three further hypotheses have been developed to explain the origin of the circular structure. Underhill (2004) notes that the structure lies within a salt province, well known from hydrocarbon exploration and suggests that the structure is a salt withdrawal feature. Smith (2004) suggests that the central uplift feature derives from a mud diapir controlled by a basement pull apart-basin. Thomson (2004) suggests that the structure is one of many similar features in the region, originating by salt-induced tectonism. In this paper, we make the proposition that: if "normal uniformitarian processes" of salt withdrawal or basement structural features were important, then several similar crater features should exist in similar structural positions in the immediate region. If such features exist, then they could be detectable by using a much more aerially extensive suite of 3-D seismic reflection data. By contrast, if a wider ranging investigation demonstrates that the Silverpit structure is unique in the southern North Sea region, then a unique origin (such as an impact) is more probable – though still not proven. In this study we utilise data from an unusually extensive combination of 3-D seismic surveys. As an aid to impartial investigation, we have established a series of structural criteria, which can be applied to itemise the attributes of the different structural features, which occur in the southern North Sea region. Our expectation was that several circular structures should exist in the region, and that the distribution of these structures would discriminate between the possibilities proposed for their origin. Our conclusion is that similar large scale structural settings do exist in the region, but that the Silverpit structure is, unexpectedly, unique. Consequently, a meteorite impact origin is the most probable explanation.

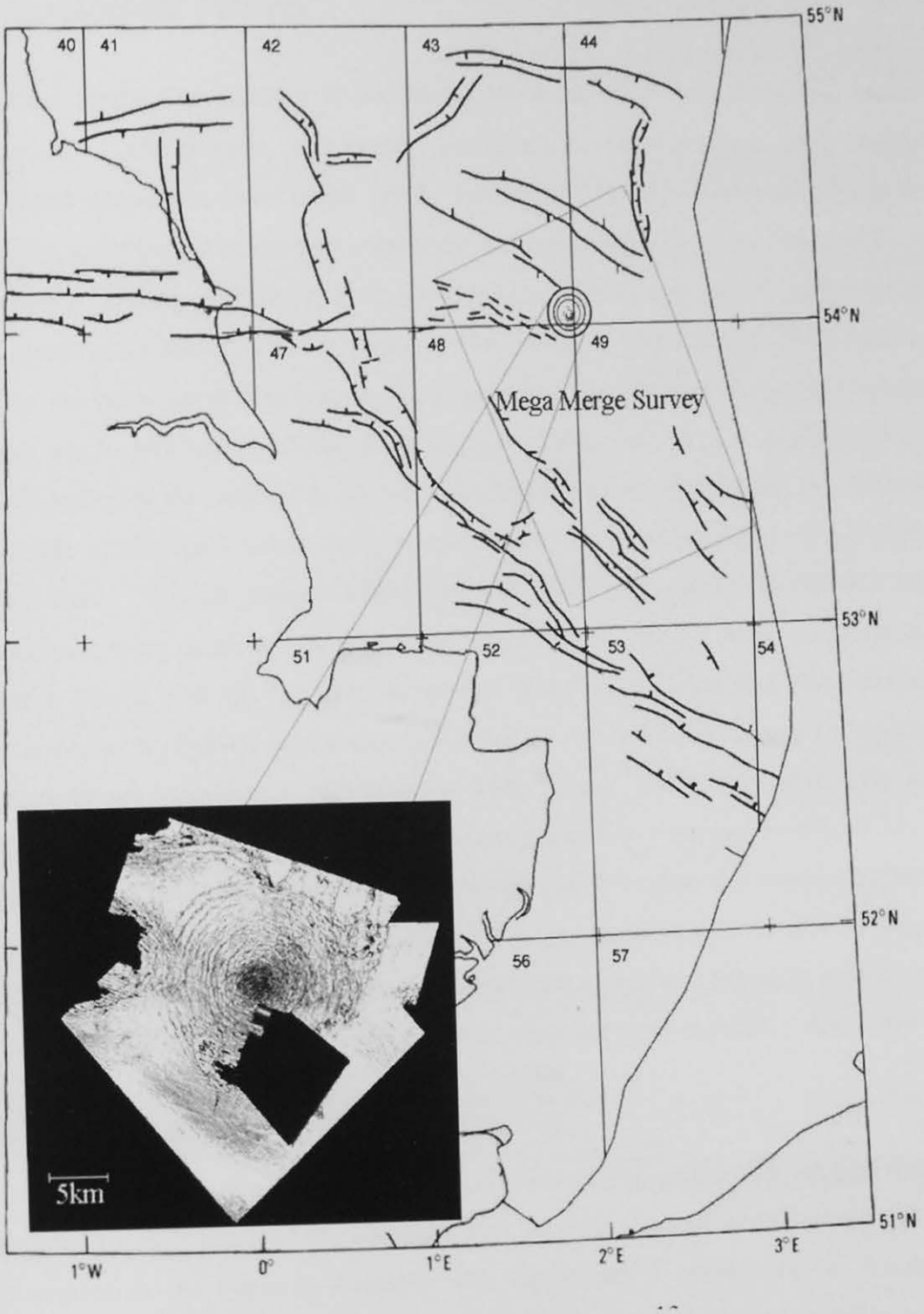

Figure 4.1: Extent of regional mega-merge seismic reflection survey, and (inset) location of Silverpit structure offshore of SE England.

4.3 Geological Setting

Southern North Sea geology is dominated by a series of post-Devonian clastic sediments. Carboniferous limestones, fluviodeltaic coal-measures, and redbed sandstone sequences, have been gently folded and faulted during the Variscan orogeny, and now act as the basement to the unconformably overlying succession of sediments. During the Early Permian, aeolian, fluvial and desert environment sediments accumulated. The late Permian saw five short lived marine transgressions across the basin producing a complex sequence of marine and evaporite deposits which are locally up to 1000m thick (Glennie 1998) and form a mobile, ductile discontinuity to the basement. Desert sedimentation continued during the Triassic although, in the late Triassic, fully marine conditions extended across the southern North Sea. Shallow marine mudstones and subsidiary paralic sandstones and limestones were deposited in the Lower and Middle Jurassic, before undergoing erosion at the end of the Jurassic period, followed by localised post-Jurassic inversion, with regional stratigraphic evidence of salt tectonics. Lower Cretaceous sediments are dominantly argillaceous, while Upper Cretaceous sediments are predominantly pelagic carbonates deposited in a chalk sea and can locally be up to 1000m thick. Early in the Paleocene there was regional uplift and regression, with commencement of major salt diapirism, followed by the deposition of up to 800m of mainly argillaceous marine sediments of the Palaeogene and Neogene within salt withdrawal synclines, adjacent to salt-cored and piercement anticlines (Cameron et al., 1992).

The southern North Sea basin is a well-documented salt province with salt movement recorded through much of the Mesozoic and Tertiary (Stewart and Coward, 1995). Movement in the Permian Zechstein salt has played a major role in structure development of the post-salt cover including the growth of salt pillows and diapirs as well as varying sinuosity salt withdrawal synclines (Glennie 1998).

4.4 The Silverpit Structure

The Silverpit structure is recorded in the Upper Cretaceous chalk of the southern North Sea and is overlain by undisturbed Upper Eocene sediments. The structure has been dated to be 49 – 53 million years old (Chapter 3). A 3 – 4km diameter centrally deformed region is surrounded by a remarkable series of concentric ring faults around the centre to a maximum diameter of 20km (Figure 4.1). A cone of uplifted material is also found affecting the base of the Chalk, located directly beneath the centrally deformed region. The present authors have determined that that ring faulting associated with the structure continues into the early Eocene, and that the structure is located near to, but not exactly on, the axis of a syncline induced by salt withdrawal.

4.5 Hypothesis and Method of approach

The centre of the Silverpit structure has not been drilled, so no direct rock evidence is available. As explained above, we seek to determine the uniqueness of the Silverpit structure in this region. Before examining our data, we briefly outline expectations derived from published work.

4.5.1 Salt Withdrawal

The southern North Sea is a well-known salt province; with salt-mobilisation structures formed across the entire survey 3500km^2 area. This can be compared to seismically surveyed salt provinces such as the Gulf of Mexico (Maione and Pickford, 2001), southern Dead Sea basin (Larsen et al., 2001) and the Eastern Mediterranean (Bertoni and Cartwright 2004). From this we can conclude that salt movement commonly produces multiple synclines of tens of kilometres in diameter, which are widespread across the province. Sometimes structures are present which are crudely circular in plan view. In the Eastern Mediterranean, salt dissolution has produced multiple circular dissolution features, similar in size to the Silverpit structure (2 – 5km in diameter), at the same stratigraphic horizon. As with the

Southern North Sea example, Eastern Mediterranean (Bertoni and Cartwright 2004) structures are formed in the stratigraphy above the withdrawing salt. The Eastern Mediterranean example is an excellent analogy for the Southern North Sea setting and as such we may expect to find a number of circular salt withdrawal structures in the study area.

4.5.2 Mudstone Diapirs

Smith (2004) suggests that the uplifted material in the centre of the Silverpit structure is present as a result of shale diapirism in the Liassic Group shales of the Jurassic. Talukder et al. (2003) comment on the mud diapirism and mud volcanoes in the Alboran Sea (Western Mediterranean), and highlight that a large number of these 2 - 3km diameter crater structures exist in the contracting Western Alborian Basin. It is clear from other areas prone to mudstone diapirism and volcanism, such as Trinidad (Deville et al., 2003) and offshore Brunei (Van Rensbergen and Morley, 2003) that it is normal for more than one mudstone diapir or volcano to be formed in these tectonic settings. Once again, we may expect to find evidence of one or more of these mudstone diapirs in the Silverpit regional study area. Importantly, there are no references to suggest that the Liassic shales has at any stage been mobile elsewhere in the southern North Sea.

4.5.3 Mud Volcanoes

Giant mud volcanoes have been imaged seismically by Davies and Stewart (2005). These produce circular craters about 2 -4 km diameter, and importantly, can also be underlain by a central uplift. Such craters occur in alignments along structural features and are overlain by sediment which has thinned. A difference with the Silverpit structure, is that the sediment overlying the crater feature is thickened.

4.6 The Seismic Dataset

The Southern North Sea Mega Merge Survey stretches from 10800E – 24400E latitude and 544000N – 533600N longitude. The Mega-merge survey has been compiled by Petroleum Geo-Services (PGS) by joining together and reprocessing a large number of different 3-D surveys, acquired by different companies between 1992 -99, at different times, and with different objectives (PGS, 2006). This has a variable line spacing, but no more than 30m in any one of the merged surveys. A tight grid of 3-D seismic lines from this survey, with a 100m separation, was interpreted to produce three maps of the key horizons, the Cretaceous top of the Chalk, the Permian top of the Zechstein and the Permian top of the Rotliegend. Composite well logs were used in our work to initially identify the different horizons to be interpreted, with thirty well ties over the survey. The surfaces are shown in Figures 4.2, 4.3 and 4.4. Criteria were then developed and itemised in an attempt to test the unique nature of the Silverpit structure.

4.7 The criteria

Two size-scales of categories were developed (Table 4.1), one to categorise the large-scale regional structures, the second to categorise the smaller localised features. The large-scale criteria are designed to identify similar structures by systematically examining scale, stratigraphy and structure from information which is common to all. The small-scale criteria then allow a much more refined examination of several structures to confirm if they are similar to the Silverpit structure. Once the three horizons had been mapped the criteria were applied. In the first instance the large scale features were examined. If all of the large-scale features applied to a particular syncline then the small-scale features were considered. All examination of features took place on the same Southern North Sea Mega Merge Survey.

Regional 3500km^2 Criteria	Local 400km^2 Criteria
Similar Stratigraphy	Level of Circularity
Similar Scale Synclines	Missing Top Cretaceous Reflector
Synclines in Similar Structural settings	Presence Ring Faults
	Uplift in the Base Cretaceous

Table 4.1: An outline of the regional and local criteria used to test the unique nature of the Silverpit structure.

4.8 Results

4.8.1 Large Scale Criteria

a) Similar scale synclines – five synclines on a 10km scale were identified at top Chalk level (Figure 4.4).

b) Synclines in similar structural settings – Three synclines were identified to have similar structural settings, resulting from salt withdrawal. They are of the same scale, orientation and are underlain by the same fault trend at Top Rotliegend level (Figure 4.2).

At the large scale, the Silverpit structure is not unique.

4.8.2 Small Scale Criteria

c) Level of circularity – Silverpit structure has a maximum ratio of orthogonal axes of 1.04. Other synclines exist 15km to the South West and 22km to the North East of Silverpit (Figure 4.4). However, these are elongate, with orthogonal axis maximum ratios of 2.7 and 2.2 respectively.

d) Missing top Cretaceous reflector – At Silverpit, the top Cretaceous is absent in the centre of the structure for a width of approximately 3km. This is not seen in any of the other synclines (Figure 4.5), where a complete top Cretaceous reflector can be seen through the syncline.

e) Ring faults – at Silverpit there are normal ring faults extending concentrically out to 10km away from the centre. Small normal fault features also occur on salt anticlines in this region (Thomson 2004), including the anticlines to the North East and South West of Silverpit (Figure 4.4). However, these normal faults are elongated and parallel to the anticline axis, and are not circular. No ring faults have been discovered in any of the other synclines.

f) Uplift in the Base Cretaceous – at Silverpit, there is a prominent uplift in the crater centre. We have examined data displayed, with minimal processing, as two-way-time on three different seismic surveys. The Trent and the Cavendish surveys are located adjacent to Silverpit structure, and the Southern North Sea Mega Merge Surveys are a re-processing of existing survey data; the central uplift is present on each of these independent surveys. The conical uplift can also be seen when a depth conversion is applied to the seismic data (Stewart and Allen 2002). No other synclines in this 3500 km^2 study area contain any suggestion of conical uplift on either two-way-time or on depth converted data.

At the small scale the Silverpit structure is unique.

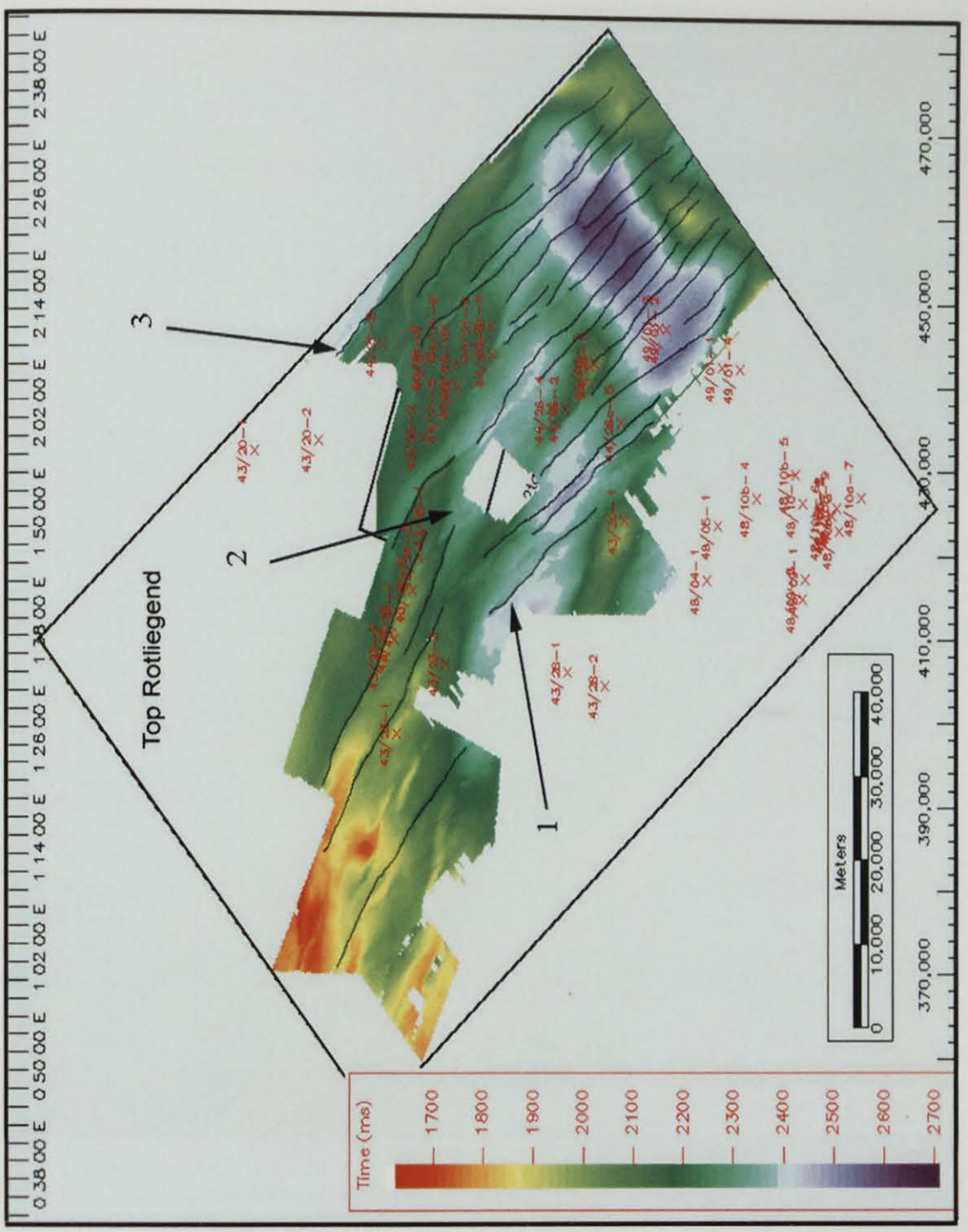

Figure 4.2: Interpreted regional surface of the Top Rotliegends, derived from new interpretation of mega-merge survey, tied to borehole stratigraphy. Locations 1, 2 (beneath the Silverpit structure), and 3 highlight points of similar structural settings.

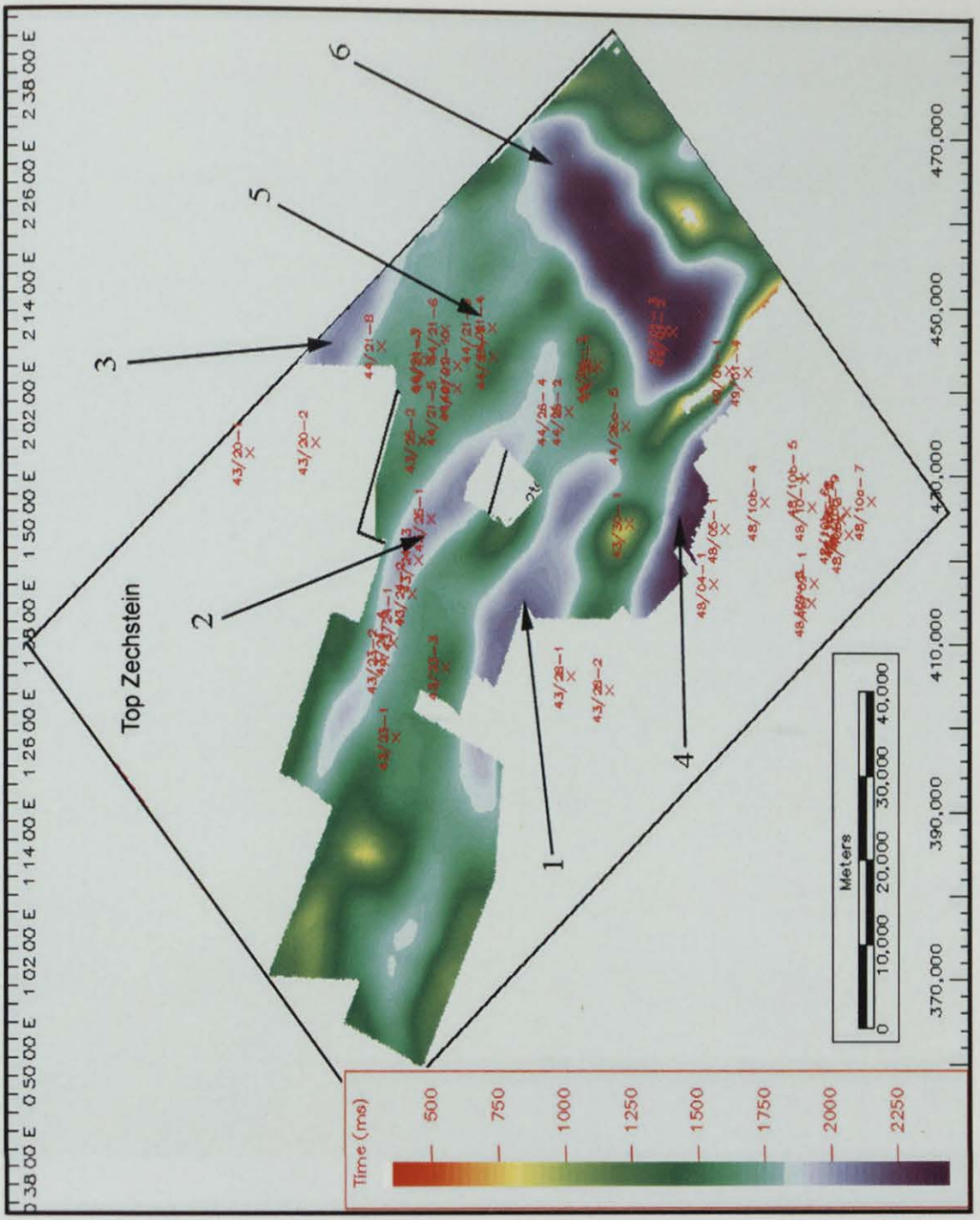

Figure 4.3: Interpreted regional surface of the Top Zechstein, derived from new interpretation of mega-merge survey, tied to borehole stratigraphy. Synclines 1, 2 (beneath the Silverpit structure), and 3 are similar in scale. Synclines 4, 5, and 6 are non-candidate synclines.

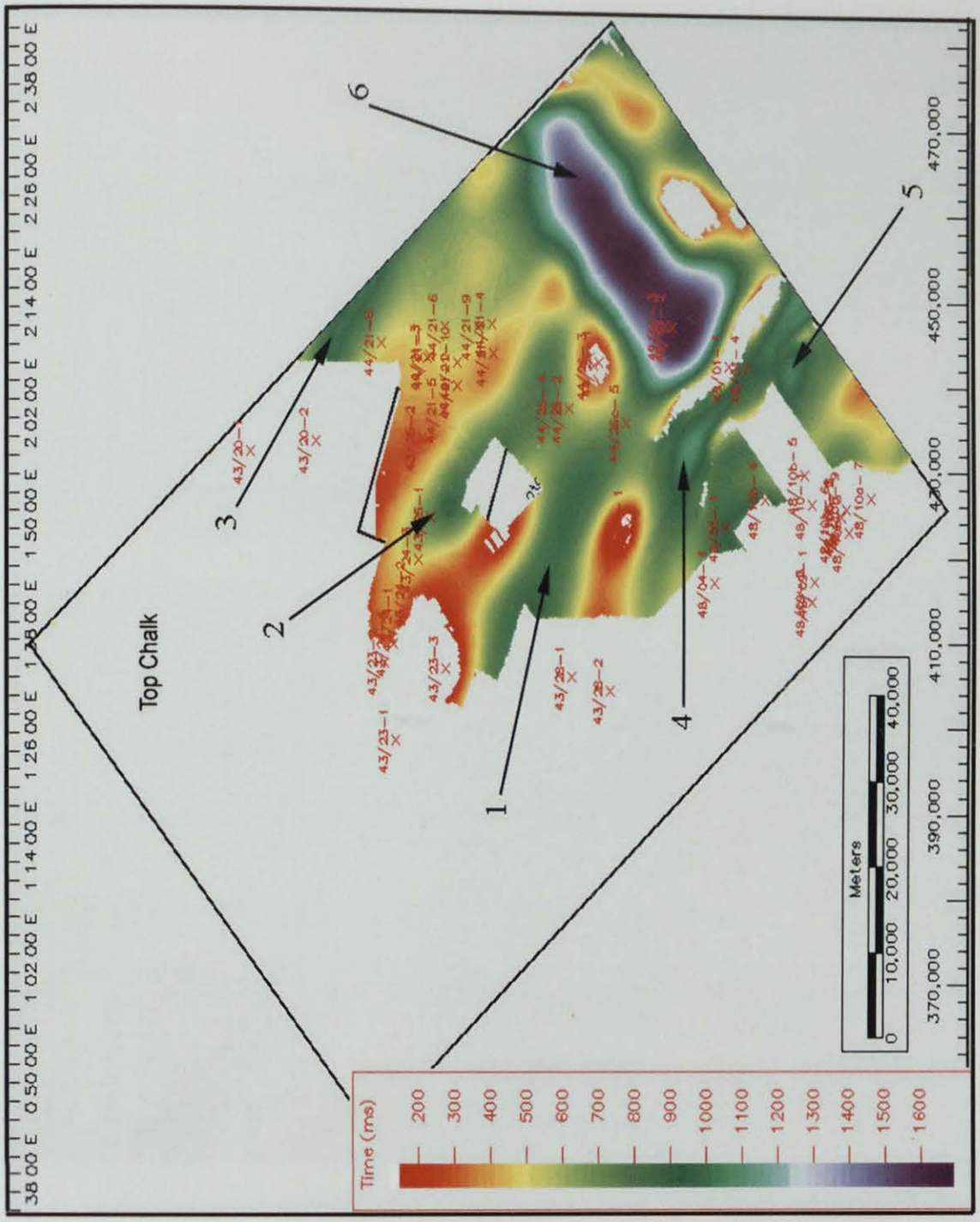

Figure 4.4: Interpreted regional surface of the Top Chalk, derived from new interpretation of mega-merge survey, tied to borehole stratigraphy. Synclines 1, 2 (the Silverpit structure syncline), and 3 are similar in scale. Synclines 4, 5, and 6 are non-candidate synclines.

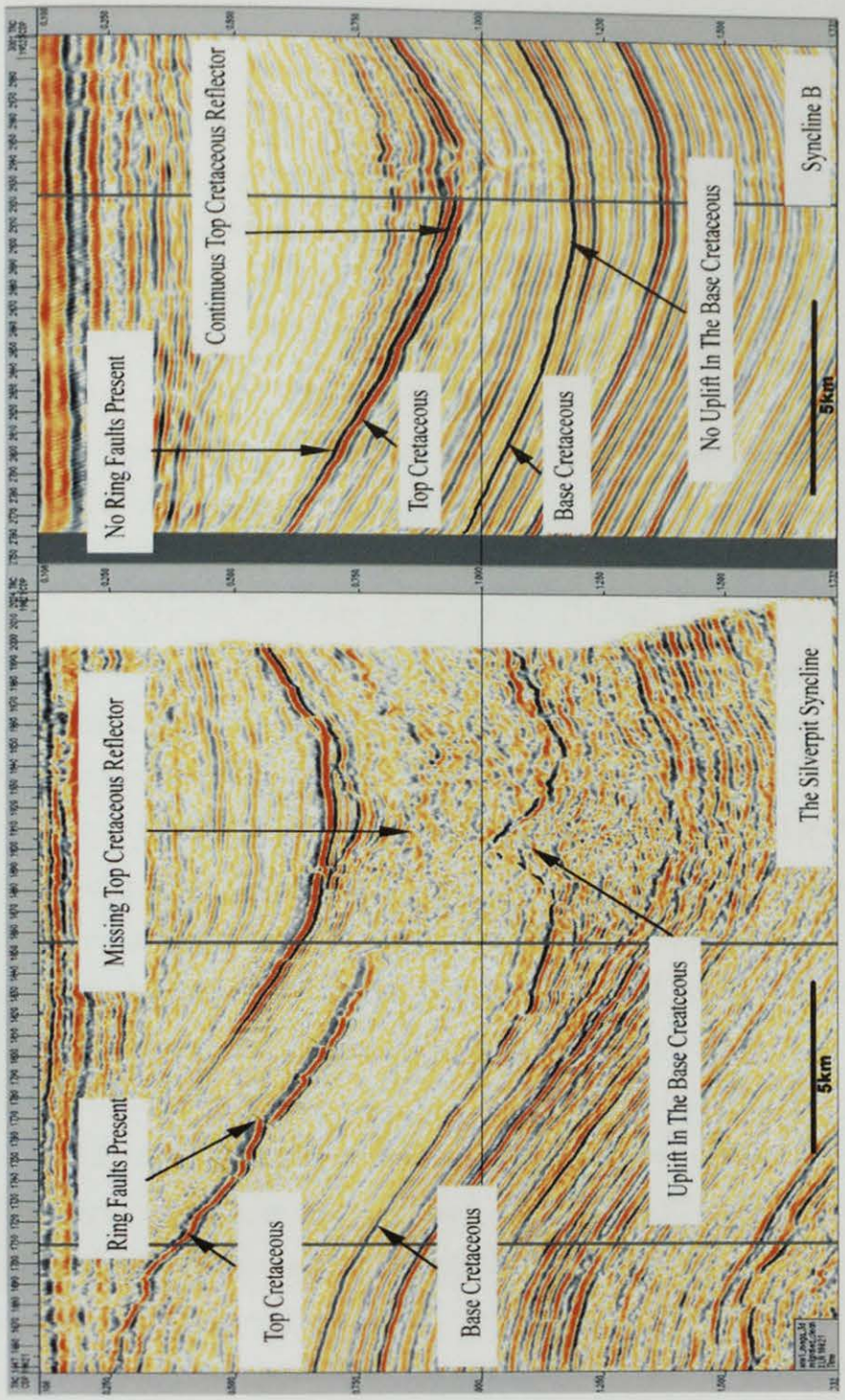

Figure 4.5: A comparison of the seismic sections through Syncline 2; the Silverpit structure and syncline 3; a salt withdrawal induced structure.

4.9 Discussion

Working with expectations from both the salt withdrawal (Underhill 2004) and the pull apart basin and mud diapirism (Smith 2004) theories for the origin of the Silverpit structure, we were surprised to find that the Silverpit structure was in fact unique in the southern North Sea, with no other structures fulfilling all of the criteria developed to test the model. In other locations worldwide, either of the salt withdrawal or mud diapirism processes result in a number of similar crater or syncline features being formed in the same structural settings, but in the southern North Sea this is not the case.

Thus the Silverpit structure is a unique structure in the Southern North Sea. Consequently, the Silverpit structure may have formed as a result of a unique event, for example, as a result of a meteorite impact. If we compare the Silverpit structure to other meteorite impact craters we do see many similarities. A good example of this is the Mjølnir Crater, Barents Sea. This complex meteorite impact crater is 40km in diameter with a central uplift and a series of ring faults concentric around the centre of the structure. It is a unique structure in the region and has been confirmed as a meteorite impact crater with the identification of shocked quartz and an iridium anomaly from core taken in the centre of the structure (Tsikalas et al., 1998).

If the Silverpit structure is indeed a meteorite impact crater, then there is still the question of why the structure is close to the axis of a salt induced syncline. It may be pure chance. Alternatively, could it be that the force produced as a result of a meteorite impact actually focussed the incipient salt movement in this part of the southern North Sea? More work is currently being carried out by the present authors to determine the exact timing of salt movement in the area, in attempt to resolve this question.

4.10 Conclusions

1) We have examined a 3500km^2 area of the southern North Sea using modern industry quality 3-D seismic reflection data. We expected to find evidence that salt withdrawal or mudstone diapirism was common across the region and had produced numerous circular structures, similar to the Silverpit structure.

2) Four synclines were identified similar in size, structural, and stratigraphic setting to the syncline containing the Silverpit structure. Of these, two showed normal faults around salt-cored anticlines, but none showed normal faults associated with the syncline axis, and none showed a circular structure (ratio of long and short axes <1.2). The top Cretaceous reflector is present and continuous in three similar synclines, but absent at the Silverpit structure. Central conical uplift is visualised at Silverpit on two-way-time data, and on depth-converted data, but is not present in any other structures.

3) Comparison to published examples of salt withdrawal or mud diapirism shows that multiple structures occur in such regions, unlike Silverpit. Comparison to the Mjølnir impact structure shows a unique structure, with a central uplift – similar to Silverpit.

4) The Silverpit structure appears to be unique in the region and so was not formed from basin-wide processes. A unique origin, from meteor impact is a more plausible explanation than salt or mud tectonism.

Acknowledgements

We are pleased to thank NERC for PhD grant NER/S/A/2003/11233. CASE sponsorship and seismic interpretation facilities were provided by P Allen and Production Geoscience Limited (Banchory). The local data sets around Silverpit were courtesy of S Stewart and BP Plc. Use of the Mega Merge Survey is thanks to PGS and J Underhill.

Chapter 5

5 Regional Salt Mobility in the Southern North Sea and its Role in the Formation of the Silverpit Structure.

Zana Conway and John Underhill

School of Geosciences, University of Edinburgh, Edinburgh, EH9 3JW

5.1 Abstract

Controversy has surrounded the genesis of the spectacularly imaged Silverpit structure in the UK southern North Sea. The prevailing view has been that the feature, which is best seen at the top of the Upper Cretaceous Chalk Group, was formed by meteorite impact. However, detailed analysis of the deeper section suggested that the mobility and withdrawal of Upper Permian Zechstein Group evaporites at depth was a plausible alternative. Results of an interpretation of a large, regional 3-D seismic volume has provided the means by which to evaluate the role of halokinesis in controlling the structural and stratigraphic evolution of the greater Silverpit area and to test the competing theories for the genesis of the "Crater". It can be demonstrated that major salt mobility affected the Silverpit area during the Tertiary with the formation of major salt walls, diapirs and pillows and intervening thinning and local grounding of Late Permian and Triassic sediments on Lower Permian sediments belonging to the Rotliegend Group. It is suggested that the episode of Tertiary salt mobility has played a role in the formation of the Silverpit structure.

5.2 Introduction

Since its recognition in 2002, controversy has surrounded the genesis of the "Silverpit Crater", a spectacular 20-km-diameter circular structure imaged through the interpretation of 3-D seismic data in the southern North Sea (Figure 5.1). Its formation was initially proposed to have been through the impact of a meteorite (Stewart & Allen 2002). Subsequent publications questioned that origin and counter-proposed that it was created by salt withdrawal at depth (Underhill 2004; Thomson 2004, Thomson et al. 2005) or the development of a pull-apart basin beneath (Smith 2004). Despite the critical assessment of the original interpretation, the view that the feature was produced by bolide impact was supported in a subsequent publication by the original proponents of the extraterrestrial genesis (Stewart & Allen, 2005).

In this paper, we investigate the role that salt mobility (halokinesis) played in the formation of tectonic structures that characterise the greater Silverpit area in general. Thorough investigation and interpretation of a large, regional 3-D seismic volume described herein provides a means by which to assess the role that salt movement had in the formation of the Silverpit structure and importantly, the results allow us to examine the genesis of the crater itself in the context of salt mobility in the southern North Sea.

5.3 Database

The structural interpretation described herein has been undertaken using a large merged 3-D seismic volume covering c.3500 km^2 released to us by PGS and provided by Shell (Figure 5.2). The interpretation has also been supplemented by another 3-D volume covering c.250 km^2 acquired and provided by BG Group that is strategically situated to the immediate north of the Silverpit structure. Together the seismic volumes extend over four southern North Sea Quadrants, encompass all or part of thirty United Kingdom Continental Shelf (UKCS) Blocks and extend over eleven producing gasfields and named discoveries (Boulton, Caister, Garrow, Ketch, Kilmar, Marjan, Murdoch, Schooner, Topaz, Trent and Watt). The stratigraphy and

seismic interpretation is excellently constrained by ties to seventy two exploration wells, all of which lie within the bounds of the 3-D volumes used.

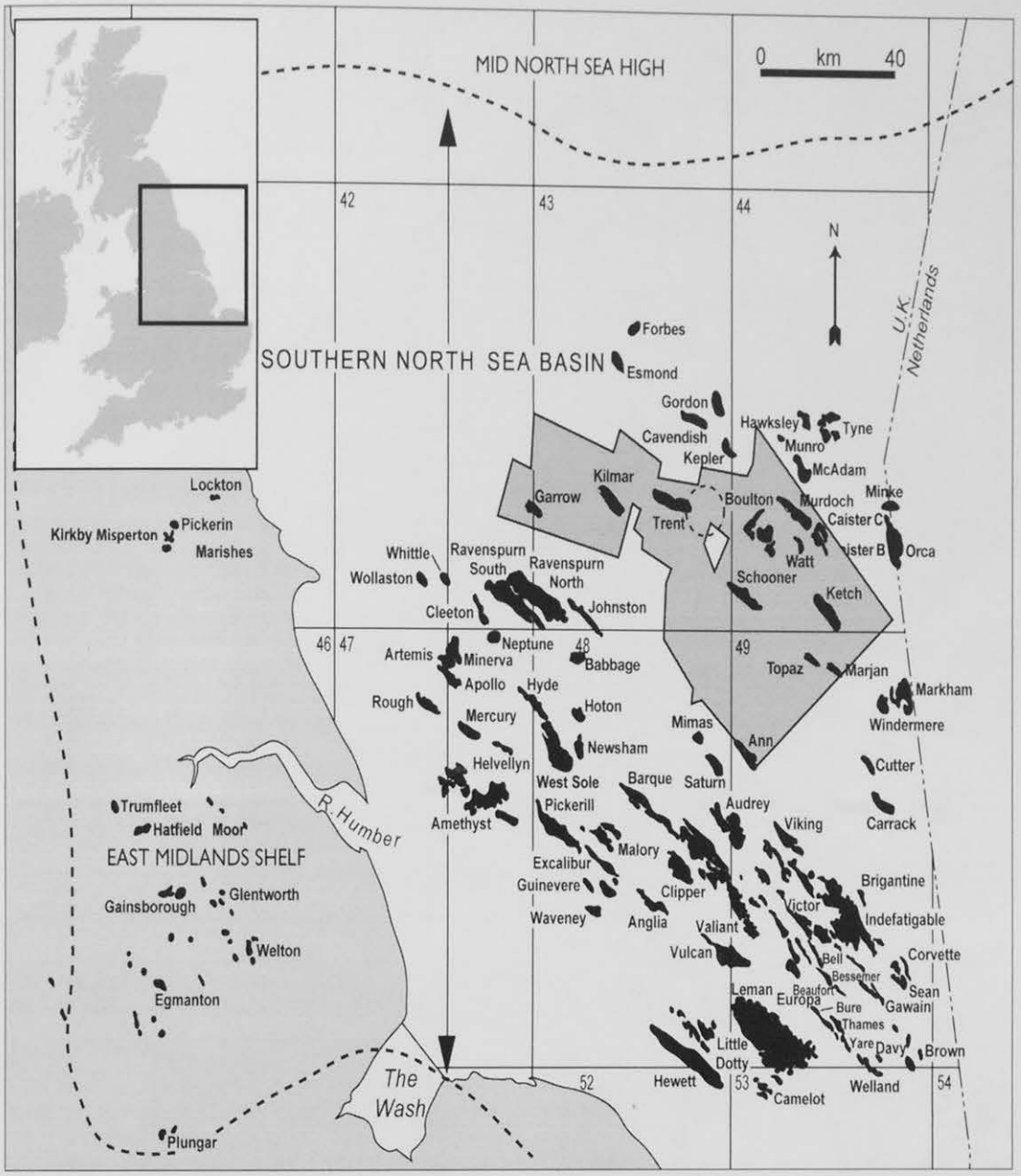

Figure 5.1: Location map of the extent study area constrained by the seismic data available shaded in grey. The Silverpit structure is outlined by the dashed circle

Figure 5.2: Extent of the combined Southern North Sea Mega Merge and Cavendish Surveys. The location of the seismic lines and transect analysed and the location of the Silverpit structure. The location of the seismic line discussed by Underhill (2004) is also highlighted.

5.4 Stratigraphy and Basin Evolution

A summary of the stratigraphy can be found in Figure 5.3. Since the primary targets for gas exploration in the Silverpit area lie in the Carboniferous (Stephanian, Westphalian and Namurian clastic reservoirs), there is a very good understanding of the stratigraphy to depths of 4km in the basin. These lie below the Variscan Unconformity and are sealed by mudstones ascribed to the Lower Permian (Rotliegend) Silverpit Formation. As in other parts of the basin, the Rotliegend is overlain by carbonates and evaporites belonging to the Upper Permian, Zechstein Group. The latter are highly variable in thickness largely as a result of evaporate mobility and they variously form diapirs, pillows and salt walls. Intervening areas are characterised by salt withdrawal, which in extreme cases leads to the overlying Triassic Bacton Group being grounded and welded directly on top of the Silverpit Formation. The presence of highly mobile evaporites in the southern North Sea has led to the effective decoupling of the sub-salt structures from those that characterise the supra-salt overburden with faults affecting the Rotliegend and Carboniferous section not demonstrable in the Triassic and younger units. The supra-salt section, consisting of Triassic-Recent sediments, is highly folded where salt mobility has occurred with the axis of anticlines and synclines being coincident with the zones of diapirism and withdrawal respectively.

The Triassic succession comprises continental red beds, the uppermost parts of which comprise interbedded shales and evaporites. The overlying Jurassic succession is truncated by a regional unconformity, the late Cimmerian Unconformity, which locally cuts down into the Triassic. Where present, the Jurassic is restricted to largely consist of shallow marine and fluvio-deltaic sediments ascribed to the Lias and West Sole Groups. The Cretaceous succession primarily consists of carbonates belonging to the Chalk Group. A disconformity marks the Mesozoic-Cenozoic boundary with the absence of rocks of Maastrichtian and Lower Danian age. Sedimentation was renewed in the Late Palaeocene with the deposition of clastic sediments. A thin Quaternary succession lies unconformably above folded Tertiary strata and record the glaciogenic history of the basin.

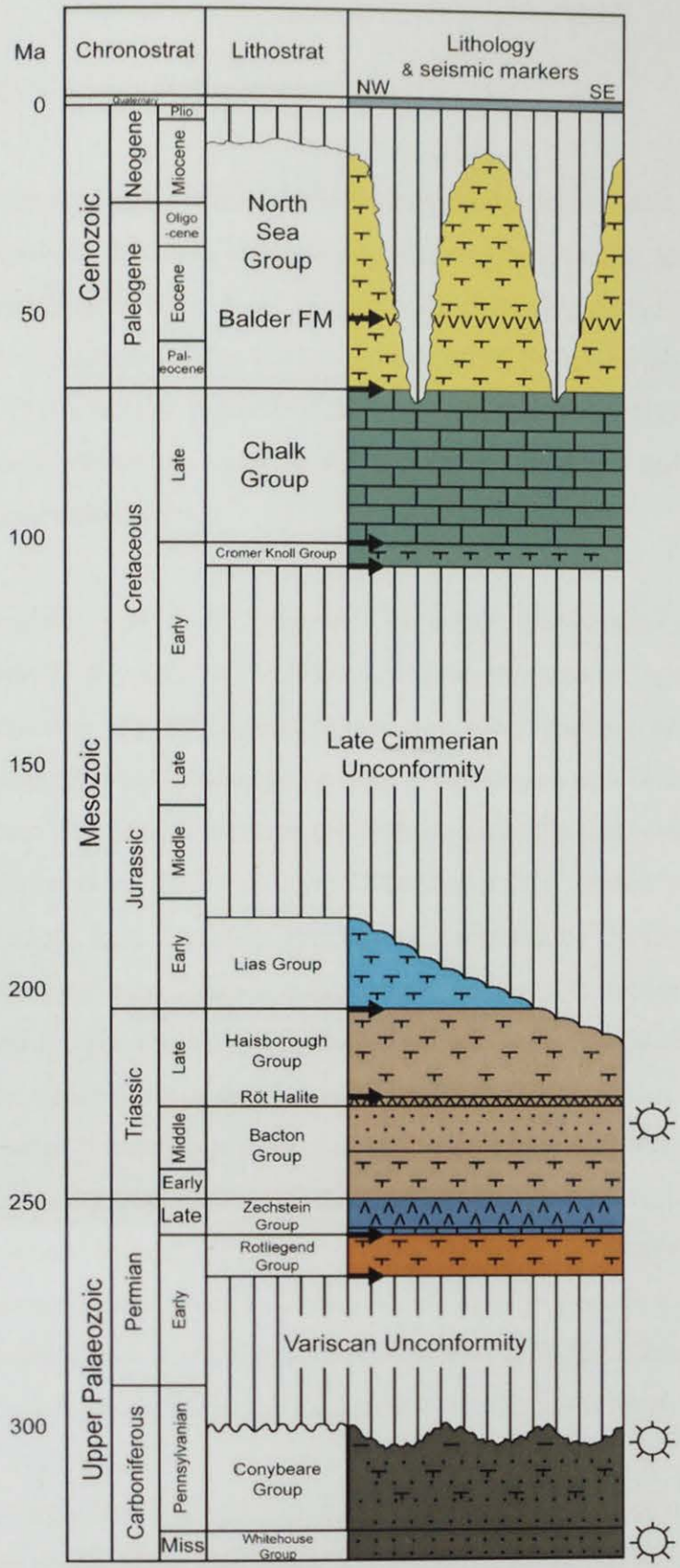

Figure 5.3: A summary of the greater Silverpit area stratigraphy.

5.5 Seismic Interpretation

5.5.1 Seismic Sections

Four strategic seismic sections have been selected from the 3-D seismic volume to highlight the main stratigraphic and structural trends found in the greater Silverpit area (Figure 5.2). A-A' (Figure 5.4), B-B' (Figure 5.5) and C-C' (Figure 5.6) are cross sections of the study area that trend SSE – NNW. The section D-D' (Figure 5.7) is a seismic traverse of the study area that trends NW – SE along the strike of the basin. All of the sections and the traverse intersect and have been calibrated with exploration wells.

Seismic line A-A' (Figure 5.4) is a representation of the structure and the stratigraphy seen in the NW part of the study area. Significant faulting can be seen affecting the Rotliegend Group and older section. Above, the Zechstein Group evaporites are extremely variable in thickness and a series of pillows and sink areas have developed. Within the pillow structures the evaporites reach a maximum thickness of 0.75 ms, across this section the minimum thickness of evaporites is 0.25ms. Post Zechstein structure is dominated by the presence of two anticlines and two synclines. Triassic sediments sit conformably on top of the Zechstein evaporites and remain a relatively constant thickness across the section. Bright reflectors within the upper parts of the Triassic section represent various evaporitic units within this group. A relatively thick succession of Jurassic sediments lie conformably on the Triassic group. Erosion of the Jurassic sediments is seen on the crest of the anticlines formed by the presence of the Zechstein evaporite domes. Whilst a major unconformity exists in crestal locations with present day sediments truncating the Jurassic sediments, Cretaceous sediments infill the centre of the synclinal structures directly above where the Zechstein evaporite has formed sink areas.

Seismic line B-B' (Figure 5.5) represents the structure and stratigraphy seen within the centre of the study area and includes the ring faults associated with the Silverpit structure. Once again the Rotliegend Group and older section has been affected by

major faulting. Above this, the Zechstein Group evaporites continue to be extremely variable in thickness with two evaporite pillows and sinks present. The maximum thickness of the evaporite section is 0.6ms, with a minimum thickness of 0.1ms. Post Zechstein structure is dominated by the presence of two anticlines and two synclines. The Triassic sediments sit conformably above the Zechstein Group evaporites and remain a constant thickness across the section. As with seismic line A-A', bright seismic reflectors in the Triassic are attributed to the presence of evaporite horizons within the group. The Jurassic sediments are much thinner in this section than in seismic line A-A' and also exhibit a clear thickness variation with the group ranging from 0.1 – 0.25ms thick. These thickness variations do not correlate with any of the present day anticline or syncline structures, but instead show erosional truncation towards the SW with formation of a regional unconformity (the Late Cimmerian event). Above the erosion surface, Upper Cretaceous sediment demonstrate constant thickness across the section. Faulting at the top of the Cretaceous is seen in the syncline to the NW of the section. This is associated with the Silverpit structure. Onlapping Tertiary sediments occur in the centre of the synclines with erosion of some of the Tertiary sediments seen on the crest of the anticlines.

Seismic line C-C' (Figure 5.6) represents the most SE section of the three dip line cross-sections used herein. Significant faulting is seen to affect the Rotliegend Group. The SW end of the section is dominated by the presence of a Zechstein Group evaporite diapir reaching a maximum thickness of 1.5ms. The Zechstein evaporites significantly reduce in thickness across the rest of the section with a maximum thickness of 0.25ms. The post Zechstein structure is dominated by the presence of the diapir to the SE and a large syncline across the rest of the section. Triassic sediments sit conformably above the Zechstein evaporites. However, due to erosion, a large amount of the Triassic sequence is not present and no Jurassic can be seen on this section. The Cretaceous sediments, which sit unconformably on top of the Triassic sediments, vary little in thickness apart from at the edge of the diapir. An extremely thick Tertiary succession fills the rest of the syncline. A large growth wedge can be seen towards the top of the Tertiary sediments, which is capped by a thin layer of Tertiary sediments of a constant thickness.

Seismic Transect D-D' (Figure 5.7) is a NW – SE trending strike. Folding in the Rotliegend Group is prominent with few faults seen. The Zechstein Group evaporites continue to vary significantly in thickness with two domes present in the southern end of the study area and two sinks one in the north and one in the south. The Zechstein overburden can be seen to be dominated by one large syncline and anticline in the furthest south of the transect. Smaller scale folding can be seen in the northern end of the transect. The Triassic sediments thin towards the south west end of the study area. The Jurassic sediments also thin towards the south west of the study area and are in fact no longer present two thirds of the way along the transect from NE to SW. The Cretaceous sediments remain relatively constant in thickness across the study area. They sit unconformably above Triassic sediments in the south west end of the transect. The edge of the Silverpit structure can be seen in the centre of the transect. Tertiary sediments are seen infilling the centre of the two main synclines. In both cases growth packages marked by pronounced onlap are well developed in the middle of the Tertiary sequence.

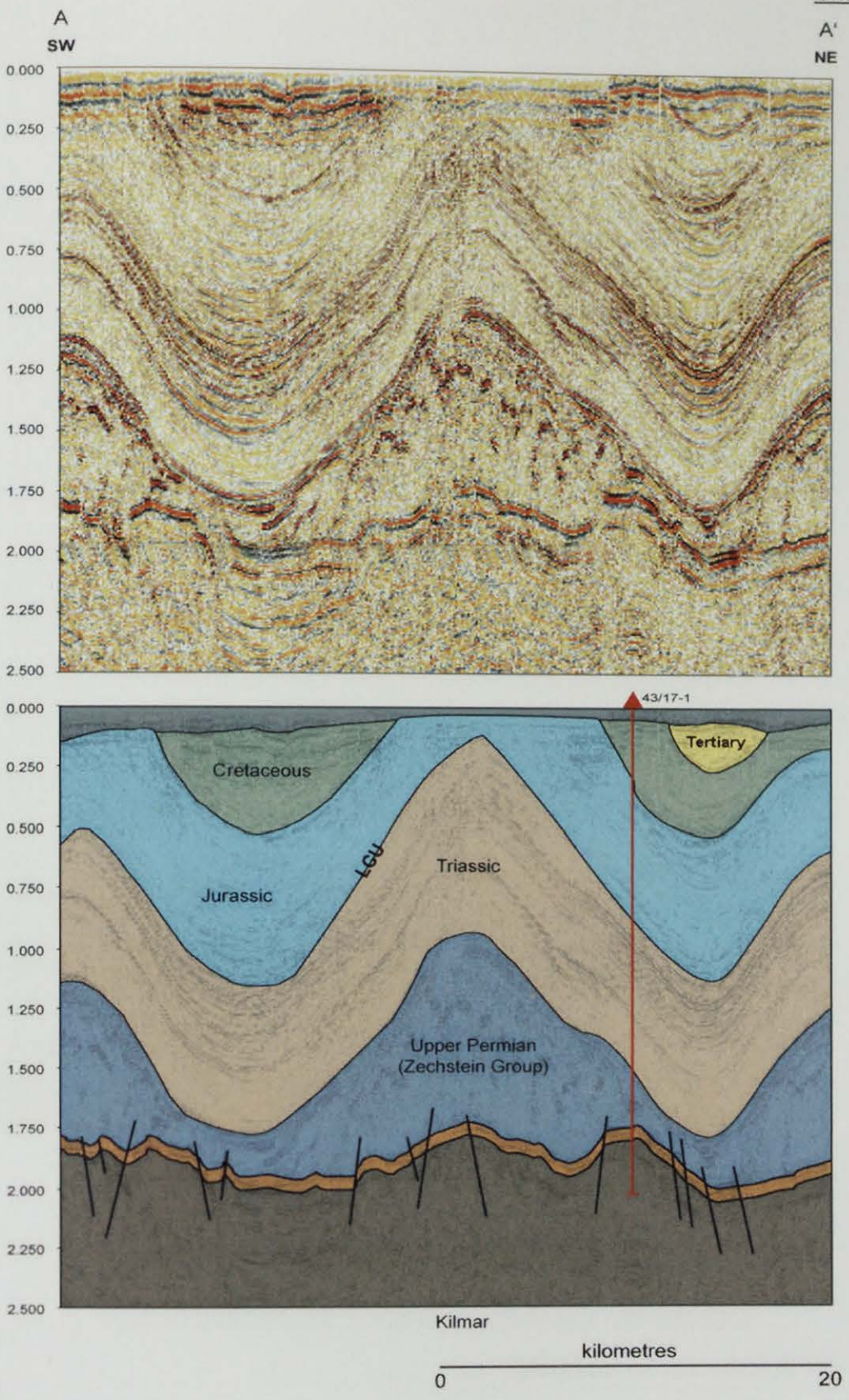

Figure 5.4: Seismic line A – A' representing the structure and stratigraphy in the NW of the study area.

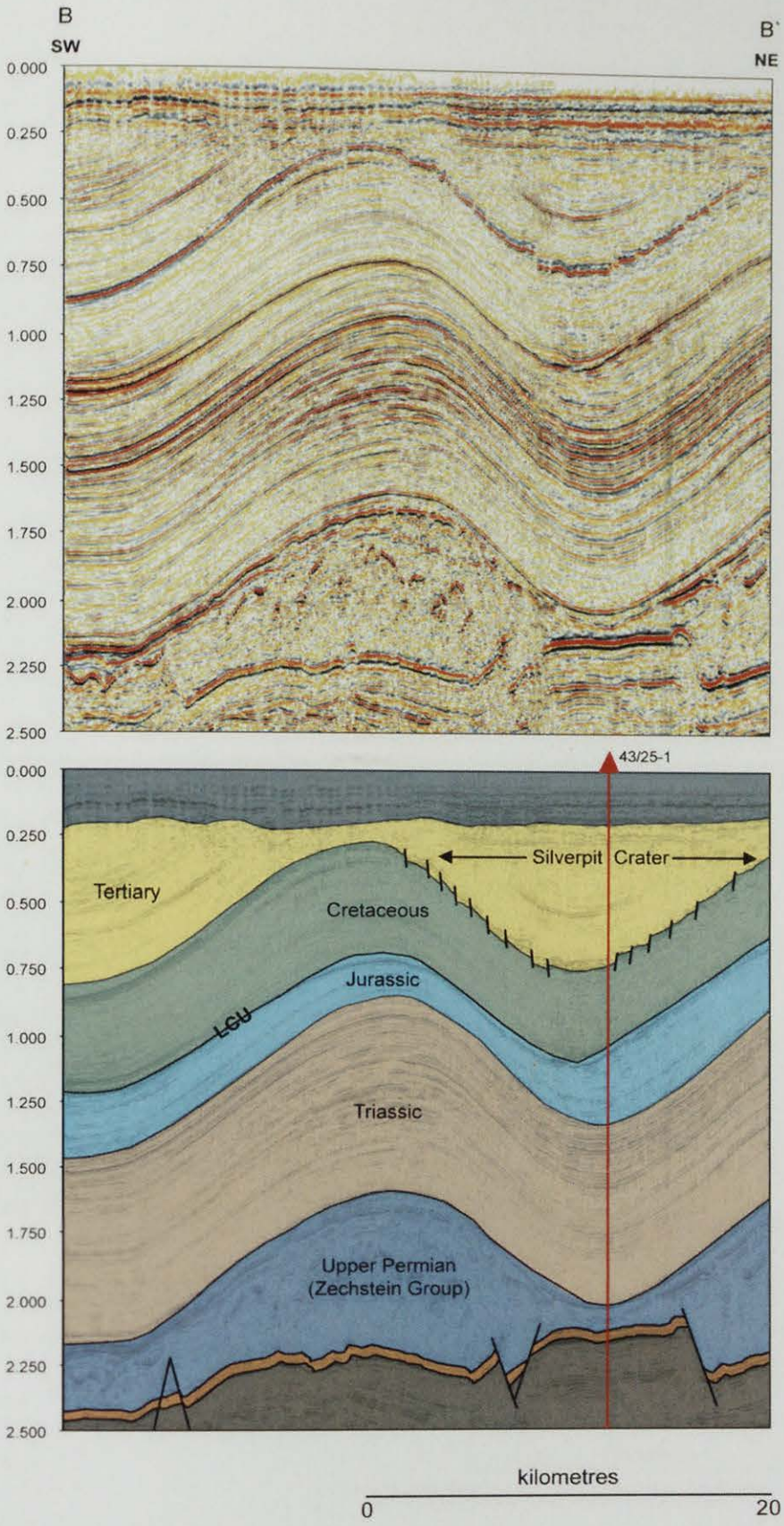

Figure 5.5: Seismic section B – B' which includes the edge of the Silverpit structure, demonstrating the presence of ring faults.

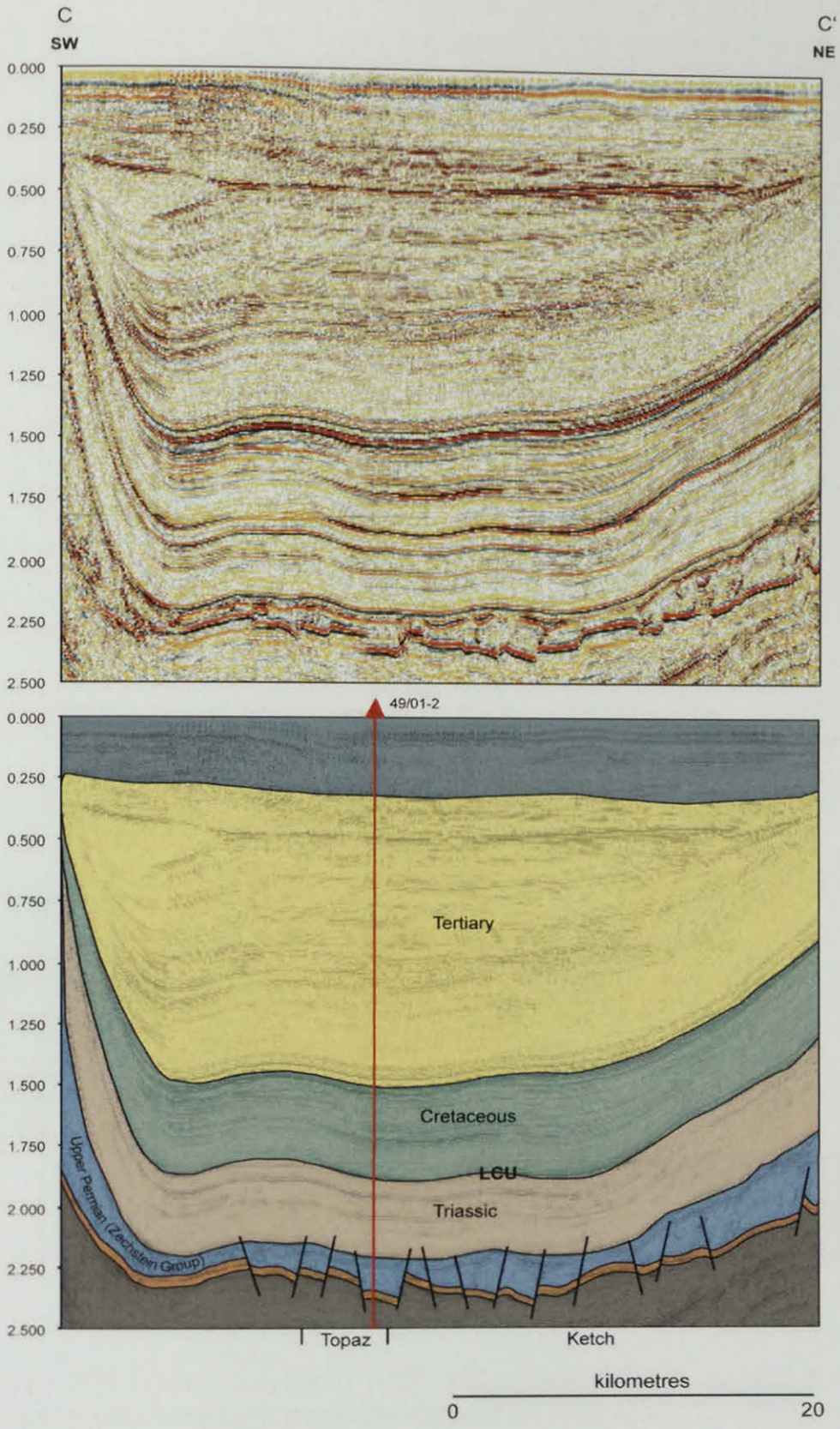

Figure 5.6: Seismic section C – C' representing the structure and stratigraphy of the SE of the study area.

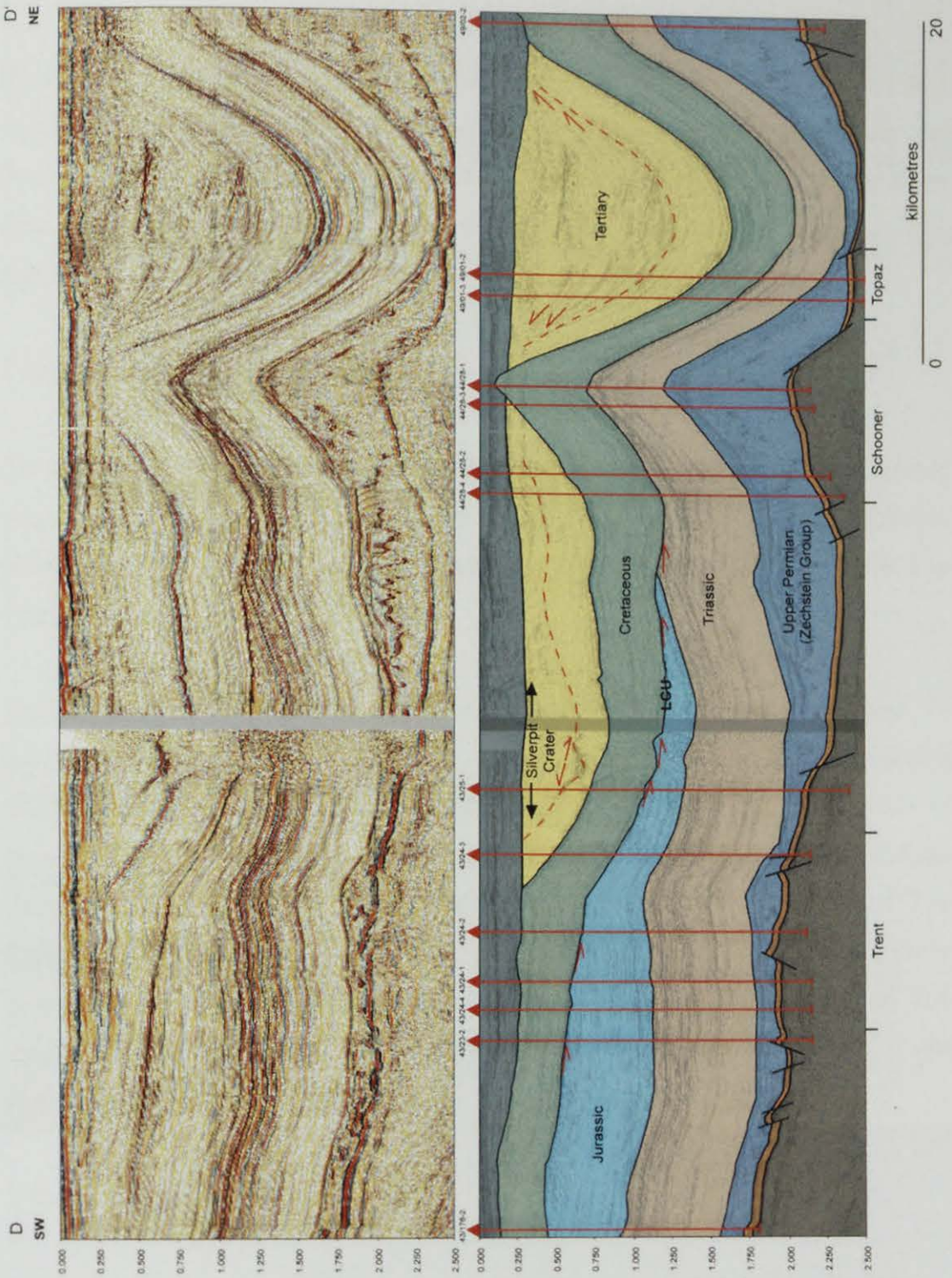

Figure 5.7: Seismic transect D – D' a representative cross section through the structure and stratigraphy seen in the whole of the study area.

5.5.2 1.00s Time Slice

Figure 5.8, is a seismic time slice taken at 1.00s. It clearly demonstrates that significant deformation has taken place in the greater Silverpit area with the juxtaposition of older Permian units and much younger Tertiary units at the same time (depth). The regional fold structures can also be seen on this time slice. The region is dominated by a series of large-scale synclines and anticlines.

5.5.3 Seismic Structure Maps

Six key horizons have been interpreted and maps of these surfaces have been created (Figure 5.9). The horizons are as follows: the Top Rotliegend Group, Top Zechstein Group, Near Top Triassic, Base Cretaceous (Mid Cimmerian unconformity) and Top Cretaceous Chalk Group.

The Top Rotliegend map indicates that two major trends of faulting can be seen. In the SE of the study a NW-SE trend is prominent. In the NW of the study area a WNW-ESE trend is prominent. The Top Zechstein map highlights the location of present day evaporite diapirs, walls, dome and sinks. The near Top Triassic, Base Cretaceous and Top Chalk maps exhibit the same structural trends as the Top Zechstein Map. The Near Top Triassic map indicates that the top of the Triassic group is not present in the SE of the study area. The Base Cretaceous and Top Cretaceous maps indicate that the Cretaceous chalk is not present in the NW of the study area.

5.5.4 Isochron Maps

The isochron mps (Figure 5.10) were created to highlight any thickness variations that may be present through the different units. Three isochron maps were created covering major time periods, the Upper Permian Zechstein, Jurassic and Cretaceous. The Zechstein isochron map exhibits significant thickness variations. The map looks very similar to the Top Zechstein structure map. As would be expected with the

presence of diapirs, domes, walls and sinks. The Triassic isochron map, which is not presented showed little to no thickness variation. The Jurassic isochron map highlights a significant thinning of the sediments towards the SE of the study area. From the seismic sections discussed earlier it is known that there is in fact no Jurassic sediment present in the far SE of the study area. The Cretaceous isochron map highlights a relatively uniform thickness of Cretaceous sediment across the study area.

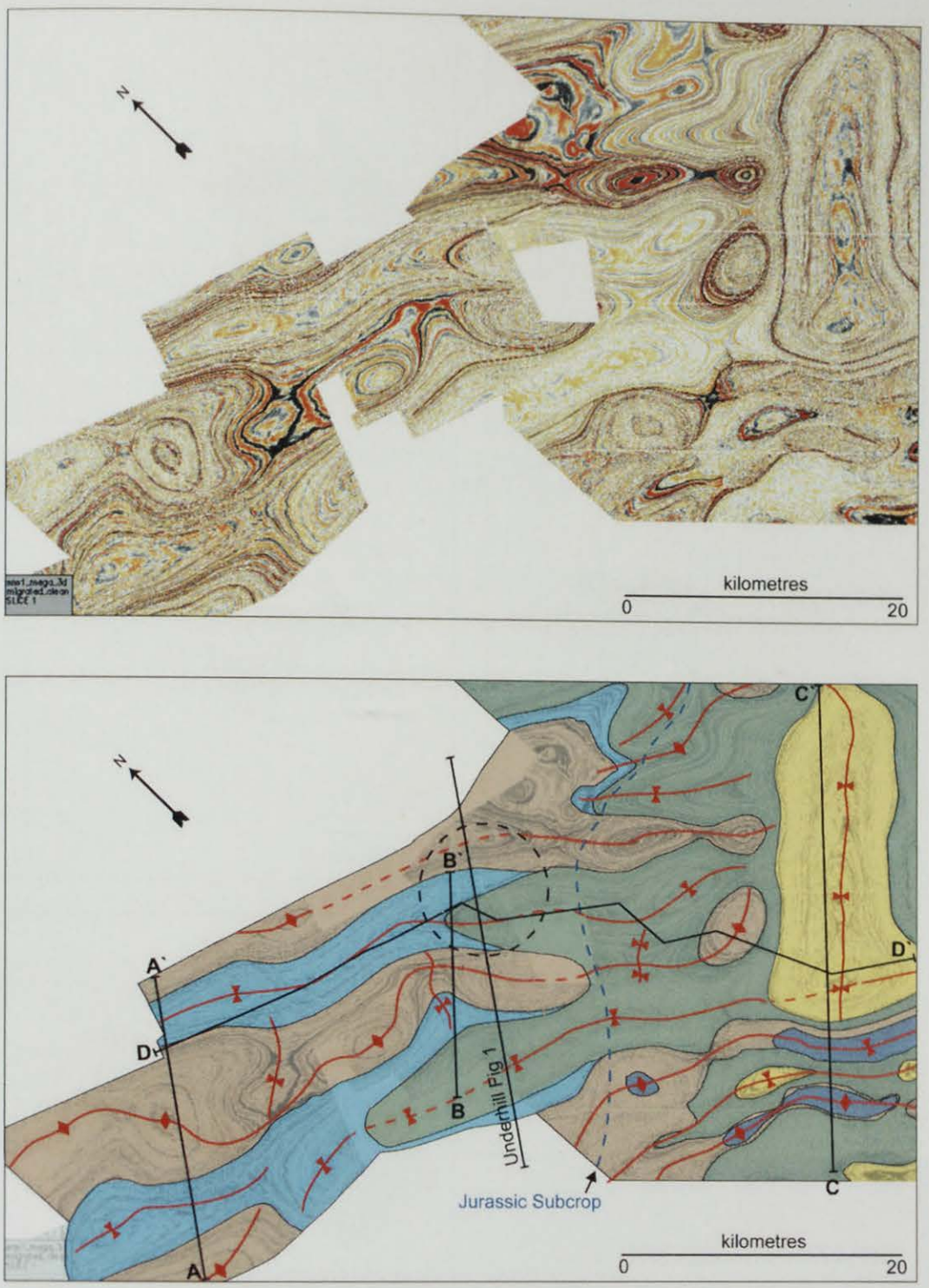

Figure 5.8: A 1.00s time slice highlighting the regional structural trends seen in the study area, dominated by a series of large-scale folds. Note the juxtaposition of both Zechstein group and Tertiary stratigraphy at the same depth.

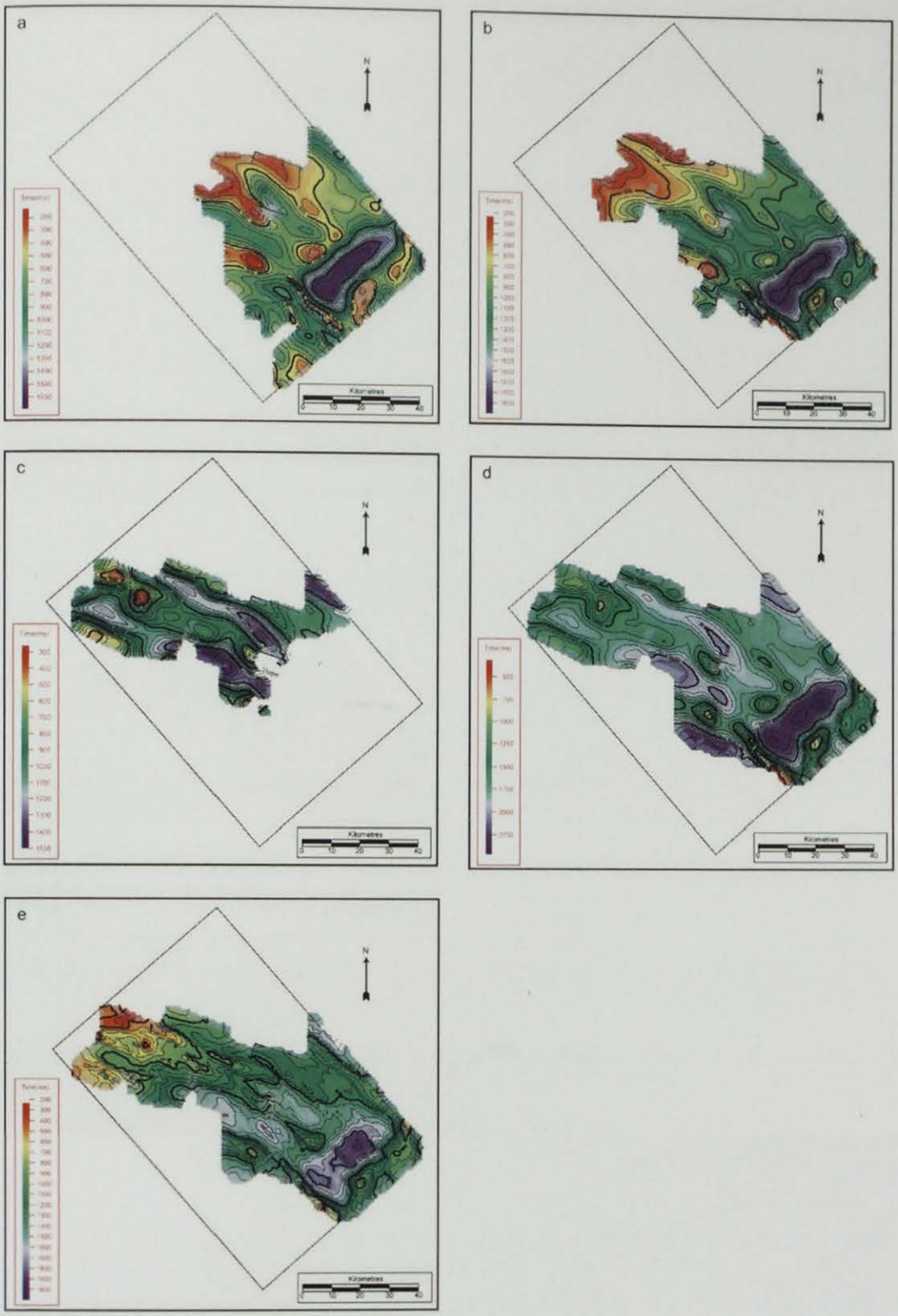

Figure 5.9: Seismic structure maps of the key interpreted horizons. Where a = top Cretaceous, b = base Cretaceous, c = nearest top Triassic, d = top Permian Zechstein group and e = top Permian Rotliegend group.

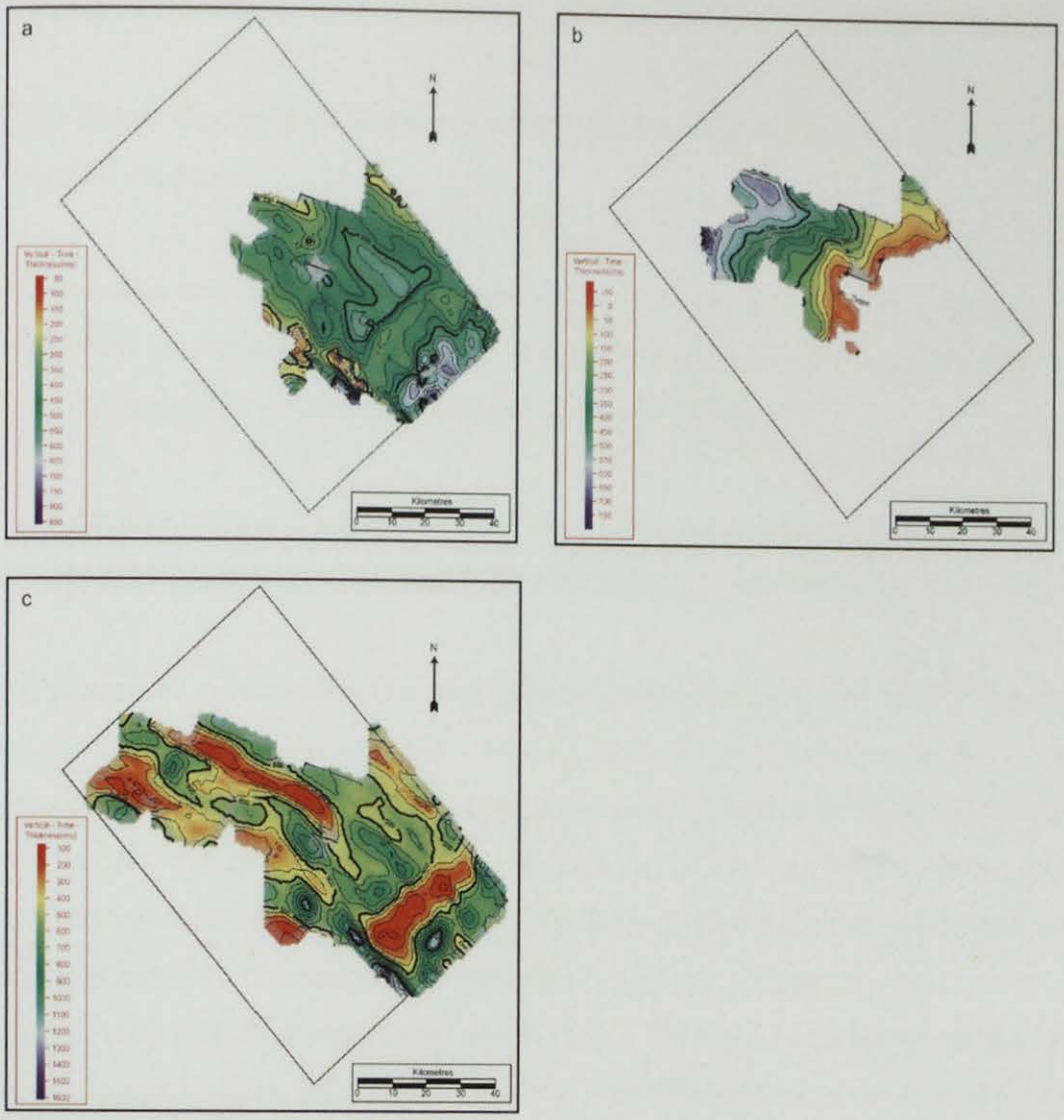

Figure 5.10: Isochron maps of the three significant stages. Where a = Cretaceous, b = Jurassic and c = Permian Zechstein.

5.6 Discussion

5.6.1 Post Zechstein Tectono-stratigraphic Evolution of the Greater Silverpit Region

Interpretation and mapping of the main stratigraphic markers allows a model to be established to explain the structural and stratigraphic features seen in the post Zechstein supra-salt overburden in the greater Silverpit area.

The virtually uniform thickness of the Triassic sediments (Figure 5.9), suggest that the only control on deposition during this time was regional subsidence.

The pattern of deformation and erosional truncation beneath the Late Cimmerian unconformity (no Middle or Upper Jurassic sediment is present in the SW of the study area), indicate that a more complex series of processes have taken place towards the end of the Mesozoic, with significant erosion having taken place. Regional uplift and erosion at the end of the Jurassic throughout the southern North Sea basin has been documented by Cameron et al (1992). Figure 5.10 shows that the Jurassic sediment thickness varies from 750ms thickness through to no Jurassic present in much of the SE of the study area. The Triassic sediments have also been affected by this uplift and erosion and can also be seen to have thinned through erosional truncation towards the southwest on the seismic traverse D – D' (Figure 5.7). The nearest top Triassic seismic surface map and Triassic isochron highlight where the top of the Triassic has been eroded.

However, the Jurassic that is present has also been affected by other deformation, which has been overprinted by the regional erosion and uplift. Seismic sections A – A' and B – B' show that the thickness of the Jurassic sediment is variable. No faulting which may explain these thickness variations is seen. As such we suggest that perhaps an episode of folding resulting from syn-sedimentary salt mobility has taken place during the Jurassic.

The Cretaceous units are relatively constant thickness which suggests that following the formation of the Late Cimmerian unconformity, regional subsidence is dominant once again. There has been more recent erosion of the Cretaceous towards the NW of the study area.

The significant thickness variations and pronounced onlap seen in the Tertiary units throughout the study area are attributed to the onset of salt mobility during this time. The present day structure is dominated by a series of salt-induced synclines, anticlines, diapirs, pillows and walls. The Tertiary deposits are at their thickest in the large basin seen in seismic section C – C' (Figure 5.6). In its extreme case no Tertiary is present where salt diapirs have penetrated through the overburden and subcrop at the sea floor.

Evidence from our seismic interpretation of the greater Silverpit region allows us to establish some understanding of the mechanisms that have caused the salt to move. We suggest that the salt has moved in response to a critical overburden thickness. In the case of the Tertiary episode of salt movement, it is relatively simple to calculate the critical thickness of sediment that existed at the time of onset of halokinesis. In all cases, 1350ms of non-Tertiary salt movement sediment is present above the Zechstein evaporites. Where Jurassic sediments sit conformably beneath the Cretaceous sediments in the NW of the study area, as seen on seismic section A – A' (Figure 5.4), it is assumed that little to no erosion of the Jurassic sediments has taken place. Therefore it has also been possible to establish the approximate thickness of post Zechstein overburden that would have been present at the time of onset of halokinesis in the Jurassic and 1100ms of sediment has been identified. The thickness of sediment above the Zechstein evaporites before each phase of salt movement is very similar. We therefore suggest that salt mobility occurs when a critical thickness of overburden exceeds approximately 1200ms, some variation will exist depending on the density of the overburden.

5.6.2 Genesis of the "Crater"

The timing of the regional Zechstein Group evaporite movement in combination with the location of the Silverpit structure, in the centre of a salt withdrawal induced syncline (Figure 5.5) mean that the role of salt withdrawal in the formation of the Silverpit structure cannot be ignored. Ring faulting similar to that associated with the Silverpit structure has been identified in other salt withdrawal provinces such as the Santos Basin, Brazil (Correia et al 2005) and in the Eastern Mediterranean (Bertoni and Cartwright 2005). Where evaporite overburden has faulted in response to the withdrawing or dissolving evaporite. We suggest that the ring faults associated with the Silverpit structure have formed as a result of regional Tertiary salt withdrawal.

5.7 Conclusions

1) Detailed analysis of the structural and stratigraphic evolution of 3500km^2 of the greater Silverpit region has been carried out.

2) Regional uplift and erosion has taken place at the end Jurassic and affects both Jurassic and Triassic stratigraphy.

3) Salt mobility during the Tertiary has played a significant role in the development of stratigraphic and structural styles seen in the greater Silverpit area and is likely to have had an influence on the genesis of the Silverpit structure.

Chapter 6

6 Geophysical and Geochemical Evidence for Anomalous Chalk Diagenesis Associated with the Circular Silverpit Structure, UK North Sea.

Zana Conway[1], Stuart Haszeldine[1], Malcolm Rider[1] & Anthony Fallick[2]

[1] School of Geosciences, University of Edinburgh, Edinburgh, EH9 3JW

[2] SUERC, Rankin Avenue, Scottish Enterprise Technology Park, G75 0QF

6.1 Abstract

The presence of both a geophysical and a geochemical anomaly has been identified in the Cretaceous Chalk beneath the Silverpit structure, UK North Sea. Detailed analysis of the geophysical well logs available through the Silverpit structure has identified an anomalous low sonic response in the base of the chalk beneath the structure, in comparison to the rest of the study area. This has been attributed to a significant decrease in porosity. Stable oxygen and carbon isotope analyses of chippings collected through the chalk have also revealed an anomalous stable oxygen isotope depth trend in the chalk beneath the structure. It is suggested that these anomalous attributes have formed as a result of unusual diagenesis of the chalk beneath the Silverpit structure, the most probable cause of which is unusual heat flow associated with the Silverpit structure.

6.2 Introduction

Work on determining the origin of the 20 km diameter Silverpit structure, UK southern North Sea, which was identified by Stewart and Allen (2002), has principally been focussed on the available seismic data. This has been used to examine the morphology, the geometry and the structural setting of the Silverpit structure. A number of different hypotheses of origin have arisen as a result of this

seismic interpretation, none of which has produced a categorical explanation for the formation of the Silverpit structure. The two most likely origins are that the Silverpit structure is either a meteorite impact crater (Stewart and Allen 2002) or a regional salt withdrawal structure (Underhill 2004).

The Silverpit structure has not been cored and so no rock material is available from the centre of the structure. Only regularly sampled chippings are available from wells at the outer edges of the Silverpit structure. As such, conventional methods of meteorite crater identification, such as the presence of shocked minerals (most commonly quartz) or the detection of a geochemical anomaly (such as an increased iridium content) (Koeberl 2002) are not viable. This being the case, the data that are available have been used to develop novel methods, to better understand the structure and to test the competing hypotheses.

6.3 Data

The data available for this study originate entirely from the exploration activities of hydrocarbon companies in the southern North Sea. The Common Access Database (CDA) was used to acquire the geophysical well log data. CDA is an online database that holds the information from all of the wells drilled and logged in the UK offshore sector. Edinburgh University is a member of CDA and has access to all of the publicly released wells made available by the Government approximately four years after the well has been drilled. Fifty wells have been used to examine the sonic log response of the Cretaceous Chalk in the southern North Sea study area.

Rock chippings collected when the wells were drilled have also been used. Two wells, 43/25-1 and 43/24-3, were drilled through the Silverpit structure (Figure 6.1). The chippings from these two wells, in addition to a control well 49/01-4, have been used to carry out bulk analysis of the carbon and oxygen stable isotope signatures of the Cretaceous Chalk. The control well was selected as it is located in a setting with the same structural trend as the two Silverpit wells, a salt withdrawal induced syncline. The control well also includes the thickest succession of Cretaceous Chalk

in the study area. The chippings from the wells 43/25-1 and 43/24-3 used for the isotopic analysis were acquired from the Department of Trade and Industry (DTI) Oil and Gas core store, Edinburgh. The chippings for well 49/01-4 were acquired from RWE (UK).

Although the age of the structure has been estimated as Early Eocene (Chapter 3), this study focuses on the characteristics of the Cretaceous Chalk in the southern North Sea. This is primarily because there are few to no available data from any of the Palaeocene deposits around the Silverpit structure and other areas of the basin. Only in the deepest syncline in the south east of the basin are there any data collected through the Tertiary horizons and these are patchy and unreliable. The Cretaceous Chalk is still a relatively shallow horizon and limitations in the data available are still a significant problem; this study utilises the two consistent sources of information available through the chalk, the sonic geophysical well log and the rock chippings collected when the wells were drilled. Previous work on both the reservoir and non-reservoir Cretaceous Chalk throughout the whole of the North Sea provides a good understanding of the behaviour and characteristics expected of the chalk.

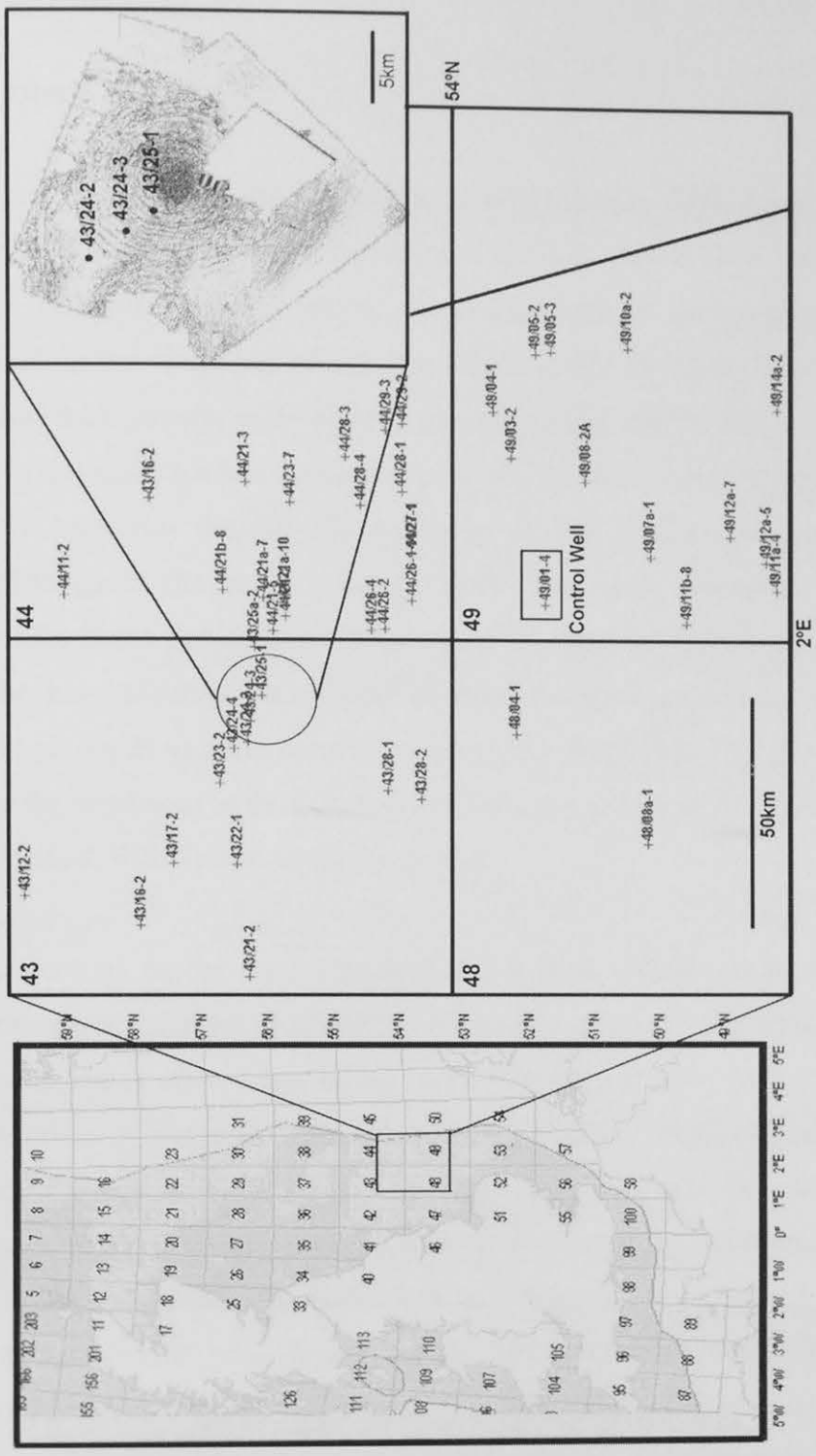

Figure 6.1: Location map of the study area including the location of the Silverpit structure. The wells inside and just outside of the structure are seen. The control well is also located.

6.4 The Sonic Log

6.4.1 Rationale

The sonic log is one of the many geophysical well logs run when a well is drilled. The sonic is the measure of a formation's interval transit time (Δt), i.e. the formation's ability to transmit waves and is measured in microsecond per foot (μs/ft), which is the reciprocal of velocity. Geologically the sonic log varies with lithology and rock texture, most notably porosity (Rider 2002). The sonic log has been used in this study for two main reasons: firstly it is one of the very few logs that has actually been run through the relatively shallow Cretaceous chalk and is available throughout the entire southern North Sea basin. Secondly, the sonic signature of the North Sea chalk has been studied in depth by Mallon and Swarbrick (2002), who have developed a compaction trend for the non-reservoir Cretaceous chalk, highlighting its uniform nature throughout the North Sea. This has been used to compare the trend seen in the Silverpit wells and the section of the southern North Sea basin studied, with the rest of the North Sea.

Significant controls on the sonic signature of the chalk include the porosity, fluid content and texture (Røgen et al 2001). Burial diagenesis of the chalk plays an important role and is often a controlling factor of the sonic velocity of the chalk as well as the porosity (Fabricus 2003). Compaction trends of chalk can be estimated from the sonic values when compared with depth. This study uses the wells that pass through chalk, which is assumed to have been modified only by burial diagenesis. As such only wells through non-reservoir chalk and chalk that has not been penetrated by salt diapirs, have been used. Reservoir chalk and chalk which is directly above or that has been penetrated by salt diapirs has often been subjected to unusual fluid flow leading to modification of the porosity and cementation, which in turn affects the sonic velocity (Jensenius and Munksgaard 1989, Røgen et al 2001).

6.4.2 Method and Results

Sonic curves through the non-reservoir Cretaceous Chalk in fifty wells in the southern North Sea basin have been examined and correlated. Four wells crucial to this study (Figure 6.1) were 43/25-1 and 43/24-3, the two wells located in the Silverpit structure; 43/24-2 located just outside of the Silverpit structure; and 49/01-4 located in the south east of the basin and which contains the thickest succession of chalk in the study-area. In general an average sonic curve was apparent (Figure 6.2), which can be compared with other non-reservoir chalk seen throughout the North Sea; this includes well 43/24-2. The trends seen are similar to that of the Central North Sea Cretaceous Chalk (Mallon and Swarbrick 2002), with a linear decrease of Δt with increasing depth. The only wells that do not fit this trend are the two wells that penetrate the outer rings of the Silverpit structure, wells 43/25-1 and 43/24-3 (Figure 6.2). Correlation of these curves with the average trend of the Cretaceous chalk highlights a significant and unusual decrease in the sonic value at the base of the chalk.

To confirm that the Silverpit structure sonic curves are indeed anomalous, a single basin wide sonic curve was created. Regional deformation of the southern North Sea basin as a result of salt movement has led to uplift of the chalk in some areas (Chapter 5). However, the chalk retains the sonic trend it acquired when it was at its maximum burial depth before uplift took place. This means that if the trends were compared at their present-day depths, they would not produce an "appropriate" sonic trend: low sonic values would be recorded at too shallow depths. As such, all of the sonic curves have been compared with one curve that contains the thickest succession of chalk in the basin from well 49/01-4. This method is based on the idea that uniform deposition of different facies takes place within the chalk (Tucker and Wright 1990). These facies produce small-scale variations on the sonic curve that can be correlated from curve to curve (Rider 2002), so that the depth of the uplifted chalk can be reconstructed back to its original depth by looking for the same series of small-scale variations as in the deepest well. The basin-wide sonic curve highlights the uniform nature of the chalk throughout the basin and confirms that the Silverpit

wells are anomalous. In fact, it was impossible to correlate the sonic curves from the two Silverpit structure wells with the control curve at all (Figure 6.3).

Analysis of the sonic trend provides limited information about the cause of the unusual characteristics of the chalk beneath the Silverpit structure. To understand what has caused the anomalous sonic response in the chalk, it is necessary to consider what controls the sonic values of the chalk. Røgen et al (2001) indicate that major controls on the sonic values are the rock fluid content, texture and porosity. Rock fluid content has relatively limited effect on the sonic response and would not be the cause of such a large variation in the sonic trend. Textural variations in the rock can only be established from petrological analysis of the chalk, which could not viably be carried out in this study in the absence of core. However, the rock texture and porosity are inherently linked and any variation in the rock texture would change the porosity of the chalk. Therefore, we can reasonably consider a likely cause of the anomalous sonic response in the chalk beneath the Silverpit structure to have arisen as a result of anomalous porosity.

By extracting the porosity trend from the sonic trend we will have a greater insight into what has affected the chalk. The sonic log can be used to calculate the porosity of the chalk; however, the method used to do this, the Wylie Time Average calculation is often imprecise and is not suitable for the detailed nature of this study. In most cases the porosity is calculated using a combination of the sonic and density or neutron logs. However, neither the density log nor the neutron log is available through the chalk beneath the Silverpit structure. Instead, the porosity has been calculated using the data that Mallon and Swarbrick (2002) present on the non-reservoir chalk of the North Sea. Their method produced a graph of sonic interval transit time versus density-derived porosity. Using their equation:

$$y = 0.6779x - 32.5 \text{ (eqn. 6.1)}$$

where y = density-derived porosity (%) and x = sonic interval transit time (μs/ft), it has been possible to calculate the porosity of the chalk beneath the Silverpit structure and the control well (Figure 6.4). The study by Mallon and Swarbrick (2002) did not

include the chalk beneath the Silverpit structure and so may not be an entirely accurate representation of the porosity in this setting. However, it can be considered as a fair approximation of the porosity of the chalk beneath the Silverpit structure.

On this interpretation there is a significant decrease in the porosity at the base of the chalk unit beneath the Silverpit structure. The 8 – 10% porosity seen at this relatively shallow depth of between 3000ft and 4000ft is equivalent to the porosity seen at the base of the much deeper, 7500ft chalk in the control well. The two Silverpit wells exhibit a much less linear decrease in porosity than the rest of the basin; the most significant porosity reduction takes place in the bottom 600ft of the chalk jumping from 30% to less than 10% in this interval. The top section of chalk in well 43/25-1 is not available. In the top section of the chalk in well 43/24-3 the overall porosity decrease is relatively linear with no significant variations from the control well.

Analysis of the sonic curves suggests that there is a significant decrease in the porosity of the chalk in the wells beneath the Silverpit structure. However, that is the limit of the sonic data and it is not possible to establish what has caused the porosity variations using just this method.

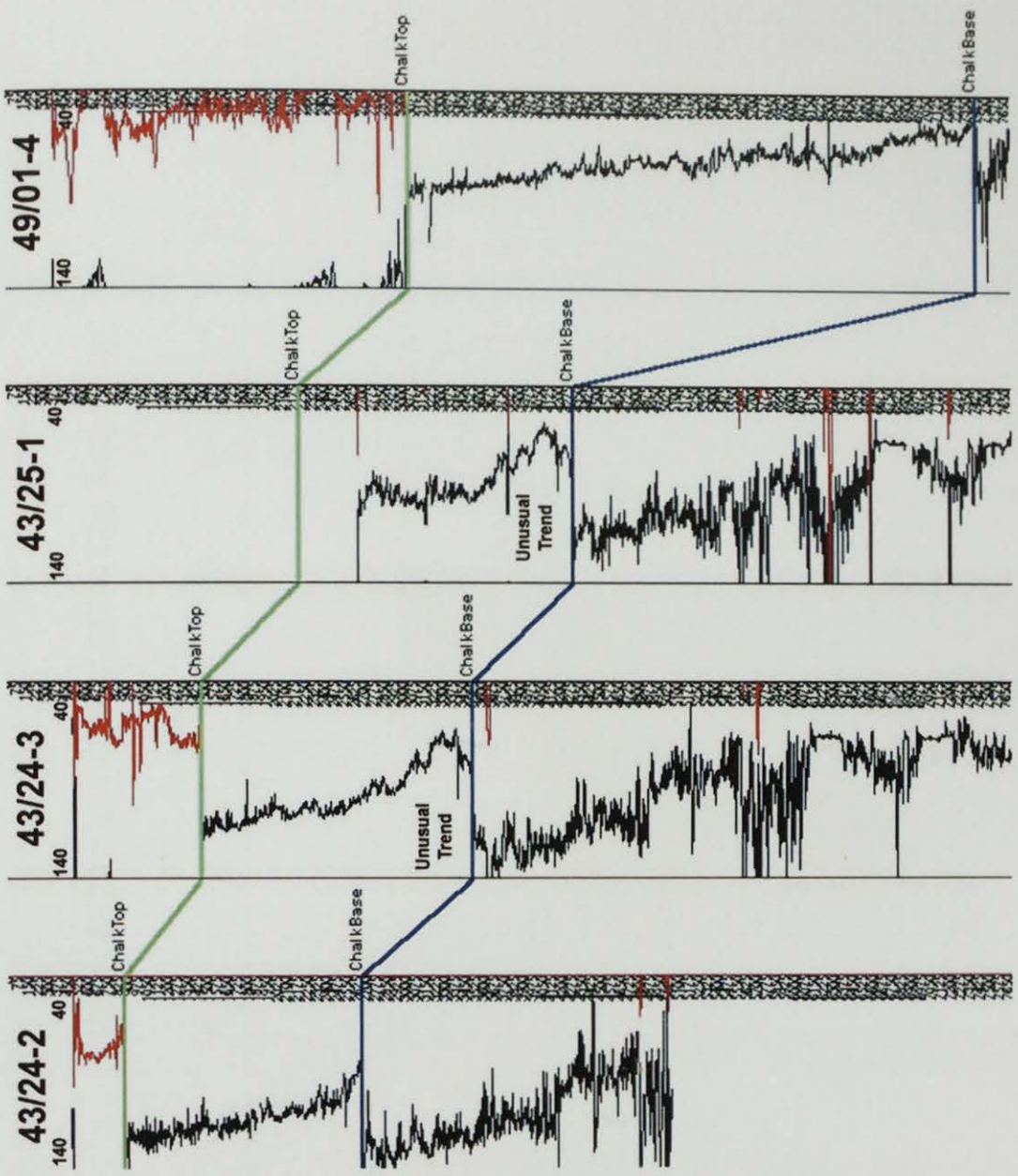

Figure 6.2: Panel highlighting the normal sonic response seen throughout the basin, 43/24-2 (just outside the structure) and 49/01-4 (the control well). 43/25-1 and 43/24-3 indicate the unusual trend seen within the Silverpit structure.

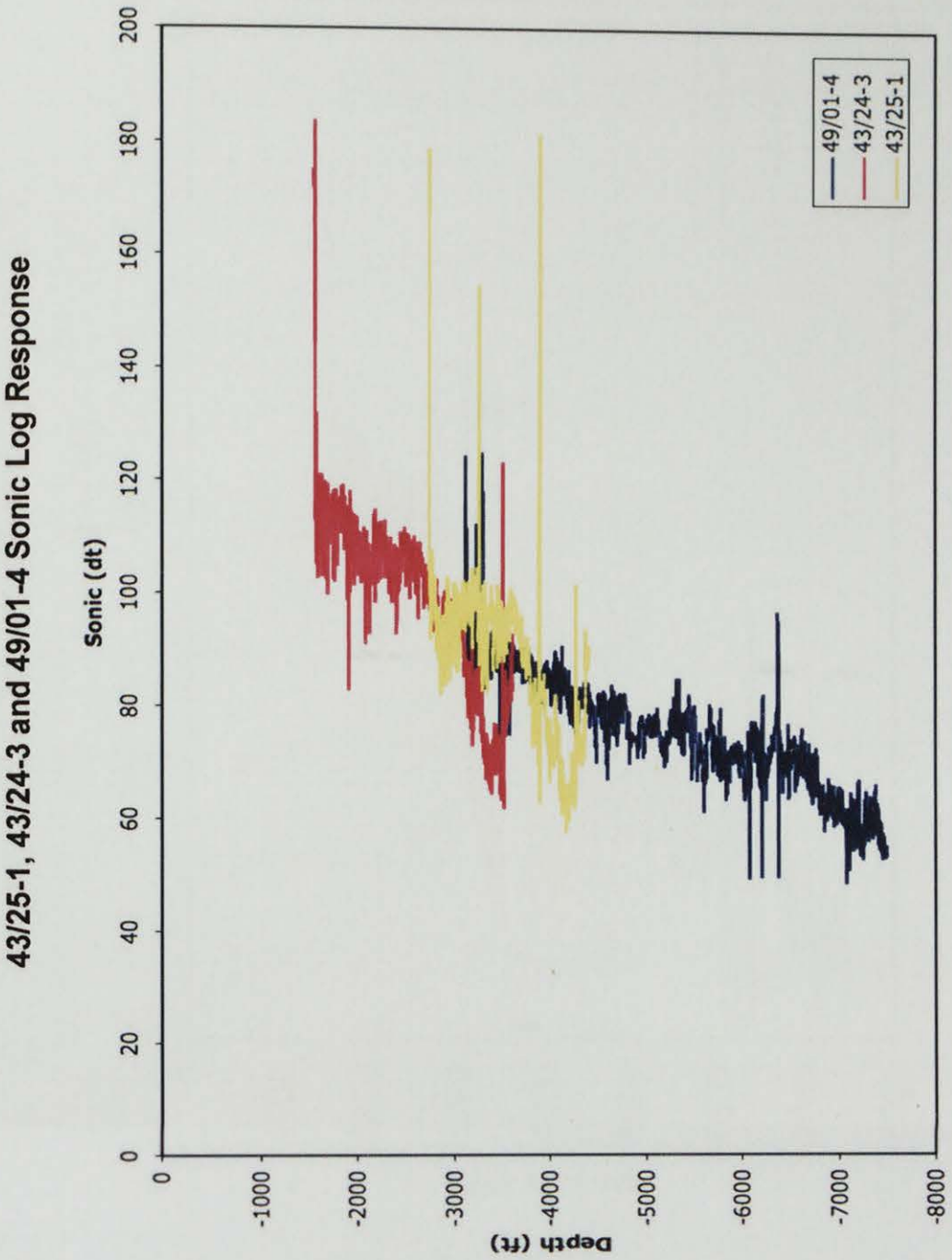

Figure 6.3: The sonic log response seen in the chalk beneath the Silverpit structure and the trend which represents the rest of the basin. The Silverpit structure trends are clearly anomalous.

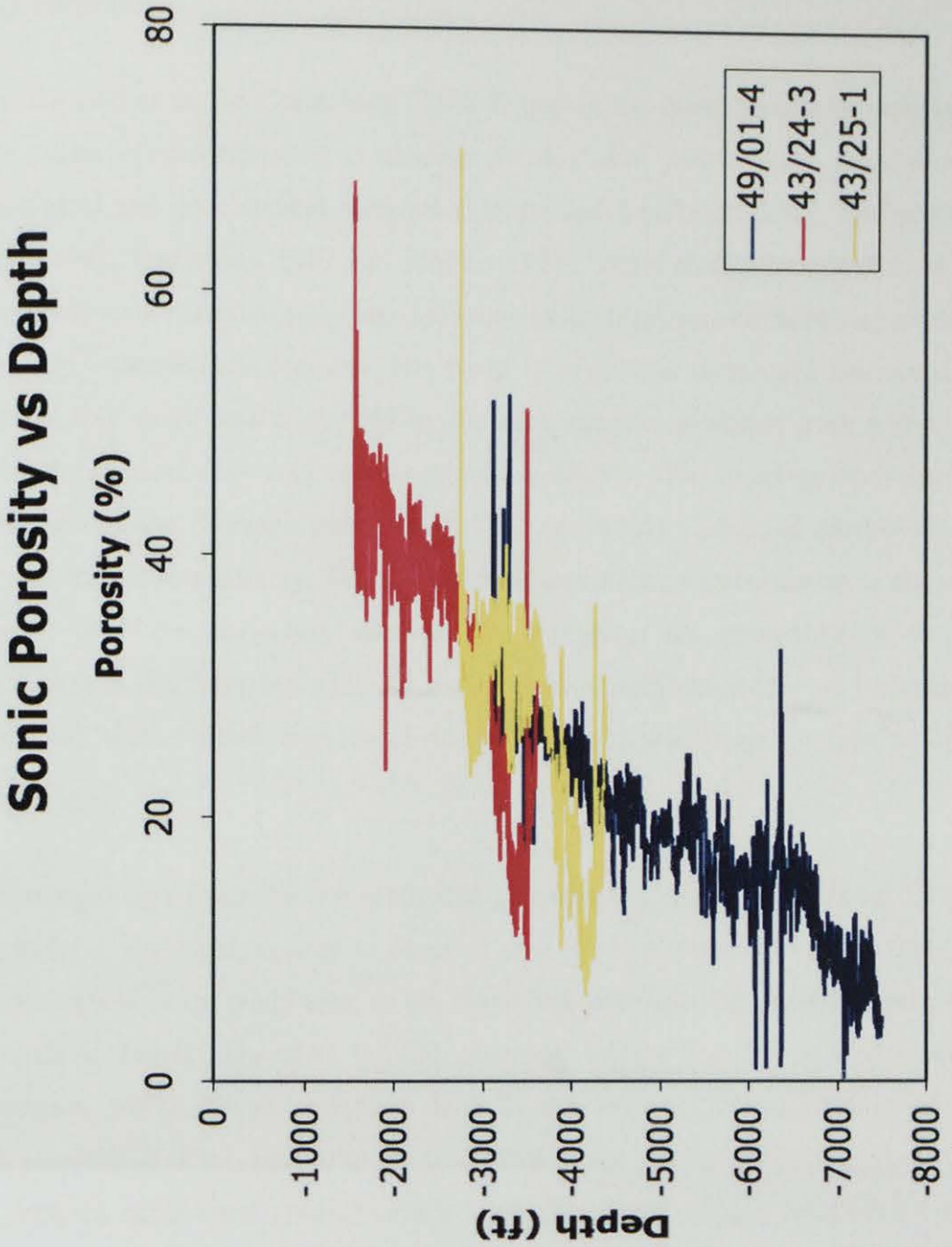

Figure 6.4: The porosity calculated using equation 6.1 from Mallon and Swarbrick. The porosity in the chalk beneath the Silverpit structure is significantly lower than other chalk in the study area at the same depth.

6.5 Stable Isotope Analysis

6.5.1 Rationale

Previous studies of the Cretaceous Chalk Group in the North Sea have included a wide range of petrophysical (including porosity and permeability calculations), petrological and geochemical methods (Mallon and Swarbrick, 2002, Egeberg and Saigal, 1991, Jorgensius, 1987 and Scholle, 1977). These studies have had access to a range of rock material and data including rock chippings, offshore and onshore cores and onshore field sections. The range of analytical techniques that could be used for this study was controlled by the rock material available from within the Silverpit structure: only rock chippings were available. The chippings from the two wells through the Silverpit structure, 43/25-1 and 43/24-3 were sampled every 50 feet and 25 feet respectively. The chippings collected are a representation of the rock material from the collection interval. The chippings are approximately 2 – 3 millimetres in diameter. As such, the most valuable analytical technique was judged to be mass spectrometric analysis of the stable carbon and oxygen isotope ratios of the chalk.

The isotopic data from the two wells that penetrate the Silverpit structure, 43/25-1 and 43/24-3 will be compared to those of well 49/01-4 which represents the non-reservoir chalk in the study area. In the North Sea, non-reservoir chalk progressively responds to burial diagenesis through chemical compaction and recrystallisation (Jørgensen 1987). These processes lead to the isotopic re-equilibration of the carbonate phase of the rock with the interstitial water at a temperature governed by the imposed geothermal gradient. An isotopically lighter oxygen composition with increasing depth should be seen (Scholle 1977). Studies of the Austin Chalk, Texas, USA show no correlation between the isotopic signature of the chalk and the depth. It is suggested that this is because this is a closed system (Czerniakowski et al 1984). Thus it has been inferred that the diagenesis of the non-reservoir chalk in the North Sea is a partially open system in order to allow the isotopic re-equilibration to take place (Jørgensen 1987).

It is anticipated that investigating the stable oxygen and carbon isotope signatures of the chalk beneath the Silverpit structure may contribute to an explanation of why the porosity anomaly exists beneath the structure.

6.5.2 Material and Analytical Method

Rock chippings from the three wells were sampled at varying intervals. The chippings from the well 43/25-1 were sampled at 30m intervals, the chippings from the well 43/24-3 were sampled at 15m and the chippings from the well 49/01-4 were sampled at 30 – 40m intervals. The samples were ground using an agate pestle and mortar. Contamination between samples was avoided using a system of washing the pestle and mortar in a weak acid solution followed by de-ionised water after grinding each sample.

Stable isotope data are reported as delta per mil values relative to VPDB (Vienna Pee Dee Belemnite) or VSMOW (Vienna Standard Mean Ocean Water). The data were generated by reacting c. 1mg of powdered carbonate with phosphoric acid at 90°C in a modification of the method of McCrea (1950). The reaction was carried out in an Analytical Precision automated system lined to an AP2003 triple collector continuous flow isotope ratio mass spectrometer (CF-IRMS). Daily correction to VPDB was via an in-house carbonate standard MAB ($\delta^{13}C$ + 2.48, $\delta^{18}O$ – 2.40 VPDB) and this in turn was calibrated against international reference material NBS 19.

The external precision and accuracy are about 0.1 per mil (one sigma) for both $\delta^{13}C$ and $\delta^{18}O$ based on replicate analyses over an extended time interval. The oxygen isotope fractionation factor for production of CO_2 from calcium carbonate by phosphoric acid reaction was taken from Rosenbaum and Sheppard (1986).

6.5.3 Analytical Results

The analytical results are given in Figures 6.5 – 6.8. The stable carbon isotope data have been plotted as $\delta^{13}C$ VPDB versus $\delta^{18}O$ VPDB. The $\delta^{13}C$ data (Figure 6.6) show a negative correlation with the $\delta^{18}O$. Significantly, there are no differences between the three wells.

The stable oxygen isotope results have been plotted in Figure 6.7 versus depth (in feet), highlighting three trends. Well 49/01-4 shows a change in $\delta^{18}O$ VPDB from –1.00‰ to –3.80‰ over 3360ft. Importantly these ratios are from the depths of 3870ft – 7230ft. The results from the two Silverpit wells exhibit almost identical trends, but offset by approximately 1000ft. Well 43/24-3, which includes all of the chalk, has $\delta^{18}O$ ranging from –1.03‰ to –4.29‰ occurring between 1750ft and 3500ft. Well 43/25-1, which has the top 200ft of chalk missing (as this was not collected when the well was drilled), has $\delta^{18}O$ ranging from –1.64‰ to –4.26‰, occurring at the much shallower depths of between 3000ft and 4300ft.

In order to confirm that the results from well 49/01-4 are representative of those of the Cretaceous Chalk Group in the North Sea as a whole, data from the Danish Sub-Basin has also been added to the graph of $\delta^{18}O$ versus depth (Figure 6.7). These data have been taken from Jørgensen (1987), which includes data from both the reservoir units of the North Sea Central Graben and the Danish sub-basin. For the same reason as the sonic trends chosen, this study uses only the non-reservoir Danish sub-basin chalk results.

Initially it would appear as if the results between 49/01-4 and the Danish sub basin are anomalous and that four separate trends exist. However, statistical analysis of the best fit lines generated from the data sets highlights that analysis of the gradient of the best fit lines ($\underline{a}$), within error, can be separated in to two groups; the two sets of data from 43/25-1 and 43/24-3, from the chalk beneath the Silverpit structure and 49/01-4 and the Danish sub-basin. All of the gradients of the best fit lines were

considered statistically normal. The details of the statistical analysis can be found in Table 6.1.

The Danish Sub basin underwent significant uplift during the Palaeogene (Clausen et al 2000). This suggests that the two sets of data representing the "normal" North Sea chalk are not necessarily different to each other. Instead it suggests that although the Danish chalk has been uplifted it has retained the isotopic signature of its deeper burial depth. This also resolves the issue of the two trends seen in the two wells that penetrate the Silverpit structure. The chalk in this area has also been affected by Tertiary uplift driven by salt movement (Chapter 5) and the chalk in 43/24-3 has been uplifted by approximately 1000ft relative to the chalk in 43/25-1. As such, whereas Figure 6.7 initially suggests that there are four different trends that need to be considered, there are in fact only two. The two trends that will be discussed and considered as representative of the settings are 49/01-4 and 43/24-3 (Figure 6.8). Well 43/24-3 has been considered despite the uplift as it includes the whole of the chalk section available.

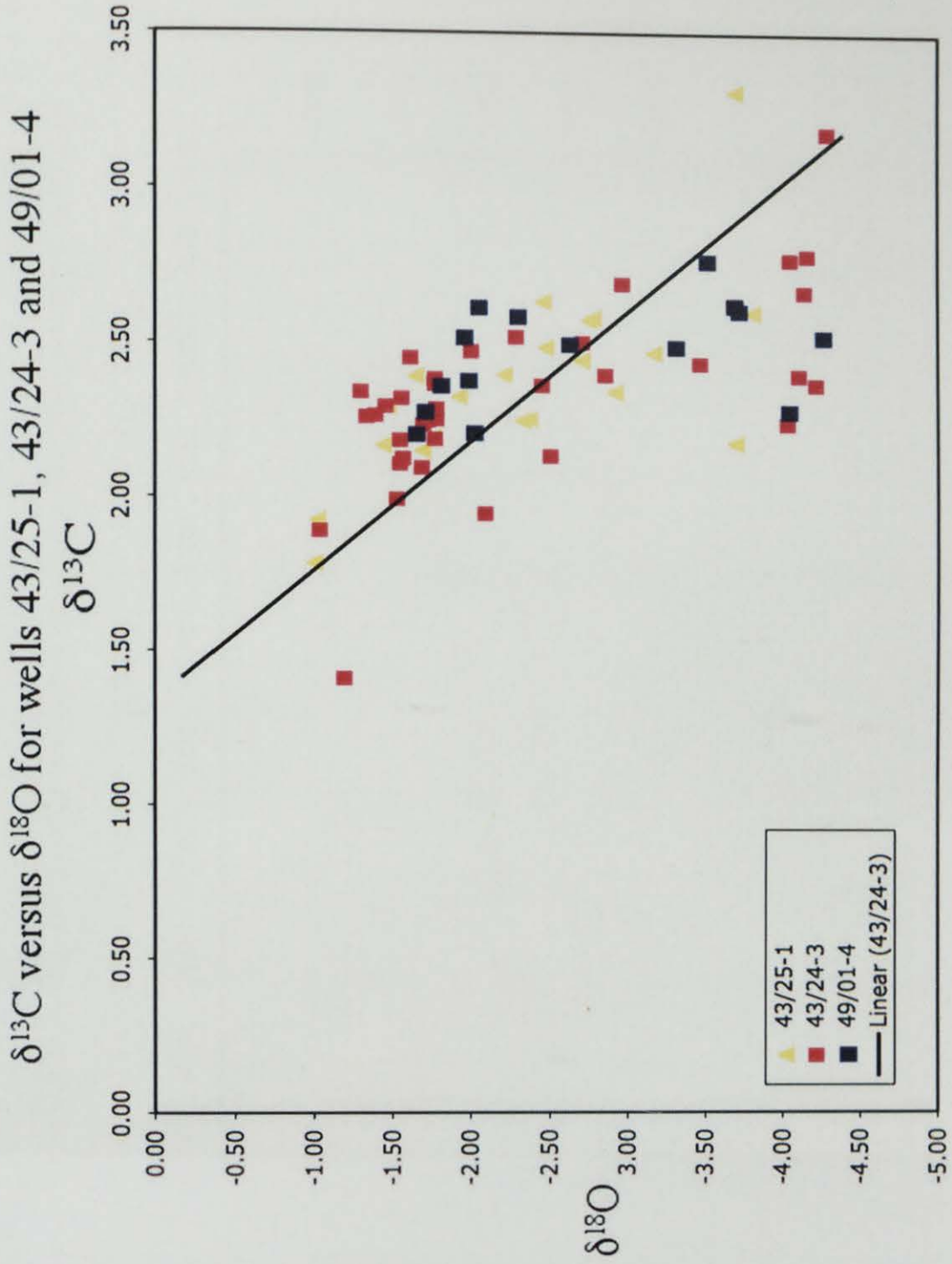

Figure 6.5: A negative correlation between stable carbon versus stable oxygen composition is recognised. There are no variations between the three wells.

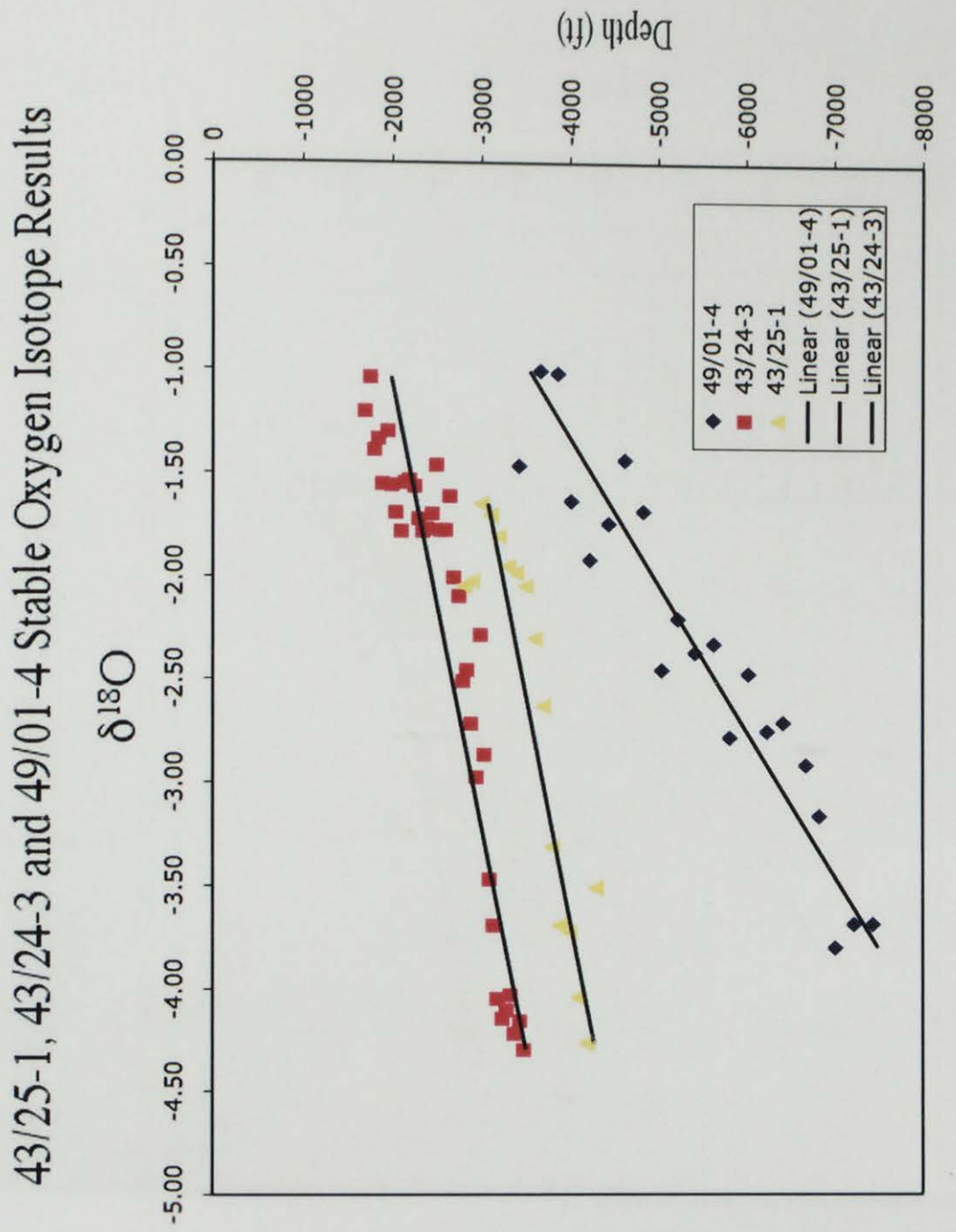

Figure 6.6: Stable oxygen isotopic compositions versus depth. Note that there are three trends of data but that the two Silverpit wells, 43/25-1 and 43/24-3 have similar gradients on the best fit lines.

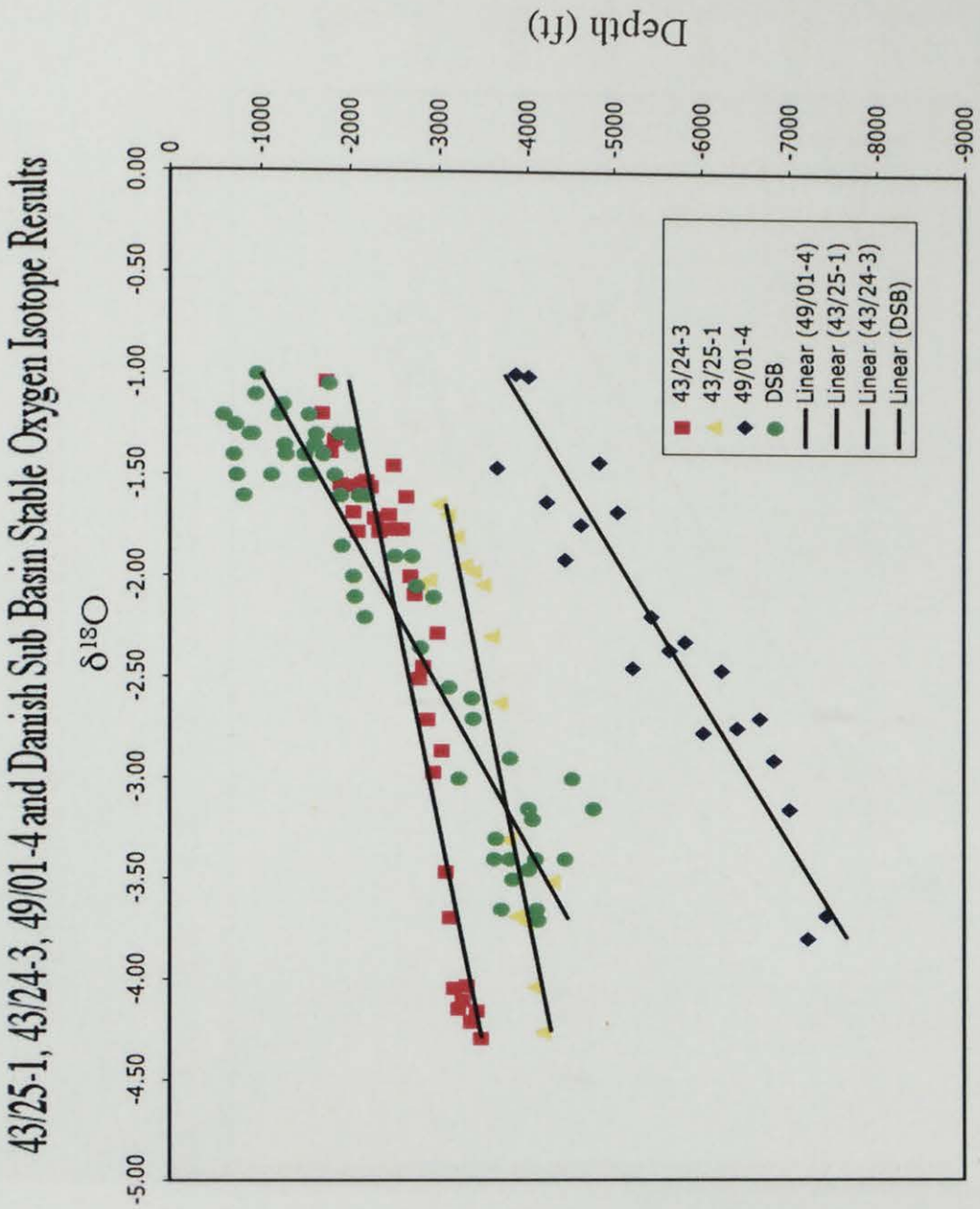

Figure 6.7: Stable oxygen isotope composition versus depth for the three analysed wells and the data from the Danish Sub Basin (DSB) taken from Jørgensen (1987). Note that four trends are now present but that they can be grouped together, 43/25-1 and 43/24-3 as one and 49/01-4 and the Danish Sub Basin as the other.

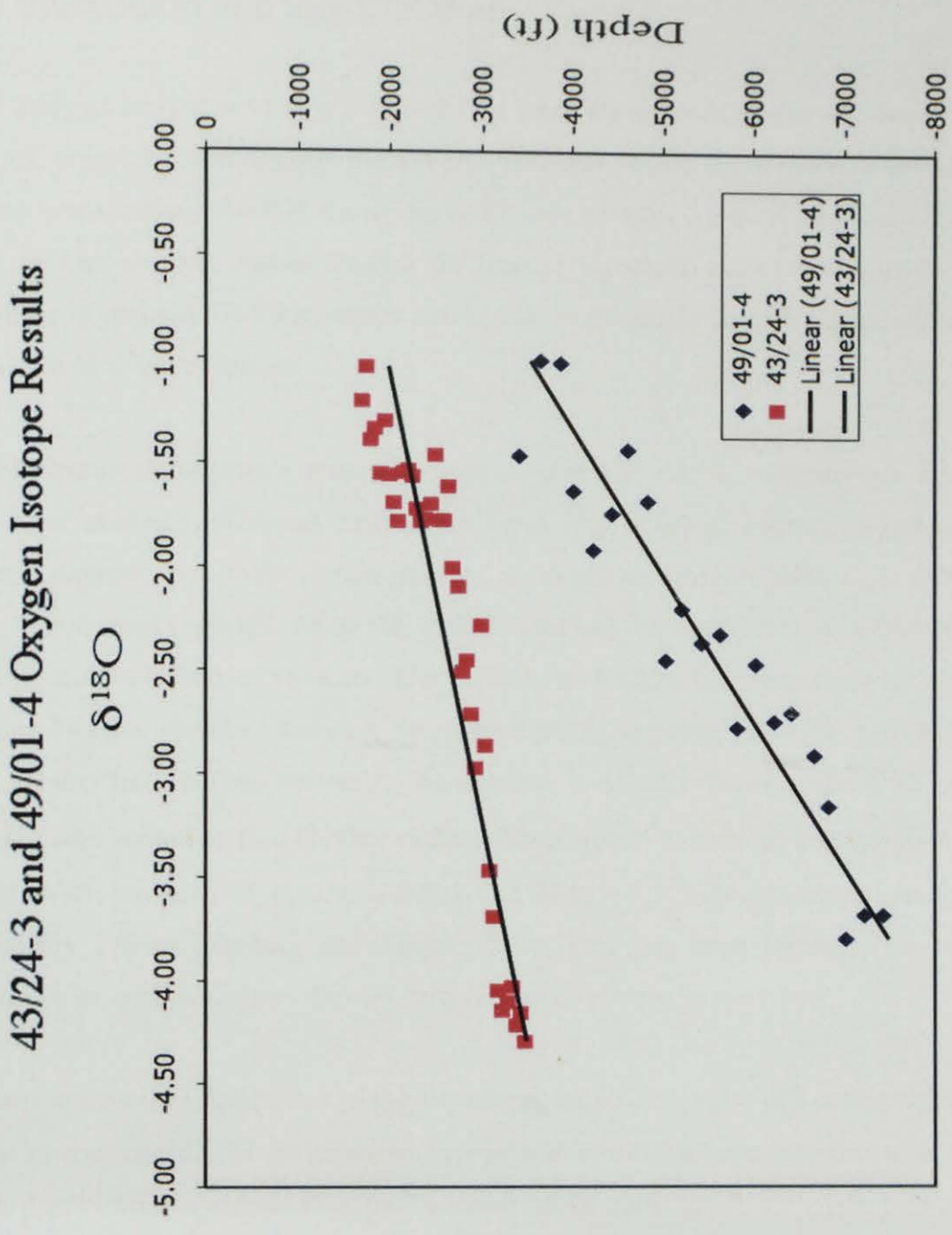

Figure 6.8: Stable oxygen isotope composition versus depth for the two trends that are considered representative of the normal non-reservoir chalk (49/01-4) and the anomalous Silverpit structure chalk (43/24-3).

6.6 Discussion and Interpretation

The analysis carried out has highlighted that there are anomalous characteristics in the non-reservoir chalk beneath the Silverpit structure, which are not seen in the rest of the non-reservoir chalk in either the study area or other areas of the North Sea. The anomalous sonic values through the base of the chalk can be attributed to a decrease in porosity. The anomalous trends seen in the stable oxygen isotope values results need to be explained.

Little variation in the stable carbon isotopic composition, <2.5‰, suggests that there has been minimal additional bicarbonate input from external sources. Jørgensen (1987) suggests that stable carbon isotopic compositions from +0.50‰ to +3.00‰ are within the expected range of carbon isotopic compositions of carbonate precipitated from normal seawater. The majority of the data from this study sit with the +1.5‰ to +3.00‰ and can be considered to be dominated by carbonate precipitated from normal seawater. The negative correlation between the $\delta^{13}C$ and $\delta^{18}O$ results has been noted in other studies. Where access to core has been available, analysis of fracture fill has highlighted that higher $\delta^{13}C$ can be present in the secondary calcite (Egeberg and Saigal 1991). This has been attributed to the influence of organic matter / derived carbon from fermentation reactions.

Understanding the implications of the anomalous stable oxygen isotope compositions requires consideration of the question: Can we understand the linear decrease of $\delta^{18}O$ with depth? This is seen in both the "normal" chalk trend and in the chalk beneath the Silverpit structure.

If we consider that the $\delta^{18}O$ of the carbonate ($\delta^{18}O_{CARB}$) is a function of the temperature (T) and the $\delta^{18}O$ of the water ($\delta^{18}O_W$), then, with depth as Z, the variation of $\delta^{18}O$ with depth is:

$$\frac{d\delta^{18}O_{CARB}}{dZ} = \frac{\partial\delta^{18}O_{CARB}}{\partial t}\frac{dt}{dZ} + \frac{\partial\delta^{18}O_{CARB}}{\partial\delta^{18}O_{W}}\frac{d\delta^{18}O_{W}}{dZ} \quad \text{(eqn. 2)}$$

Note that $\frac{dt}{dZ}$ is the geothermal gradient.

If we then consider that at isotopic equilibrium:

$\delta^{18}O_{CARB} - \delta^{18}O_{W} = 2.78 \times 10^{6} T^{-2} - 2.89$ (eqn. 3) Chacko et al (2001).

And we differentiate eqn. 3:

$$\frac{\partial\delta^{18}O_{CARB}}{\partial t} - \frac{\partial\delta^{18}O_{W}}{\partial t} = -2 \times 2.78 \times 10^{6} T^{-3} \quad \text{(eqn. 4)}$$

Then if $\frac{\partial\delta^{18}O_{W}}{\partial t} = 0$, $\frac{\partial^{18}O_{CARB}}{\partial t}$ is a weak (i.e. T^{-3}) function of temperature.

Further if $\frac{d\delta^{18}O_{w}}{dZ} = 0$, the second term on the right hand side of equation 6.2 is zero and $\frac{d\delta^{18}O_{CARB}}{dZ}$ depends strongly on $\frac{dt}{dZ}$, the geothermal gradient.

Because the unusual oxygen isotope results in the chalk beneath the Silverpit structure also have a linear trend we suggest that this trend may have arisen as a result of a higher than average geothermal gradient.

If a higher than average geothermal gradient has been present in the chalk beneath the Silverpit structure, then the anomalously reduced porosity in the base of the chalk may be attributed to increased cementation, since carbonate has a retrograde solubility, i.e. more carbonate is precipitated at higher temperatures.

6.6.1 Suggested Origin of the Silverpit Structure

A number of different processes may have caused the unusual diagenesis seen in the chalk beneath the Silverpit structure. By systematically analysing the suggested origins of the Silverpit structure and considering if the described geophysical and geochemical anomalies could be produce in these settings it is possible to suggest the most likely origin of the Silverpit structure.

Regional salt withdrawal (Underhill 2004) cannot explain the increased geothermal gradient. The anomalous characteristics are seen only beneath the Silverpit structure and are not seen anywhere else in the study area. Salt mobility has affected the whole of the study area (Chapter 5) and no other anomalous chalk has been identified. As such this is not a viable explanation for the process that has led to the development of the increased porosity and elevated geothermal gradient seen in the chalk beneath the Silverpit structure.

Meteorite impact is in fact the most likely explanation for the presence of the increased geothermal gradient imposed on the chalk beneath the Silverpit structure. On first appreciation this does not seem possible. The heat source associated with the impact would have dissipated from the top down. However, further investigation into the kinetics of meteorite impacts highlights that there is heat flow associated with the formation of the central uplift (Pirajno 2005). Rebound of the hot rocks from below activates hydrothermal circulation in the rocks beneath the target horizon. This would explain the presence of the decreased porosity seen in the base of the chalk beneath the Silverpit structure as carbonate has retrograde solubility and with an increased temperature or geothermal gradient more carbonate will be precipitated.

The heat flow associated with the rebound of target rocks and the formation of a central uplift has been well documented in impact craters that contain economically valuable suites of rock. Examples include the Cu-Ni-PGE deposits of the Sudbury impact structure, Canada (Molnár 2001) and the Witswatersrand gold deposits at the Vredefort impact structure, South Africa (Grieve 2005). However, little has been

documented on the post impact fluid flow in smaller, sedimentary rock-based impacts. We suggest that in structures that have restricted access to the impact horizon, for example in buried structures, utilising geophysical and more limited geochemical techniques could be the key to determining the origin of the structure.

Dataset	R^2	a	Std Error of a	y0	Std Error of y0	Normality Test
Well 49/01-4	0.9954	1415	106	-2122	262	Passed
Danish Sub Basin	0.9730	1290	68	286	152	Passed
Well 43/25-1	0.9967	462	61	-2318	172	Passed
Well 43/24-3	0.9937	470	34	-1493	87	Passed

Table 6.1. Statistical analysis of the linear stable isotopic compositions versus depth trends, y=y0+ax, where y = y-axis, y0 = intercept, a = gradient and x = x-axis.

6.7 Conclusions

1) An anomalous sonic well log response is present in the base of the Cretaceous Chalk Group beneath the Silverpit structure and nowhere else in the study area.

2) Stable isotope analysis of carbon and oxygen isotopic compositions of the chalk highlight a linear $\delta^{18}O$/depth trend in the chalk with an anomalous gradient, beneath the Silverpit structure.

3) Unusual and unique diagenesis of the chalk beneath the Silverpit structure has occurred.

Acknowledgements

We are pleased to thank NERC for PhD grant NER/S/A/2003/11233. CASE sponsorship was provided by Production Geoscience Limited (Banchory). Chippings were provided by the DTI core store and RWE UK Ltd. Thanks also go to Alex Whittaker for his assistance with the statistical analysis and to Mark Wilkinson for his helpful suggestions.

Chapter 7

7 Fieldwork and Onshore Core Analysis

7.1 Fieldwork

Having determined an age range for the central zone of deformation of the Silverpit structure as 49 – 53 Ma, Lower Eocene, fieldwork was carried out to search for onshore UK distal deposits associated with a meteorite impact. The other hypotheses of origin do not produce characteristic distal deposits and are not considered in this chapter. As discussed in Chapter 2, meteorite impact craters are only confirmed once either or both a mineralogical (such as shocked quartz) and a geochemical (such as an anomalously high iridium content) signature have been identified. Because these features can only be formed as a result of a meteorite impact they make the identification of the structure as a meteorite impact crater unambiguous.

7.1.1 Fieldwork Locations

Figure 7.1, taken from Cameron et al (1992) summarises the Tertiary standard stages and the deposits that are associated with each of these. In Eastern England, where the fieldwork was based, the Lower Eocene deposits consist of the London Clay Formation, the Virginia Water Formation and the Bagshot Beds. Locations of these deposits were established from the following references: Booth et al (1994), Pattison et al (1993), Lake (1986), Chatwin (1961) and Sherlock (1947). Figure 7.2, documents the locations that were visited.

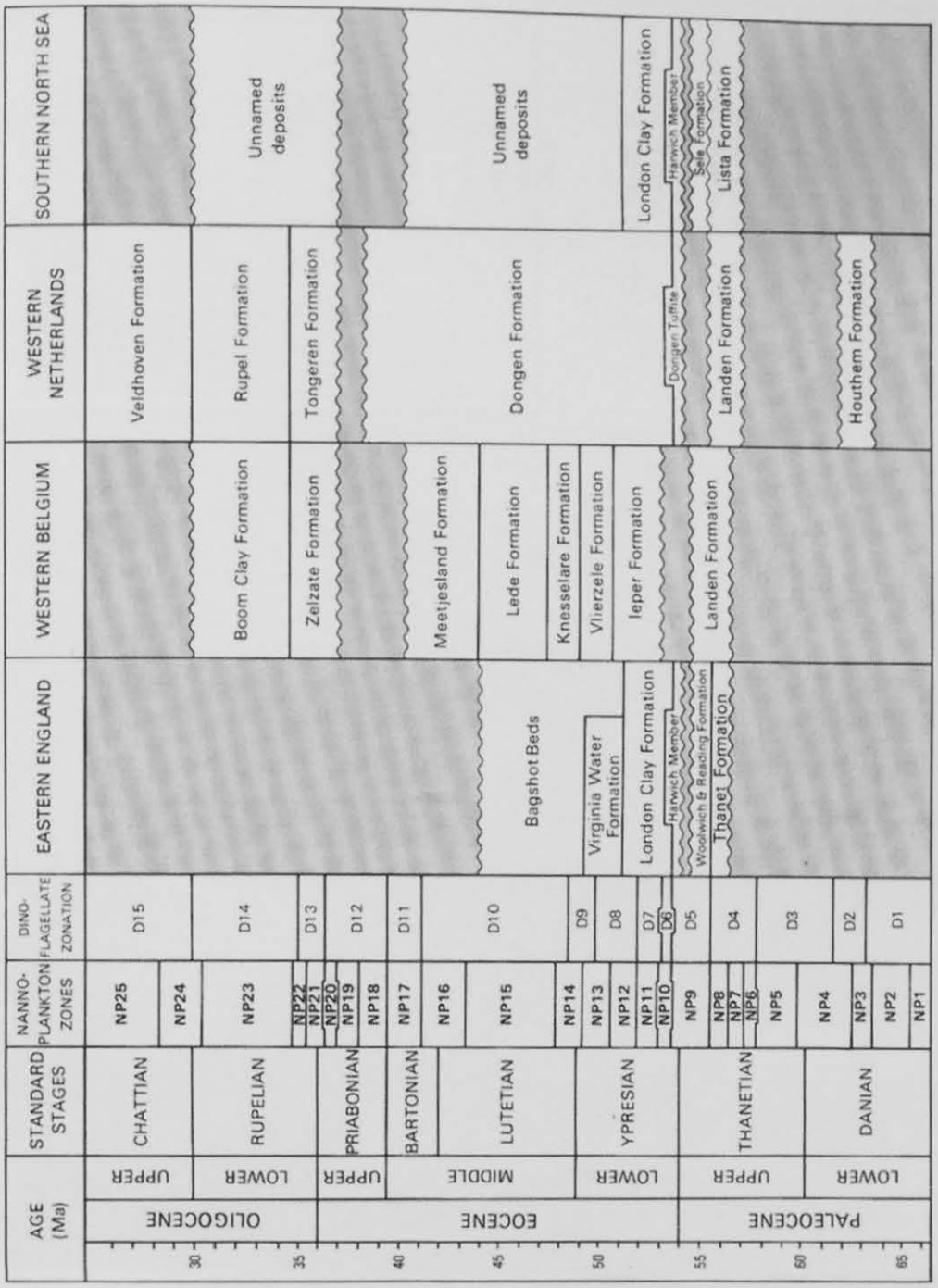

Figure 7.1: A panel highlighting the age of Tertiary stratigraphy. From Cameron et al (1992).

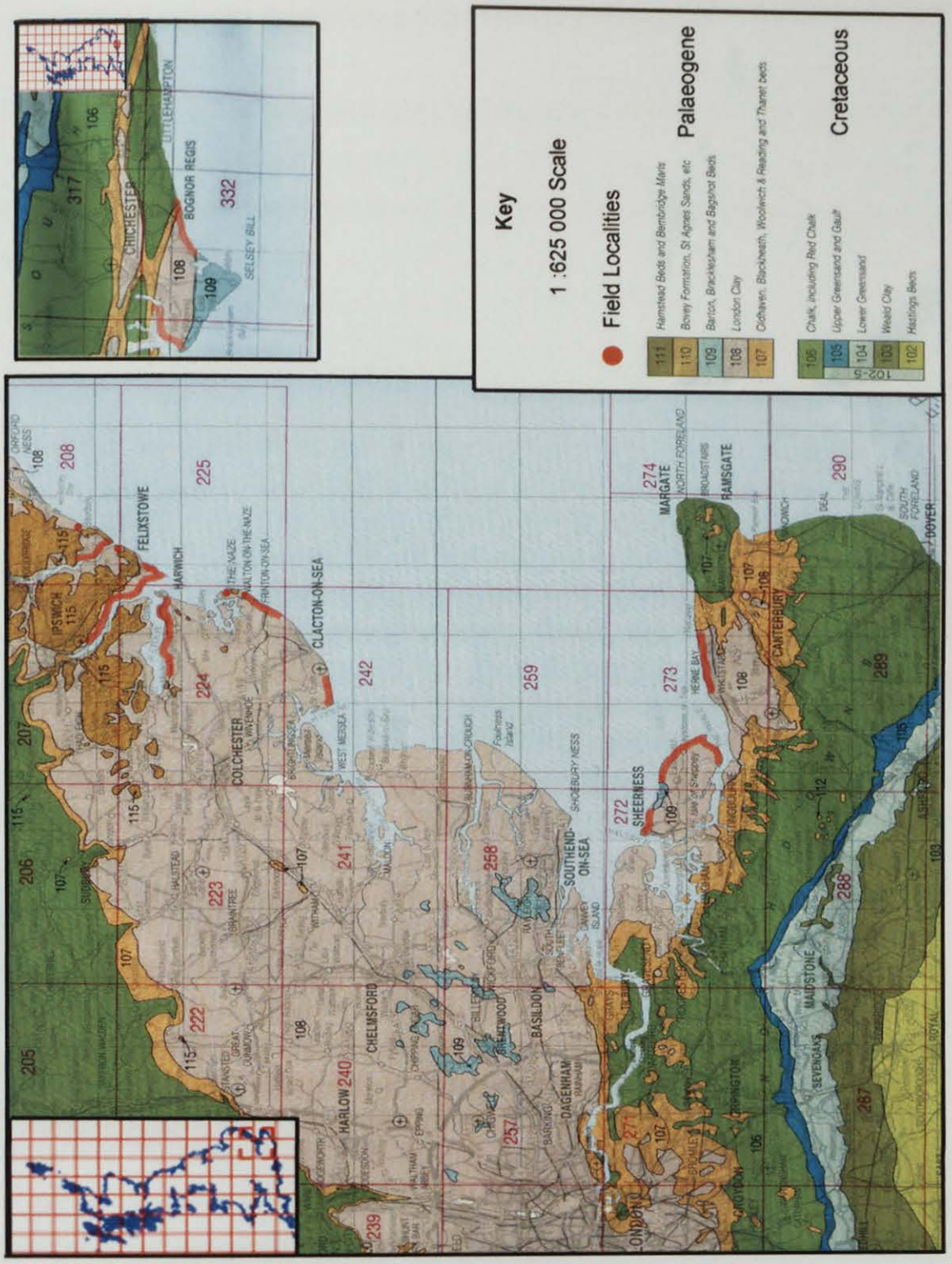

Figure 7.2: Location Map of fieldwork localities. Map from the solid geology map, UK south sheet, BGS (2001).

7.1.2 Distal Deposits Associated With Meteorite Impacts

Before fieldwork could be carried out an understanding of the types of deposits that are associated with meteorite impacts was needed. This understanding can further be refined if we consider that if the Silverpit structure formed as a result of a meteorite impact, it would have been a marine meteorite impact. Cameron et al (1992) show that the southern North Sea was a shallow marine environment during the Eocene with sea level reaching no more than 200m deep. This has significant implication for the type of deposit that may be found in the present day onshore stratigraphic record. Dypvik and Jansa (2003) review the sedimentary signatures and processes during marine bolide impacts. They suggest that the main mechanism of transport of impact material following collision is through shock-generated waves, tsunami deposits and resurge currents. These often result in the formation of turbidity current, grain flow, mud flow, debris flow and resuspension of finer particle deposits. The only way to distinguish if these deposits have been formed by meteorite impact and not by other processes such as seismic events or slope failures is by the presence of impact-produced sedimentary particles such as the various forms of melts, impact spherules, shocked quartz and geochemical anomalies.

The search for possible deposits associated with the Silverpit structure was therefore focused on trying to find the presence of anomalous turbidite, grain flow, mud flow, debris flow and tsunami deposits. Because of the relatively large age range the formation of the Silverpit structure is currently bracketing in, the initial identification of any deposits that could be associated with a meteorite impact were to be carried out by eye. Therefore only melts and impact spherules would clearly be recognised in the stratigraphic record. Melts and spherules would introduce a different mineralogy into the unit that may be a different colour, grain size or texture.

As a result of the wide range of deposits that may be associated with the impact, it has been difficult to establish the likely thickness of these deposits. However, because of the relatively small size of the impact (3 – 4km) and the distal location of

the field sites (approximately 150km away from the impact), centimetre to millimetre scale deposits were expected, if any were to be found at all.

7.1.3 Results and Problems associated with the Fieldwork

The fieldwork proved to be unsuccessful. The extremely populated nature of eastern England meant that the only readily accessible exposure was along the coastline or along riversides. In many of the localities visited the exposure could not be accessed or had been covered by coastal defence systems (Figure 7.3). Where exposure was accessible it was often extremely weathered making the identification of anomalous features completely impossible (Figure 7.4). One of the most significant problems is that the lithology of the Eocene deposits makes the identification of the features such as turbidite or mudflow deposits extremely difficult. King (1981 & 1984) details the stratigraphy of the London Clay and associated deposits. The deposits primarily consist of a series of interbedded clays, silts and silty sands. The problem is that turbidites, mud flows and debris flows in very distal locations are usually identified by the presence of a fining up sequence of sand, silt and finally clay. This meant that trying to distinguish normal London Clay deposits apart from anomalous meteorite impact created deposits was virtually impossible.

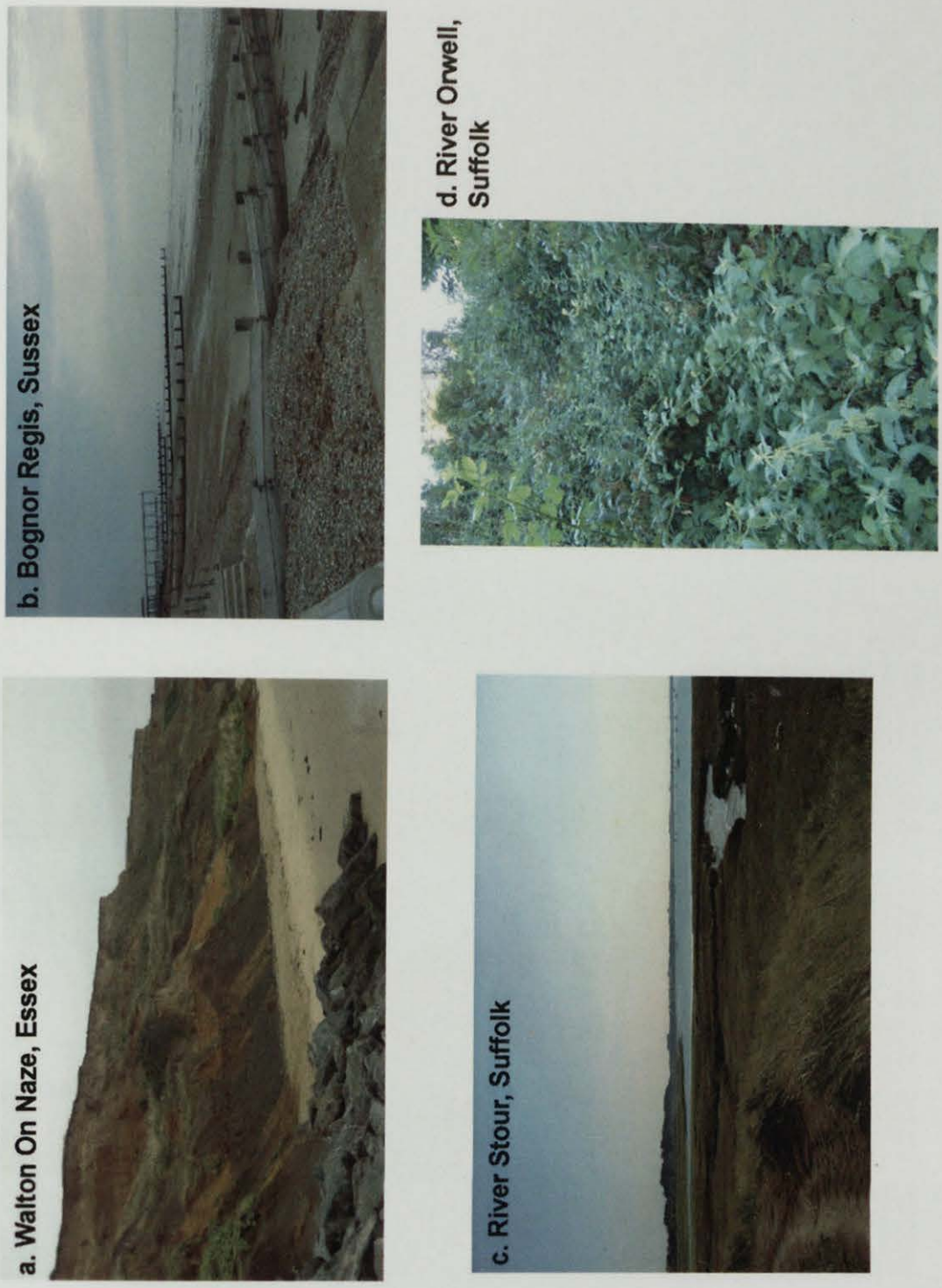

Figure 7.3: Photographs from the fieldwork localities: a. and b. highlight the coastal defence systems covering the exposure, c. highlights the lack of exposure and d. the inaccessible nature of much of the exposure.

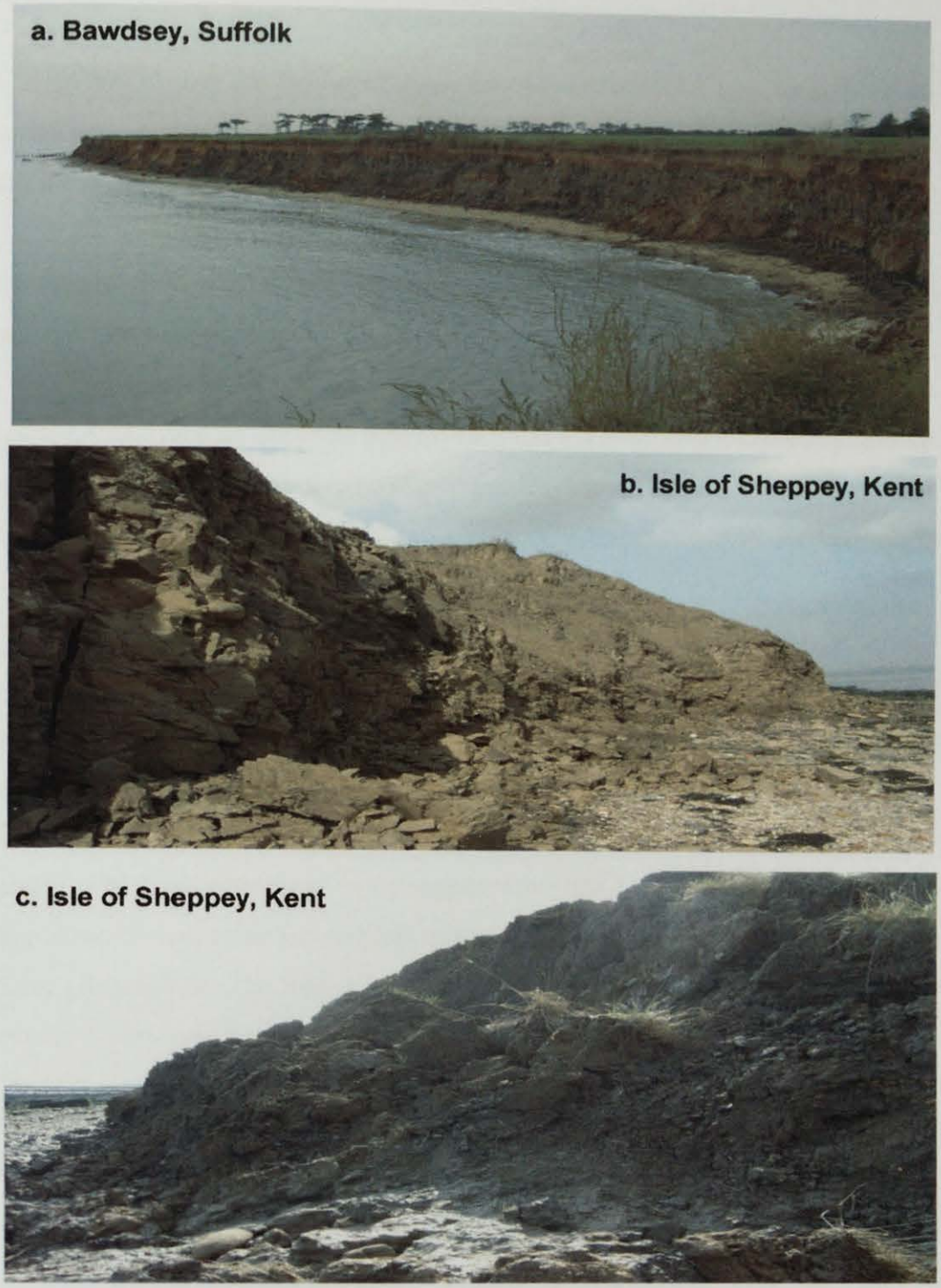

Figure 7.4: Photographs highlighting the extremely weathered nature of much of the exposure

7.2 Onshore Core Analysis

The main reason that the fieldwork proved to be unsuccessful was because of the lack and poor quality of Lower Eocene deposits. Therefore analysis of the available onshore core through the Lower Eocene was carried out.

7.2.1 Onshore Core Locations, Results and Problems Associated With Onshore Core Analysis

Cores were analysed at the BGS Keyworth. Figure 7.5 locates the cores that were examined. The analysis involved looking for the same features as the fieldwork, trying to identify anomalous beds or sequences of beds, as well as anomalous mineralogy and unusual grains / textures within the beds.

Once again the onshore core analysis proved to be unsuccessful. Of the thirty cores initially identified as potentially containing Lower Eocene deposits only three were logged. The majority of recent cores were restricted and so could not be analysed. Many of the older cores (drilled during the 1940s – 1970s) have significantly degraded. The high concentration of pyrite within the Lower Eocene deposits had broken down to iron oxide and sulphur that had overprinted any other features within the core (Figure 7.6). The logs of the three cores that were usable can be found in Appendix I. However, no unusual features were identified within these three cores.

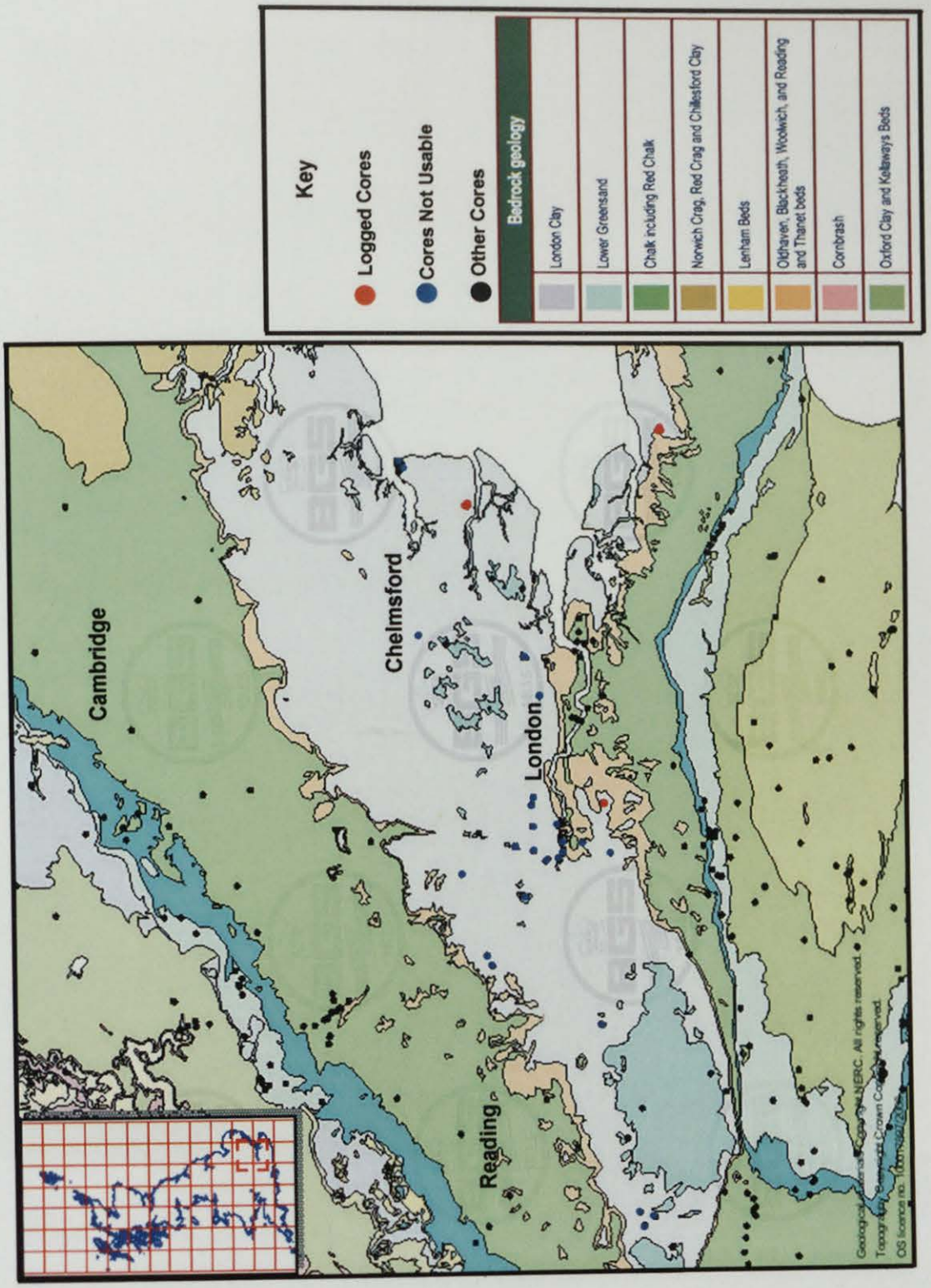

Figure 7.5: Location of the onshore cores. Only three were finally logged. Map from http://www.bgs.ac.uk/geoindex/index.htm.

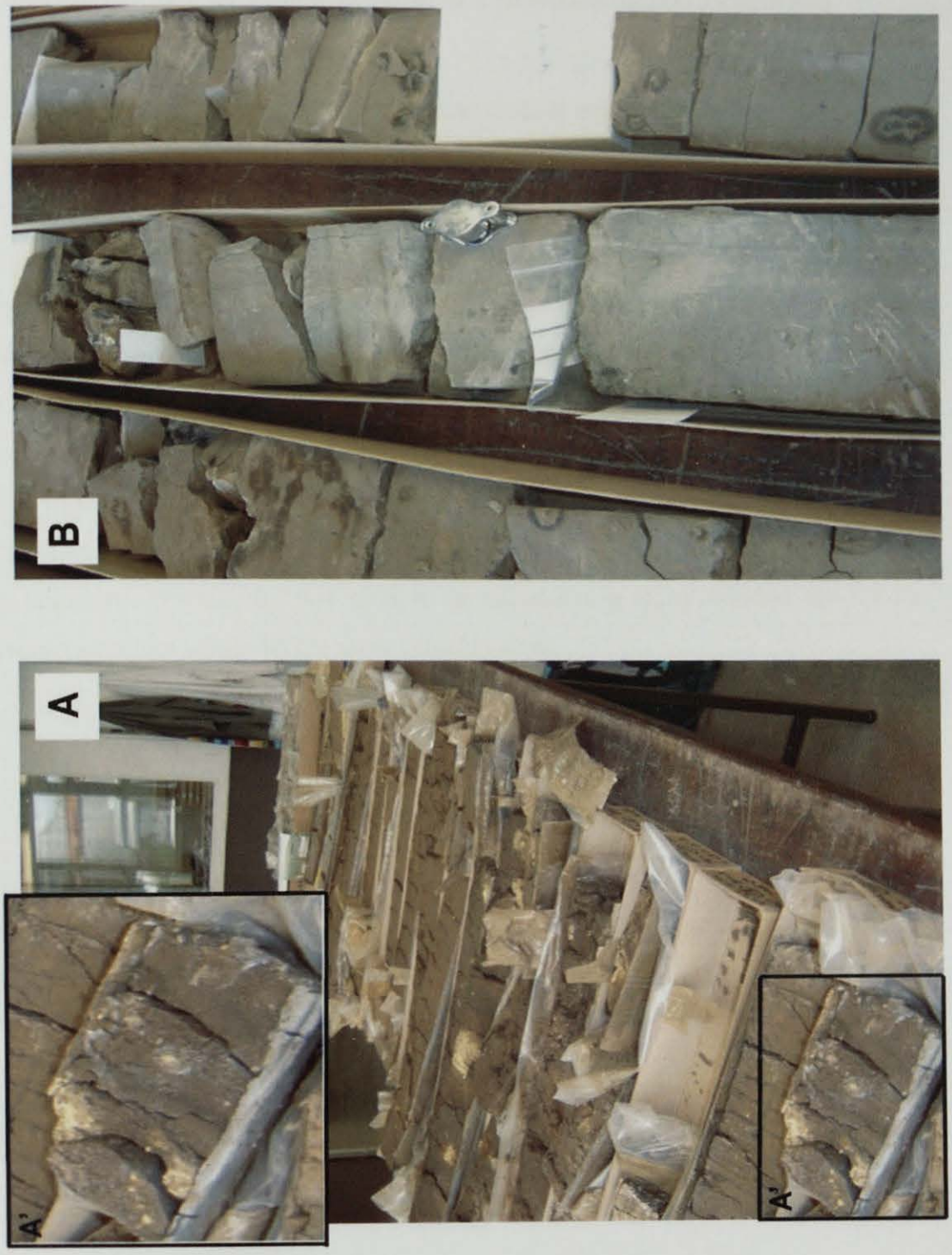

Figure 7.6: Photographs showing the varying condition of the available core. A. highlights a degraded core, A' shows the pyrite breaking down to iron oxide and sulphur. B. highlights core TQ19SE102 which was logged.

7.3 Discussion of Fieldwork and Onshore Core Analysis

It could be argued that because no meteorite impact evidence was identified during the fieldwork and onshore core analysis that meteorite impact is not responsible for the formation of the Silverpit structure. However, the results were inconclusive and as such neither strengthen nor weaken the meteorite impact hypothesis. The large age range that the Silverpit structure is currently attributed to means that this work was relatively loosely constrained. Attempting to examine in great detail the lithology of the Lower Eocene deposits and identify any anomalous features requires significantly more time and resources than were available during this study. It is an entire PhDs work in itself. The onshore core analysis could be greatly enhanced if access to the more recently drilled, but restricted, cores was available as these will be less degraded. Overall, for this work to be successful a more accurate age for the Silverpit structure would be the most valuable asset.

Chapter 8

8 Discussion

This chapter discusses and synthesises the main findings of this thesis presented in chapters 3 – 7. In this chapter the proposed hypotheses for the origin of the Silverpit structure will be systematically analysed. It will link together the different techniques used, including seismic interpretation, well log interpretation and stable isotope geochemistry to propose a model for the origin of the Silverpit structure. This chapter also discusses the limitations of this study and the wider implications of the research.

8.1 Viability of Proposed Hypotheses of Origin

The different features associated with Silverpit structure and the possible origins of their formation have been summarised in Table 8.1.

8.1.1 Pull-Apart Basin Tectonics

Smith (2004) suggested that the Silverpit structure formed as a result of underlying pull-apart basin tectonics, which forms the ring faulting. This is combined with a Jurassic shale diapir, which explains the conical uplift found in the centre of the structure. This thesis highlights that this is an unlikely mode of formation of the structure. Chapter 4 indicates that the faulting which affects the stratigraphy below the Zechstein evaporites is not unique to the Silverpit structure. The two adjacent synclines are the same scale and have the same structural setting. This being the case you may expect to find at least two more structures similar in geometry as the Silverpit structure.

The suggestion that the conical uplift formed as a result of a shale diapir is also unlikely to have taken place in the structural setting seen at the Silverpit structure. Chapter 4 discusses the ubiquitous nature of mudstone diapirs in contracting settings such as the Western Alborian basin (Talukder et al 2003). Again the work presented in Chapter 4 proves that the Silverpit structure is unique in the 3500km^2 studied.

The aspect ratio of the Silverpit structure is also not what you may expect to find if pull-apart basin tectonics were responsible for it's formation. Pull-apart basins generally have an aspect ratio of between 2 – 5 (Aydin and Nur 1982). The Silverpit structure has an aspect ratio of 1.04. The Silverpit structure is too circular to have formed as a result of pull-apart basin tectonics.

8.1.2 Salt Diapir Withdrawal

Salt withdrawal has been discussed at length throughout out this thesis. However, it is important to consider that two different salt withdrawal processes take place. Here we discuss the possibility that the Silverpit structure was formed as a result of a previously intruded salt diapir, which has then withdrawn. Regional salt withdrawal is discussed in section 8.1.3. Features associated with the Silverpit structure that could be attributed to the withdrawal of the Silverpit structure include: Ring faulting and the unusual diagenesis found in the chalk beneath the structure. Ring faults associated with salt diapir withdrawal have been identified in the East Texas basin (Maione and Pickford 2001) and are similar in dimensions as those seen at the Silverpit structure. The ring faults form where accommodation space is created as a result of the withdrawing diapir.

In Chapter 6, additional heat flow is suggested as the likely cause of the anomalous diagenesis in the chalk beneath the Silverpit structure. Hot water migration systems surrounding salt diapirs and their influence on chalk diagenesis is discussed by Jensenius and Munksgaard (1989). Additional carbonate material is precipitated in the hot water system. However, the trends seen at the Silverpit structure are not exactly the same. No additional fluids have entered the system at Silverpit. Also,

with salt diapirs, lateral temperature gradients are also present, this is not seen at the Silverpit structure. Never the less a salt diapir without the additional fluid flow, would still be a good explanation for possible elevated heat flow experienced by the chalk. Because the salt diapir would have risen up through the stratigraphy, with the source being the much deeper Zechstein Group evaporites, this hypothesis also explains why the unusual diagenesis is seen at the base of the chalk.

However, it is in fact very unlikely that the withdrawal of a salt diapir is responsible for the formation of the Silverpit structure. Detailed analysis of the stratigraphy beneath the Silverpit structure in Chapter 3 highlights that the stratigraphy beneath the structure is coherent, traceable and undeformed and that deformation decreases with increasing depth (figure 3.8). If we compare this to the East Texas basin example (figure 2.12), significant deformation is seen in the stratigraphy above and beneath the withdrawing salt diapir, with deformation seen close to the salt source in the deeper stratigraphy. The lack of deformation in the stratigraphy beneath the Silverpit structure suggests that a diapir has not penetrated the stratigraphy at any stage and that salt diapir withdrawal is not the cause of formation of the Silverpit structure.

8.1.3 Regional Salt Withdrawal

Regional salt withdrawal or dissolution is the second salt withdrawal mechanism considered as a possible origin for the Silverpit structure. Importantly, detailed analysis into the timing of the regional salt withdrawal compared with the formation of the structure correlate. Chapters 3 and 5 indicate that significant salt movement has taken place during the Tertiary. In Chapter 3 the age of the central zone of deformation of the Silverpit structure is bracketed as between 49 – 53 million years old and that the ring faults formed after that. Therefore the salt was moving at the same time the ring faults formed.

Some of the most significant features of the Silverpit structure can be explained to have arisen as a result of salt withdrawal. The Silverpit structure occurs in the centre

of a syncline that has formed as a result of salt withdrawal (Chapter 3). It is difficult to explain any other viable reason for the presence of the structure in this location. Ring faulting is also a key feature in structures associated with regional salt withdrawal and dissolution. For example in the Eastern Mediterranean (Chapter 2) ring faults arise as a result of accommodation space being created by the withdrawing evaporites at depth.

Despite the synclinal location of the Silverpit structure and the ring faults associated with it, there are still a number of features which are different from other salt withdrawal locations and that cannot be explained by salt withdrawal. The ring faulting is present only in the early Tertiary and late Cretaceous sediments (Figure 3.2). In the Eastern Mediterranean example ring faults continue down to the withdrawing evaporite unit (Figure 3.7). Unlike the Eastern Mediterranean example and other salt withdrawal provinces such Santos Basin, offshore Brazil, the Silverpit structure is unique in the 3500km^2 salt mobility affected study area. Numerous salt withdrawal structures are usually found together. Chapter 4 highlights that the Silverpit structural setting is not unique and so we may expect to find more of these features.

There are also other features that cannot be explained by the regional salt withdrawal hypothesis. The central zone of deformation and conical uplift cannot be formed as a result of regional salt withdrawal. In other examples such as the Eastern Mediterranean the centre of the ring fault structure remains undisturbed. Also, since regional salt withdrawal involves no penetration of the overburden by the evaporites, there is no explanation for the formation of the conical uplift seen at the Silverpit structure.

The unusual diagenesis found in the chalk beneath the Silverpit structure (Chapter 6) can also not be explained by regional salt withdrawal. For the same reason that the conical uplift can not be explained, there would be no mechanism with which to form any additional heat flow in the overburden which is more than 2 km above the withdrawing evaporites. Additionally, the unique nature of the diagenesis does not

correspond with the fact that there is salt withdrawal taking place throughout the study area (Chapter 4).

The timing of salt movement, location of the Silverpit structure in a salt induced syncline and the presence of ring faults agree with the salt withdrawal hypothesis of Underhill (2004). However, the unique nature of the structure, central zone of deformation and conical uplift and the unique diagenesis do not agree which suggests that salt withdrawal cannot be entirely responsible for the formation of the Silverpit structure.

Controversy surrounding the origin of circular structures in known salt provinces is not unique to the Silverpit structure example. Upheaval Dome, Utah, USA, is an exposed 5.5-km-diameter circular structure, whose origin remains contested. It consists of a complexly faulted and folded central uplift, surrounded by a ring structural depression and a circular monocline that defines its perimeter. Jackson et al (1998) suggest that the structure formed as a result of a pinched off salt diapir, whereas Kriens et al (1999) suggest that it formed as a result of a meteorite impact. The crater is extremely eroded and located in the Paradox Basin, an active salt province. It remains controversial because despite being exposed, the extreme erosion that has taken place has made it difficult to find any conclusive meteorite impact evidence. Kriens et al (1999) suggested that shatter cones and planar deformation features had been found in the centre of the structure. Despite this the debate about the origin of Upheaval Dome continues.

More recently a 20-km-diameter circular structure has been identified in the Upper Cretaceous of the Santos Basin, offshore Brazil. The Praia Grande Impact Structure is located above an active salt group, in a similar setting to the Silverpit structure (Correia et al 2005). It consists of a central high surrounded by a ring syncline and externally a series of listric normal faults. At present work on this structure is limited to seismic interpretation and similar controversies as are associated with the Silverpit structure exist.

8.1.4 Meteorite Impact

Stewart and Allen (2002) initially reported the structure as a multi-ringed impact crater. A significant proportion of the features associated with the Silverpit structure can be explained as a result of meteorite impact. The unique nature of the structure suggests that it formed as a result of a unique event, a meteorite impact is a unique event. Structurally, the central zone of deformation and conical uplift are regularly seen associated with complex meteorite impact craters, the formation of which is discussed in depth in Chapter 2. The decrease of deformation with depth as presented in Chapter 3 (Figure 3.8) is also consistent with a meteorite impact. The energy associated with the impact dissipates through the deeper stratigraphy and deformation decreases with increasing depth.

The unusual diagenesis found in the chalk beneath the Silverpit structure can also be explained by the meteorite impact hypothesis. Investigation into the kinetics of meteorite impacts highlights that there is heat flow associated with the formation of the central uplift (Pirajno 2005). Rebound of the hot rocks from below activates hydrothermal circulation in the rocks beneath the target horizon. This explains the presence of a decreased porosity at the base of the chalk. The Shoemaker impact of western Australia is a good example of this (Pirajno 2005). Higher-grade metamorphism is seen associated with the conical uplift than impacted horizon. If the heat source comes from the base of the chalk then more carbonate will be precipitated where the temperature is highest and a lower porosity would be expected.

The heat flow associated with the rebound of target rocks and the formation of a central uplift has been well documented in impact craters that contain economically valuable suites of rock. Examples include the Cu-Ni-PGE deposits of the Sudbury impact structure, Canada (Molnár 2001) and the Witwatersrand gold deposits at the Vredefort impact structure, South Africa (Grieve 2005). However, little has been documented on the post impact fluid flow in smaller, sedimentary rock based impacts.

The ring faults associated with the Silverpit structure present more of a problem. Stewart and Allen (2002) suggest that the ring faults form part of the multi-ringed impact crater. However, as discussed in Chapter 2, multi-ringed impacts are usually 100s – 1000s of kilometres in diameter. There is also still much debate as to whether any multi-ringed impact craters have been identified on Earth. Even the largest meteorite impact craters seen on Earth such as, the Vredefort impact crater, South Africa, the Sudbury crater, Canada and the Chicxulub impact crater, Gulf of Mexico have been questionably described as multi-ringed impacts (Grieve and Therriault 2000). Only Chicxulub has some morphological ring features and they are usually described as complex impact craters. The Silverpit structure is much smaller than these impacts and it is not simple to explain why it would be a multi-ringed meteorite impact. It could be as a result of the coherence of the sediment that the meteorite impacted into, but this is beyond the scope of the work carried out in this thesis.

It could be suggested that the reason that the Silverpit structure sits in the centre of a salt withdrawal induced syncline is because the meteorite impact has focussed the salt withdrawal. However, careful consideration of the evidence presented in thesis indicates that this is unlikely. Chapter 5 proves that the salt withdrawal is taking place regionally. Figure 4.4 shows that the Silverpit structure sits in an elongate syncline and not a circular basin shape as you might expect to find if the meteorite impact had focussed the salt withdrawal. There is also at least one other syncline of the same shape, size and orientation. Since these two synclines have the same underlying structural setting, it is likely that it is the underlying structure controlling the location of the synclines and not the meteorite impact (Stewart and Coward 1995).

There are some features associated with the Silverpit structure that cannot be explained by the meteorite impact hypothesis. The timing of formation of the ring faults (Chapter 3) is after the central zone of deformation, whereas with a multi-ringed impact you would expect the two to form at the same time. The meteorite

crater hypothesis also struggles to explain why the Silverpit structure sits in the centre of a salt induced syncline. These features will be discussed in Section 8.2.

	Pull-Apart Basin	Salt Diapir Withdrawal	Regional Salt Withdrawal	Meteorite Impact
Central Zone of Deformation	N	Y	N	Y
Conical Uplift	N	Y	N	Y
Ring Faulting	Y	Y	Y	N
Centre of a Syncline Location	Y	Y	Y	N
No Disturbance to Underlying Stratigraphy	Y	N	Y	Y
Aspect Ratio of 1.04	N	Y	Y	Y
Unusual Diagenesis	N	Y	N	Y
Unique	N	Y	N	Y

Table 8.1: Table highlighting the different features associated with the Silverpit structure and the processes that may have formed them.

8.2 Proposed Model of Formation of the Silverpit Structure

Comparing the features seen at the Silverpit structure with the hypotheses that have been suggested as possible origins for the structure, highlight that not one of the different hypotheses can explain all of the different features seen. Therefore, it is suggested that origin of the Silverpit structure is two-phase, involving a meteorite impact and regional salt withdrawal. The suggested formation is described below:

1. A small meteorite impact creates a 3 – 4 km diameter complex meteorite impact crater, which forms the central zone of deformation and conical uplift. The meteorite has been modelled by Collins et al (2005) to be approximately 120m diameter, travelling at between 20 – 50 Kms^{-1} and weighing approximately 2.0 x 10^9kg (assuming a stony meteorite).

2. Post impact heat flow leads to the formation of unusual diagenesis in the chalk beneath the crater. This additional heat enabled enhanced cementation, causing the porosity gradient to steepen. This formed a circular plug of more rigidly cemented rock to a maximum diameter of 20km.

3. The onset of salt mobility begins regionally during the Eocene. The Cretaceous Chalk that has been affected by unusual diagenesis has lower porosity and is therefore denser. The denser chalk is forced into the centre of the syncline forming as a result of salt withdrawal.

4. Ring faults are able to form in the youngest Cretaceous Chalk through to the Tertiary in response to the accommodation space being created by the withdrawing salt. This additional overburden is seen in other synclinal localities throughout the southern North Sea, but ring faults only form surrounding the Silverpit impact crater as a result of the presence of the impact modified chalk.

8.3 Problems with the study

The 3D seismic data that covers the Silverpit structure and surrounding area allow much investigation of the structure and it's relationship with the surrounding stratigraphy to take place. However, if the origin of the Silverpit structure is to be confirmed then more than just the examination of the seismic data is required. Despite having access to a database that contains all of the well data throughout the North Sea very little proved to be useful. From the two wells that penetrate the structure 43/25-1 and 43/24-3 (Chapters 3 and 6) only the sonic log produced results. The wells are run for the purpose of hydrocarbon exploration. The hydrocarbons in the southern North Sea are found in the much deeper Carboniferous and Permian units (Chapter 5). Therefore many of the geophysical well logs are not run through the very shallow Tertiary and Cretaceous deposits, which means that they are of limited use for this study. The lack of well log information in the shallow stratigraphy also means that the exact timing of salt mobility during the Tertiary cannot be established, neither can the age of the ring faults which would be useful to know.

The only rock material available from the Silverpit structure is the chippings that have been collected from two wells, 43/25-1 and 43/24-3 that penetrate the ring faults. These chippings are not collected continuously through the stratigraphy but are sampled at regular intervals. The chippings are only between 2 – 7mm in diameter. Without a continuous record through the stratigraphy the exact age of the structure cannot be determined. Chapter 7 highlights the problems associated with finding distal deposits with a wide age range to work with. The small size of the chippings and the non-continuous sampling also makes the search for key meteorite impact identifiers, such as shocked quartz or glass spherules extremely difficult. Koeberl and Reimold (2006) did investigate the chippings collected through the appropriate Tertiary horizons, but found nothing. Their conclusions suggested that it is not that these features do not exist just that the sampling may not have included the impact horizon.

8.4 Future of this research

8.4.1 Silverpit Structure Research

Much has now been published on the structural attributes and features associated with the Silverpit structure and the possible origins of these. Detailed seismic interpretation has allowed the shape of the structure to be studied in great depth, but it remains an unconfirmed meteorite impact crater. Although not particularly useful for confirming the origin of the structure, it would be useful to have the section of missing data found in the SE area of the structure imaged.

In order for the research to progress and diversify, ideally the centre of the structure needs to be cored. This would provide rock with which detailed mineralogical and geochemical analysis could test the meteorite impact hypothesis. It would also allow the age of the structure to be more clearly constrained. This would support much more targeted fieldwork in the UK and Europe to find distal deposits associated with the impact. A detailed study of the offshore core material looking for both proximal and distal deposits associated with the impact would also be useful, but again relies on a well-constrained age to be successful.

As this thesis was being completed unusual rock material was discovered in the chippings collected from well 43/19a-C1 drilled by RWE UK. The well is located at 54° 28' 43.53"N, 001° 44' 24.87"E. Unfortunately the samples arrived too late to be analysed and included in this thesis. However, as it is unlikely that the Silverpit structure will be cored in the foreseeable future, these chippings may hold the key to confirming the origin of the Silverpit structure.

8.4.2 Buried Meteorite Impact Craters: Can Extra-Terrestrial Criteria Be Used on Earth?

As discussed by Stewart (2003), buried meteorite impacts pose a unique geologic problem. Even if the shape and structural elements match exactly what is seen and

what is expected to be seen in a meteorite impact crater, the structure cannot be confirmed as a meteorite impact crater. Only if certain mineralogical or geochemical responses (such as shocked quartz or an unusually high iridium content) are found in rock material from or surrounding the structure, is the structure confirmed as a meteorite impact crater. Drilling and coring costs are often expensive and prohibit the acquisition of rock material from buried circular structures, as is the case with the Silverpit structure.

The Silverpit structure is a good example of a structure that has many of the distinguishing features associated with a meteorite impact, but remains an unconfirmed crater. It is likely that with more and more of the Earth's surface being seismically imaged that more of these buried circular structures will be identified. This being the case, the classification system that has been reserved for extra-terrestrial impact may have to be used. Extra-terrestrial impacts are recognised by their shape and distinguishing features. Rock samples are not available to carry out mineralogical and geochemical analysis, but the structure is still recognised as a meteorite impact crater. The detailed investigation that has been carried out in this thesis by systematically considering and discussing / rejecting the different hypotheses that may be responsible for the formation of the structure and demonstrating that only meteorite impact could be responsible for these features will have to become a more accepted identification method.

Unless there is a change in confirming that a circular structure on Earth is a meteorite impact crater, many of the buried structures will remain unclassified.

9 Conclusions

1) The Silverpit structure is unique within the 3500km^2 area studied.

2) The ring faults of the Silverpit structure formed after the central deformation and conical uplift.

3) The age of the central deformation zone and conical uplift of the Silverpit structure has been determined to be 53 – 49Ma, Ypresian, Early Eocene.

4) Deformation associated with the structure decreases with increasing depth suggesting that the deformation occurred from the top down rather than the bottom up. No disturbance of the horizons beneath the structure exists.

5) Zechstein salt movement has played the dominant role in the deposition of the post Triassic sediment and has continued to move into the Tertiary, with a significant change in direction of movement of the salt at some stage between the Jurassic and late Tertiary.

6) An anomalous sonic well log response, with a more rapid transit time is present in the base of the Cretaceous Chalk Group beneath the Silverpit structure and nowhere else in the study area.

7) Stable isotope analysis of carbon and oxygen isotopic compositions of the chalk highlight a linear $\delta^{18}O$/depth trend in the chalk with an anomalous gradient beneath the Silverpit structure and nowhere else in the study area. This is compatible with increased cementation.

8) Unusual and unique diagenesis of the chalk beneath the Silverpit structure has occurred.

9) The formation of the Silverpit structure occurred in two-phases. Meteorite impact created the central zone of deformation, conical uplift and provoked unusual diagenesis in the chalk around the impact site. Subsequent withdrawal of salt on a regional scale led to the formation of subsidence rings. The circular rings are controlled in their shape and position by the extensively cemented plug of chalk. This rigid plug controlled the position of a salt induced syncline axis, orientated parallel to the regional structural trend.

Bibliography

Allemand, P. & Thomas, P. 1999. Small-scale models of Multiring basins. *Journal of Geophysical Research.* **104**, 16 501–16 514.

Alvarez, L. W. 1987. Mass extinctions caused by large bolide impacts. *Physics Today.* **40**, 24–33.

Arthurthurton, R. S., Booth, S. J., Morigi, A. N., Abbott, M. A. W. & Wood, C. J. 1994. Geology of the country around Great Yarmouth. *Memoir of the British Geological Survey.* Sheet 162 (England and Wales).

Aydin, A. & Nur, A. 1982. Evolution of pull apart basins and their scale independence. *Tectonics.* **1**, 91–105.

Becker, L., Poreda, R.J., Bash, A. R, Pope, K. O., Harrison, T. M. Nicholson, C. & Lasky, R. 2004, Bedout: A Possible End-Permian Impact Crater Offshore of Northwestern Australia. *Science.* **304**, 1469-1476.

Bertoni, C. and Cartwright, J.A. 2005. 3D Seismic analysis of circular evaporite dissolution structures, Eastern Mediterranean. *Journal of the Geological Society, London.* **162**, 909-926.

Bidgood, M. D., Jutson, D. J., Johnson, B. (in prep) Results of the Microfossil & Nannofossil Analysis of the base Tertiary to uppermost Late Cretaceous interval from two wells in the locality of the U.K. North Sea "Silverpit Crater" – Biostratigraphic support for an impact origin to the structure. *Journal of Micropalaeontology.*

British Geological Survey 2001. Solid Geology Map, UK South Sheet 1:625 000 (4th Edition).

British Geological Survey Geoindex website: http://www.bgs.ac.uk/geoindex/index.htm - accessed 15/11/06.

Cameron, T. D. J., Crosby, A., Balson, P.S., Jeffery, D. H., Lott, G.K., Bulat, J. & Harrison, D. J. 1992. United Kingdom Offshore Regional Report: The geology of the southern North Sea. London. *HMSO, for the British Geological Survey.*

Correia, G. A., Corrêa de Menezes, J. R., Bueno, G. V. & Marques, E. J. J. 2005. 3D Seismic Interpretation of the Praia Grande Impact Structure – Upper Cretaceous of Santos Basin, Offshore Brazil. Presented: *9th International Congress of the Brazilian Geophysical Society.*

Chacko, T., Cole, D. R. & Horita, J. 2001. Equilibrium oxygen, hydrogen and carbon isotope fractionation factors applicable to geologic systems. *Reviews in Mineralogy and Geochemistry*. **43**, 1-81.

Chatwin, C.P. 1961. British regional geology, East Anglia and adjoining areas. HMSO.

Clausen, O. R., Nielson, O. B., Huuse, H. & Michelsen, O. 2000. Geological indications for Palaeogene uplift in the eastern North Sea Basin. *Global and Planetary Change*. **24**, 175-187.

Collins, G. S., E. P. Turtle, H. J. Melosh 2003. Numerical Simulations of Silverpit Crater Collapse: A Comparison of Tekton and SALES-2. In: Impact Cratering: Bridging the Gap Between Modeling and Observation, LPI Contribution No. 1155, Lunar and Planetary Institute, Houston, p 18.

Czerniakowski, L. A., Lohmann, K. C. & Wilson, J. L. 1984. Closed-system burial diagenesis: isotopic data from the Austin Chalk and its components. *Sedimentology*. **31**, 863-877.

Davies, R. J. & Stewart, S. A. 2005. Emplacement of giant mud volcanoes in the South Caspian Basin: 3D seismic reflection imaging of their root zones. *Journal of the Geological Society, London*. **162**, 1–4.

Davison, I., Alsop, I. & Blundell, D. Salt tectonics: some aspects of deformation mechanics. In: Alsop, G. I., Blundell, D. J. & Davison, I. 1996. Salt Tectonics. *Journal of the Geological Society, London, Special Publications*. **100**, 1–10.

Deville, E., Battani, A., Griboulard, R., Guerlais, S., Herbin, J. P., Houzay, J. P., Muller, C. & Prinzhofer, A. 2003. The origin and processes of mud volcanism: new insights from Trinidad. *Geological Society of America, Special Publication*. **216**, 475-490.

Dypvik, H., Attrep Jr., M., 1999. Geochemical signals of the late Jurassic, marine Mjølnir impact. *Meteoritics and Planetary Science*. **34**, 393–406.

Dypvik, H., Ferrell Jr., R. E., 1998. Clay mineral alterations associated with a submarine meteorite impact. *Clay Minerals*. **33**, 51 – 64.

Dypvik, H. & Jansa, L. F. 2003. Sedimentary signatures and processes during marine bolide impacts: a review. *Sedimentary Geology*. **161**, 309–337.

Earth Impact Database: www.unb.ca/passc/impactdatabase/index.html - Accessed September 2006.

Egeberg, P. K and Saigal, G. C. 1991. North Sea chalk diagenesis: cementation of chalks and healing of fractures. *Chemical Geology*. **92**, 339–354.

Fabricus, I. 2003. How burial diagenesis of chalk sediments controls sonic velocity and porosity. *AAPG Bulletin.* **87**, 1755-1778.

Farris Lapidus, D., 1990, Dictionary of geology: Collins, London and Glasgow, 349–350.

Glennie, K. W., 1998, Petroleum Geology of the North Sea: Basic concepts and recent advances (4th Edition). Blackwell Science Ltd, London, 172 - 211.

Grieve, R. A. F. 2005. Economic natural resource deposits at terrestrial impact structures. *Geological Society Special Publication.* **248**, 1-29.

Grieve, R. A. & Therriault, A. 2000. Vredefort, Sudbury, Chicxulub: Three of a Kind? *Annual review of Earth and Planetary Sciences.* **28**, 305– 38.

Hartmann, W. K. & Yale, F. G. 1971: Mare Orientale and its basin system. *Communications in Lunar Planetary Laboratory.* **7**, 327–356.

Head, J. W. 1977. Origin of the outer rings in lunar multi-ring basins. Evidence from morphology and ring spacing. In *Impact and explosion cratering* (eds. D. J. Roddy, R. O. Pepin, R. B. Merrill). Pergamon Press, New York, 563–573.

Hodges, C. A. & Wilhelms, D. E. 1978. Formation of lunar basin rings. *Icarus.* **34**, 294–323.

Jenyon, M.K. 1988. Overburden deformation related to the pre-piercement development of salt structures in the North Sea. Journal of the Geological Society, London. **145**, 445-454.

Jackson, M. P. A., Schultz-Ela, D. D., Hudec, M. R., Watson, I. A. & Porter, M. L. 1998. Structure and evolution of Upheaval Dome: A pinched-off salt diapir. *GSA Bulletin.* **110,** 1547-1573.

Jenyon, M. K. 1988. Some deformation effects in a clastic overburden resulting from salt mobility. *Journal of Petroleum Geology.* **11**, 309–324.

Jensenius, J. & Munksgaard, N. C. 1989. Large scale hot water migration systems around salt diapirs in the Danish Central Trough and their impact on diagenesis of chalk reservoirs. *Geochimica and Cosmochimica Acta.* **53**, 79-88.

Jørgensen, N. O. 1987. Oxygen and carbon isotope compositions of Upper Cretaceous chalk from the Danish sub-basin and the North Sea Central Graben. *Sedimentology.* **34**, 559-570.

Kenkmann, T. 2002. Folding within seconds. *Geology.* **30**, 231–234.

King, C. 1984. The stratigraphy of the London Clay Formation and the Virginia Water Formation in the coastal sections of the Isle of Sheppey (Kent, England). *Tertiary Research.* **5,** 121 – 160.

King, C. 1981. The stratigraphy of the London Clay and associated deposits. *Tertiary Research, Special Paper.* **6,** 7 – 39.

Koeberl, C. 2002. Mineralogical and geochemical aspects of impact craters. *Mineralogical Magazine.* **66,** 745-768.

Koeberl, C. A., Plescia, J. B., Hayward, C. L. & Reimold, W. U. 1999. A petrographical and geochemical study of quartzose nodules, country rocks, and dike rocks from the Upheaval Dome structure, Utah. *Meteoritics and Planetary Science.* **34,** 861–868.

Kriens, B. J., Shoemaker, E. M. & Herkenhoff K. E. 1999. Geology of the Upheaval Dome impact structure, southeast Utah. *Journal of Geophysical Research.* **104,** 18 867- 18 887.

Lake, R. D., Ellison, R. A., Henson, M. R. & Conway, B. W. 1986. Geology of the country around Southend and Foulness. *Memoirs of the British Geological Survey.* Sheets 258 & 259.

Larsen, B. D., Ben-Avraham, Z. & Shulman, H. 2001. Fault and salt tectonics in the southern Dead Sea basin. *Tectonophysics.* **346,** 71-90.

McCrea, J. M. 1950. On the isotopic chemistry of carbonates and a paleotemperature scale. *J. Chem. Phys,* **18,** 849-857.

Mallon, A. J. & Swarbrick, R.E 2002. A compaction trend for non-reservoir North Sea Chalk. *Marine and petroleum Geology,* **19,** 527-539.

Maione, S. J. & Pickford, S. 2001. Discovery of ring faults associated with salt withdrawal basins, Early Cretaceous, in the East Texas Basin. *The Leading Edge.* **20,** 818-829.

Melosh, H. J., 1989, Impact cratering: A geologic process: New York, Oxford University Press.

Melosh, H. J. & McKinnon, W. B. 1978. The mechanics of ringed basin formation. *Geophysical Research letters.* **5,** 985–988.

Melville, R. V. & Freshney, E. C. 1982. British regional geology, the Hampshire basin and adjoining areas. HMSO.

Mjølnir Homepage: http//folk.uio.no/ftisikala/mjolnir – Accessed September 2006.

Molnár, F., Watkinson D. H. & Jones P.C. 2001. Multiple hydrothermal processes in footwall units of the North Range, Sudbury Igneous Complex, Canada and implications for the genesis of vein type Cu-Ni-PGE deposits. *Economic Geology.* **96**, 1645-1670.

O'Keefe, J. D. & Ahrens, T. J. 1999. Complex craters: Relationships of stratigraphy and rings to impact conditions. *Journal of Geophysical Research.* **104**, 27 091–27 104.

O'Mara, P.T., Merryweather, M., Stockwell, M & Bowler, M.M. 2003. The Trent Gas Field, Block 43/24a, UK North Sea. In: Gluyas, J.G. & Hichens, H.M. (Eds.): United Kingdom Oil and Gas Fields. Commemorative Millennium Volume. Geological Society, London, Memoir, 20, 835-849.

Ormö, J. & Lindström, M. 2000. When a cosmic impact strikes the sea bed. *Geological Magazine.* **137**, 67–80.

Pattison, J., Berridge, N. G., Allsop, J. M. & Wilkinson, I. P. 1993. Geology of the country around Sudbury (Suffolk). *Memoir of the British Geological Survey.* Sheet 206 (England and Wales).

Petroleum Geo-Services (PGS), 2006, Southern North Sea Mega Merge Survey: http://www.pgs.com/Custom/templates/DataLibrary/survey____25680.aspx

Pirajno, F. 2005. Hydrothermal processes associated with meteorite impact structures: evidence from three Australian examples and implications for economic resources. *Australian Journal of Earth Sciences.* **52,** 587-605.

Rider, M. H. 2002. The geological interpretation of well logs. Rider French Consulting.

Røgen, B., Fabricus, I., Japsen, P., Høier, C., Mavko, G. & Pederson, J. M. 2005. Ultrasonic velocities of chalk samples:influence of porosity, fluid content and texture. *Geophysical Prospecting.* **53**, 481-496.

Rosenbaum, J. M. & Sheppard, S. M. F. 1986. An isotopic study of siderites, dolomites and ankerites at high temperatures. *Geochimica and Cosmochimica* Acta. **50**, 1147-1159.

Scholle, P. A. 1977. Chalk diagenesis and its relation to petroleum exploration: Oil from chalks, a modern miracle? *Bulletin of the American Association of Petroleum Geologists.* **61**, 982 – 1009.

Sherlock, R. L. 1947. British Regional Geology, London and Thames Valley. HMSO.

Shoemaker, E. M. 1998. Long Term Variations in the impact cratering record on Earth. In Grady, M. M., Hutchison, R., McCall, G. J. H. and Rothery, D. A. (eds):

Meteorites: Flux with time and impact effects. *Geological Society, London, Special Publications*. **140**, 7–10.

Smith, K. 2004. The North Sea Silverpit Crater: impact structure or pull apart basin? *Journal of the Geological Society, London*. **161**, 593-602.

Stewart, S. A. 2003. How will we recognise buried impact craters in terrestrial sedimentary basins? *Geology*. **31**, 929–932.

Stewart, S. A. 1999. Seismic interpretation of circular geologic structures. *Petroleum Geoscience*. **5**, 273-285.

Stewart, S. A. & Allen, P.J 2002. A 20-km-diameter multi-ringed impact structure in the North Sea. *Nature*. **418**, 520-523.

Stewart, S. A. & Coward, M.P. 1995. Synthesis of salt tectonics in the southern North Sea, UK. *Marine and Petroleum Geology*. **12**, 457-475.

Sylvester, A. G. 1988. Strike slip faults. *Geological Society of America Bulletin*. **100**, 1666–1703.

Talukder, A. R., Comas, M. C. & Soto, J. L. 2003. Pliocene to Recent mud diapirism and related mud volcanoes in the Alboran Sea (Western Mediterranean), *in* Van Rensbergen, P., Hillis, R. R., Maltman, A. J. and Morley, C. K. eds., Subsurface Sediment Mobilization. *Geological Society of London, Special Publications*. **216**, 443-459.

Thomson, K. 2004. Overburden deformation associated with halokinesis in the Southern North Sea: implications for the origin of the Silverpit Crater. *Visual Geosciences*. 10.1007/s10069-004-0019-0 Elsevier.

Thomson, K., Owen, P. & Smith, K. 2005. Discussion on the North Sea Silverpit Crater: impact structure or pull-apart basin? *Journal of the Geological Society. London*. **162**, 217–220.

Tsikalas, F., Gudlaugsson, S. T., Eldholm, O. & Faleide, J. I., 1998. Integrated geophysical analysis supporting the impact origin of the Mjølnir structure, Barents Sea. *Tectonophysics*. **289**, 257–280.

Tsikalas, F., Gudlaugsson, S. T. & Faleide, J. I. 1998. The anatomy of a buried impact structure: The Mjolnir structure, Barents Sea. *Journal of Geophysical Research*. **103**, 30469-30483.

Tsikalas, F., Gudlaugsson, S. T., Faleide, J. I. & Eldholm, O. 2002. The Mjølnir impact crater porosity anomaly. *Deep Sea Research II*. **49**, 1103–1120.

Tucker, M. E. & Wright, V.P. 1990. Carbonate Sedimentology. Blacwell Science Ltd.

Twiss, R. J. & Moores E. M. 1992. Structural Geology. Freeman, New York, USA.

Underhill, J. R. 2004. An alternative origin for the 'Silverpit Crater'. *Nature*, DOI 10138/nateure02476.

Van Rensbergen, P. & Morley, C. K. 2003. Re-evaluation of mobile shale occurrences on seismic sections of the Champion and Baram deltas, offshore Brunei. *Geological Society of London Special Publication.* **216**, 395-409.

Varol, O. 1998, Palaeogene. In: Bown, P. (ed.) Calcareous Nannofossil Biostratigraphy, BMS Publ. Series, Chapman & Hall, 200-224.

Walkden, G., Parker, J. & Kelley, S. 2002. A late Triassic impact ejecta in southwestern Britain. *Science.* **298**, 2185–2188.

Zanda, B. & Rotaru, M. 2001. Meteorites. Cambridge University Press, p 31 – 39.

Appendix i

Stable Isotope Results

Well No	Sample No	Depth (ft)	δ^{13} C VPDB	δ^{18}O VPDB	δ^{18}O VSMOW
49/01-4	1	3420	2.29	-1.46	29.40
49/01-4	2	3630 - 3660	1.78	-1.00	29.88
49/01-4	3	3840 - 3870	1.92	-1.01	29.86
49/01-4	4	3990 - 4020	2.39	-1.63	29.23
49/01-4	5	4200 - 4230	2.32	-1.92	28.93
49/01-4	6	4410 - 4440	2.19	-1.74	29.11
49/01-4	7	4590 - 4620	2.17	-1.43	29.43
49/01-4	8	4800 - 4830	2.15	-1.68	29.17
49/01-4	9	5010 - 5040	2.63	-2.45	28.39
49/01-4	10	5190 - 5220	2.39	-2.20	28.64
49/01-4	11	5400 - 5430	2.25	-2.36	28.47
49/01-4	12	5610 - 5640	2.25	-2.32	28.52
49/01-4	13	5820	2.58	-2.77	28.05
49/01-4	14	6030	2.49	-2.47	28.37
49/01-4	15	6240	2.57	-2.75	28.08
49/01-4	16	6420	2.44	-2.70	28.13
49/01-4	17	6680	2.34	-2.91	27.91
49/01-4	18	6810 - 6840	2.47	-3.16	27.66
49/01-4	19	6990 - 7020	2.60	-3.80	26.99
49/01-4	20	7200 - 7230	2.17	-3.68	27.11
49/01-4	21	7410 - 7440	3.31	-3.68	27.11
43/24-3	22	1700	1.41	-1.20	29.68
43/24-3	23	1750	1.89	-1.03	29.84
43/24-3	24	1800	2.26	-1.38	29.48
43/24-3	25	1850	2.26	-1.33	29.54
43/24-3	26	1900	2.18	-1.55	29.32
43/24-3	27	1950	2.34	-1.29	29.58
43/24-3	28	2000	2.32	-1.55	29.31
43/24-3	29	2050	2.09	-1.69	29.17
43/24-3	30	2100	2.25	-1.78	29.08
43/24-3	31	2150	2.11	-1.54	29.32
43/24-3	32	2200	1.99	-1.53	29.33
43/24-3	33	2250	2.12	-1.56	29.30
43/24-3	34	2300	2.25	-1.72	29.14
43/24-3	35	2350	2.28	-1.78	29.08
43/24-3	36	2400	2.19	-1.77	29.09
43/24-3	37	2450	2.23	-1.69	29.16
43/24-3	38	2500	2.29	-1.46	29.41
43/24-3	39	2550	2.38	-1.77	29.09
43/24-3	40	2600	2.36	-1.77	29.09

43/24-3	41	2650	2.45	-1.61	29.25
43/24-3	42	2700	2.47	-2.00	28.85
43/24-3	43	2750	1.95	-2.09	28.75
43/24-3	44	2800	2.13	-2.50	28.33
43/24-3	45	2850	2.36	-2.45	28.39
43/24-3	46	2900	2.50	-2.71	28.12
43/24-3	47	2950	2.69	-2.97	27.85
43/24-3	48	3000	2.52	-2.28	28.56
43/24-3	49	3050	2.39	-2.86	27.96
43/24-3	50	3100	2.43	-3.46	27.34
43/24-3	51	3150	2.62	-3.69	27.11
43/24-3	52	3200	2.77	-4.04	26.74
43/24-3	53	3250	2.67	-4.14	26.64
43/24-3	54	3300	2.39	-4.10	26.68
43/24-3	55	3350	2.24	-4.03	26.76
43/24-3	56	3400	2.36	-4.21	26.57
43/24-3	57	3450	2.78	-4.16	26.63
43/24-3	58	3500	3.18	-4.29	26.49
43/25-1	59	2800	2.04	-2.04	28.81
43/25-1	60	2900	2.20	-2.02	28.83
43/25-1	61	3000	2.20	-1.64	29.21
43/25-1	62	3100	2.27	-1.70	29.16
43/25-1	63	3200	2.36	-1.80	29.05
43/25-1	64	3300	2.51	-1.95	28.90
43/25-1	65	3400	2.37	-1.98	28.87
43/25-1	66	3500	2.61	-2.04	28.80
43/25-1	67	3600	2.58	-2.30	28.54
43/25-1	68	3700	2.49	-2.63	28.20
43/25-1	69	3800	2.48	-3.30	27.50
43/25-1	70	3900	2.62	-3.69	27.11
43/25-1	71	4000	2.60	-3.72	27.08
43/25-1	72	4100	2.28	-4.04	26.75
43/25-1	73	4200	2.52	-4.26	26.51
43/25-1	74	4300	2.76	-3.51	27.29

Appendix ii

Core Logs

Holly Hill BH3 TR06SE19

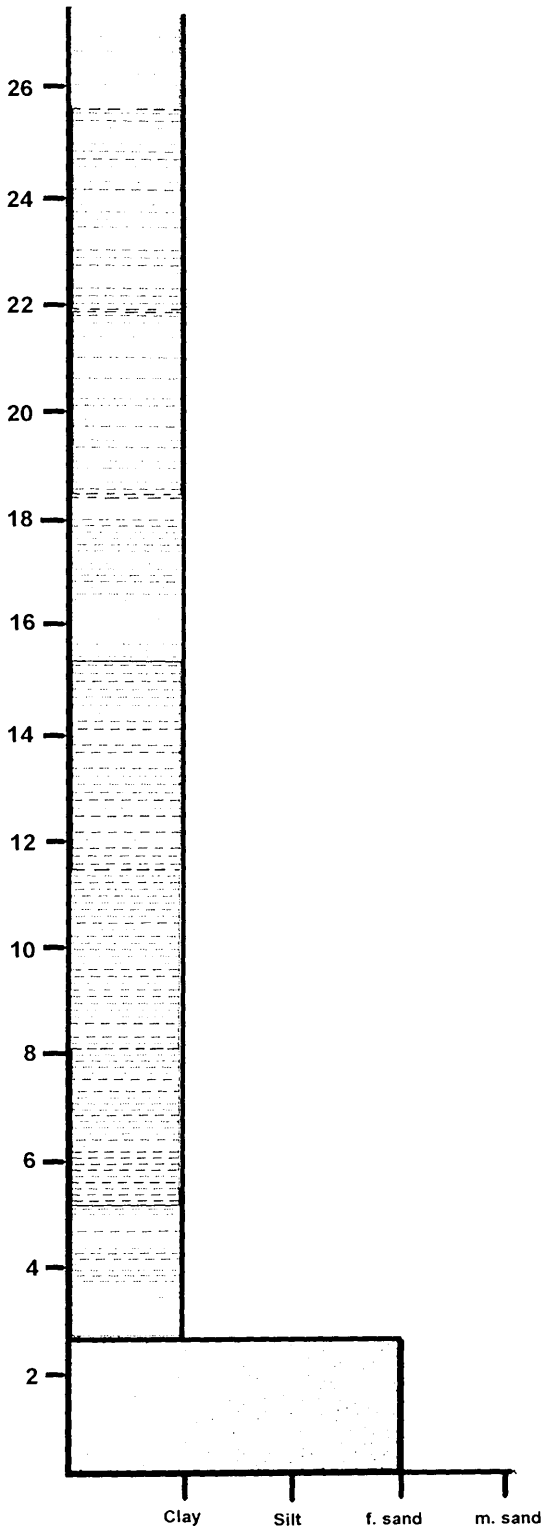

Almost impossible to see original clay lots of breakdown of pyrite. Both sulphur and iron oxide present

Many bands of orange colour with small black and sulphur rich bands replacing pyrite

Homogenous brown clay

Significant breakdown of pyrite, sulphur and iron oxide present in bands

Organic matter and sporadic fragmenetd shell material

Homogenous, sporadic an d sparse shell fragments. Sulphurus nodules from pyrite breakdown.

Clay becomes darker brown to top of bed

Homogenous brown clay, irregular distribution of small organic particles

Very fine sand, orange / brown

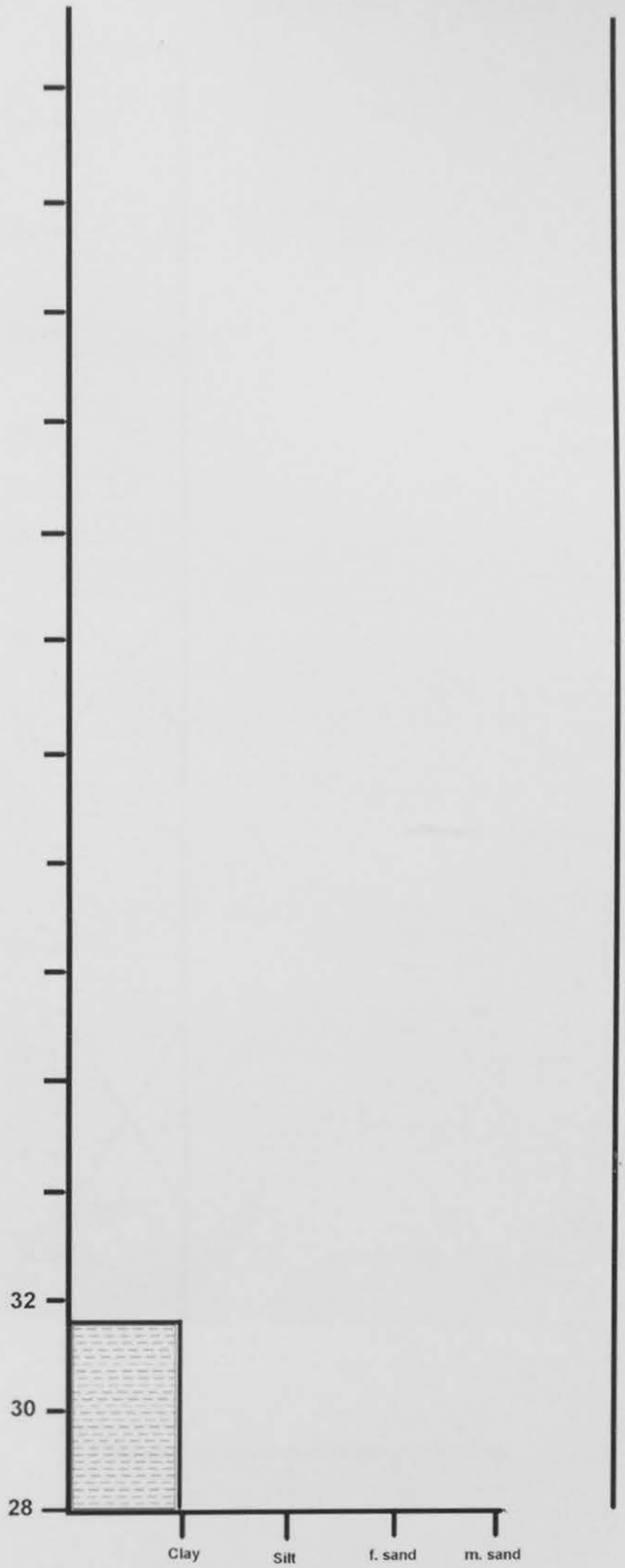

Homogenous brown clay, less breakdown products

Stanmore Common TQ19SE102

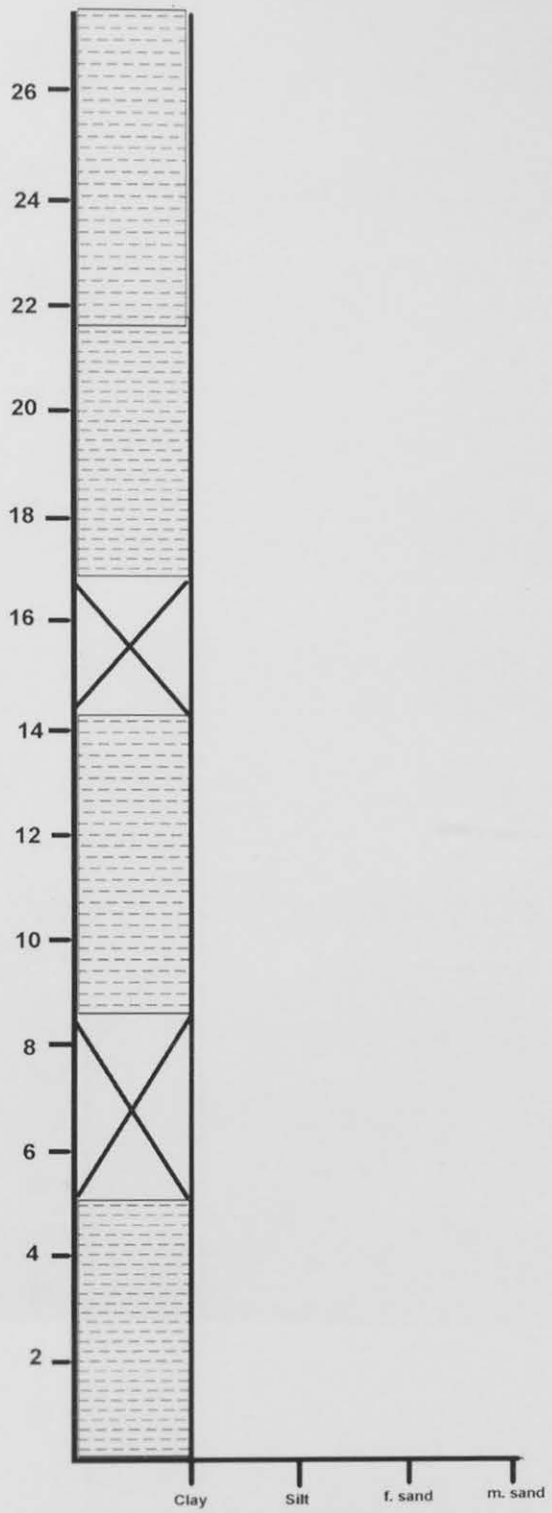

Homogenous light brown clay

Large nodules of sulphur from pyrite breakdown, sporadic small (1-2cm) pebbles

Missing Core

Darker brown homogenous clay, sulphur from pyrite breakdown present in nodules

Missing Core

Homogenous light brown clay, organic matter sporadically distributed

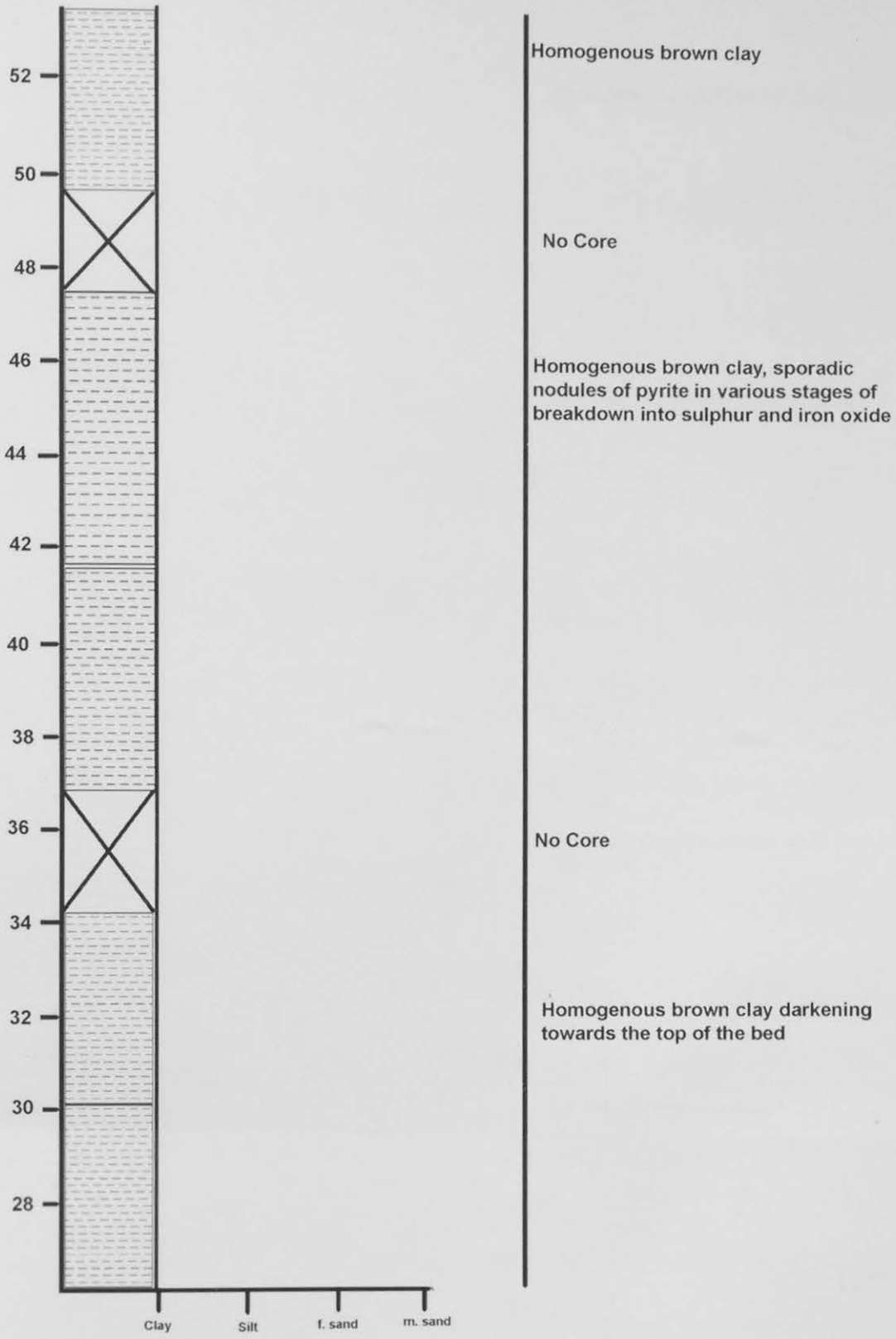
52
50
48
46
44
42
40
38
36
34
32
30
28
Clay
Silt
f. sand
m. sand
Homogenous brown clay
No Core
Homogenous brown clay, sporadic nodules of pyrite in various stages of breakdown into sulphur and iron oxide
No Core
Homogenous brown clay darkening towards the top of the bed

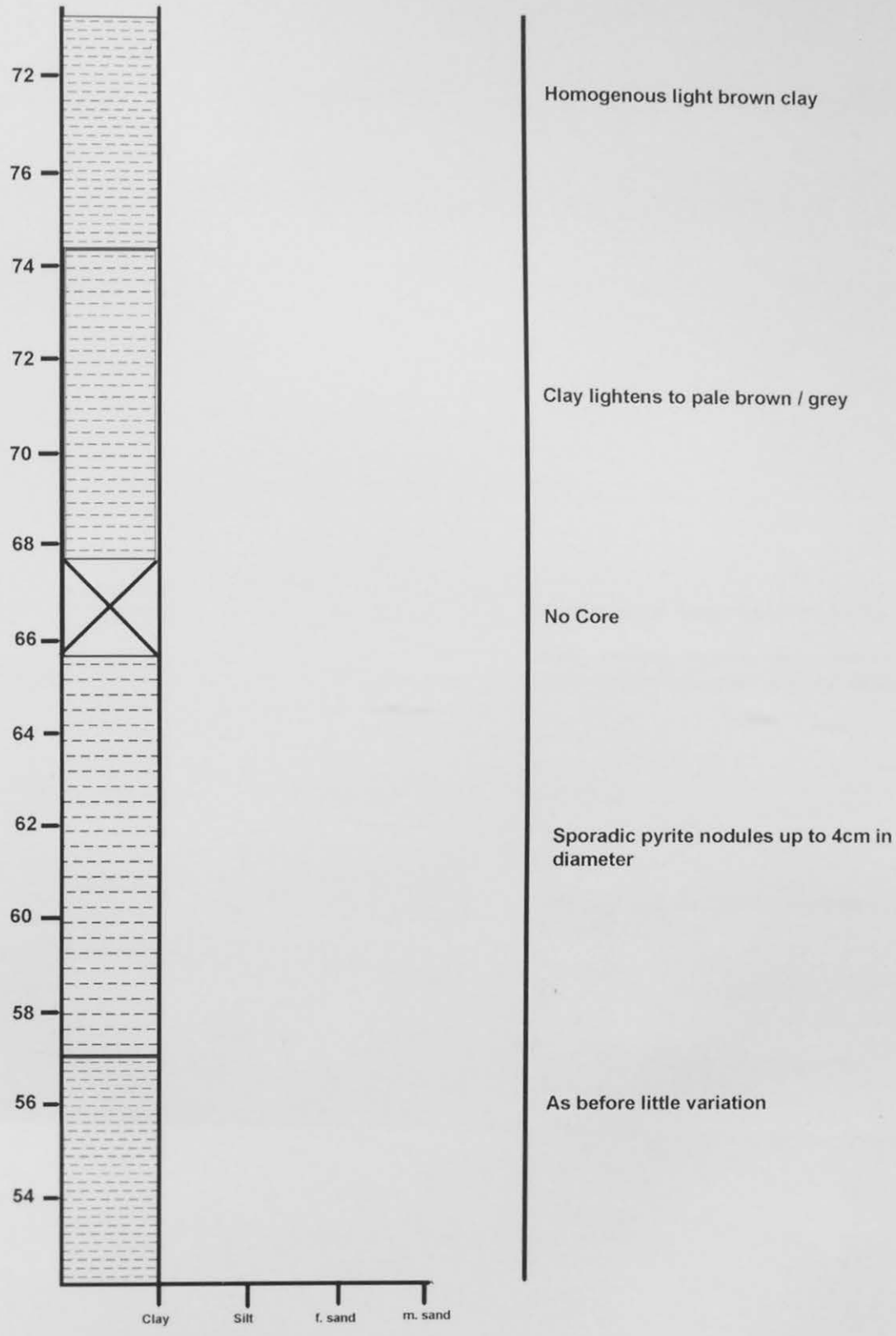
72
76
74
72
70
68
66
64
62
60
58
56
54
Clay
Silt
f. sand
m. sand
Homogenous light brown clay
Clay lightens to pale brown / grey
No Core
Sporadic pyrite nodules up to 4cm in diameter
As before little variation

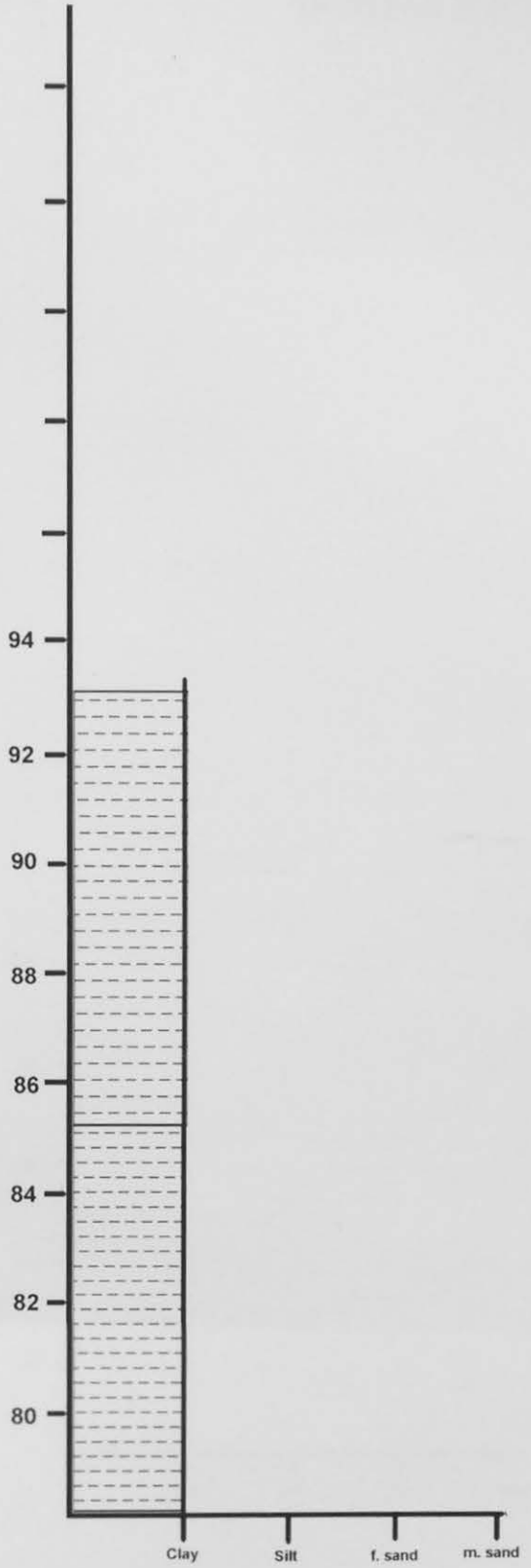

Shall material, fragmented and patchy

Pyrite nodules sporadic and partially broken down to sulphur and iron oxide

Pale grey at base of bed, becoming browner higher up

Homogenous light grey unit, some sporadic organic matter

Bradwell 205 TM00NW31

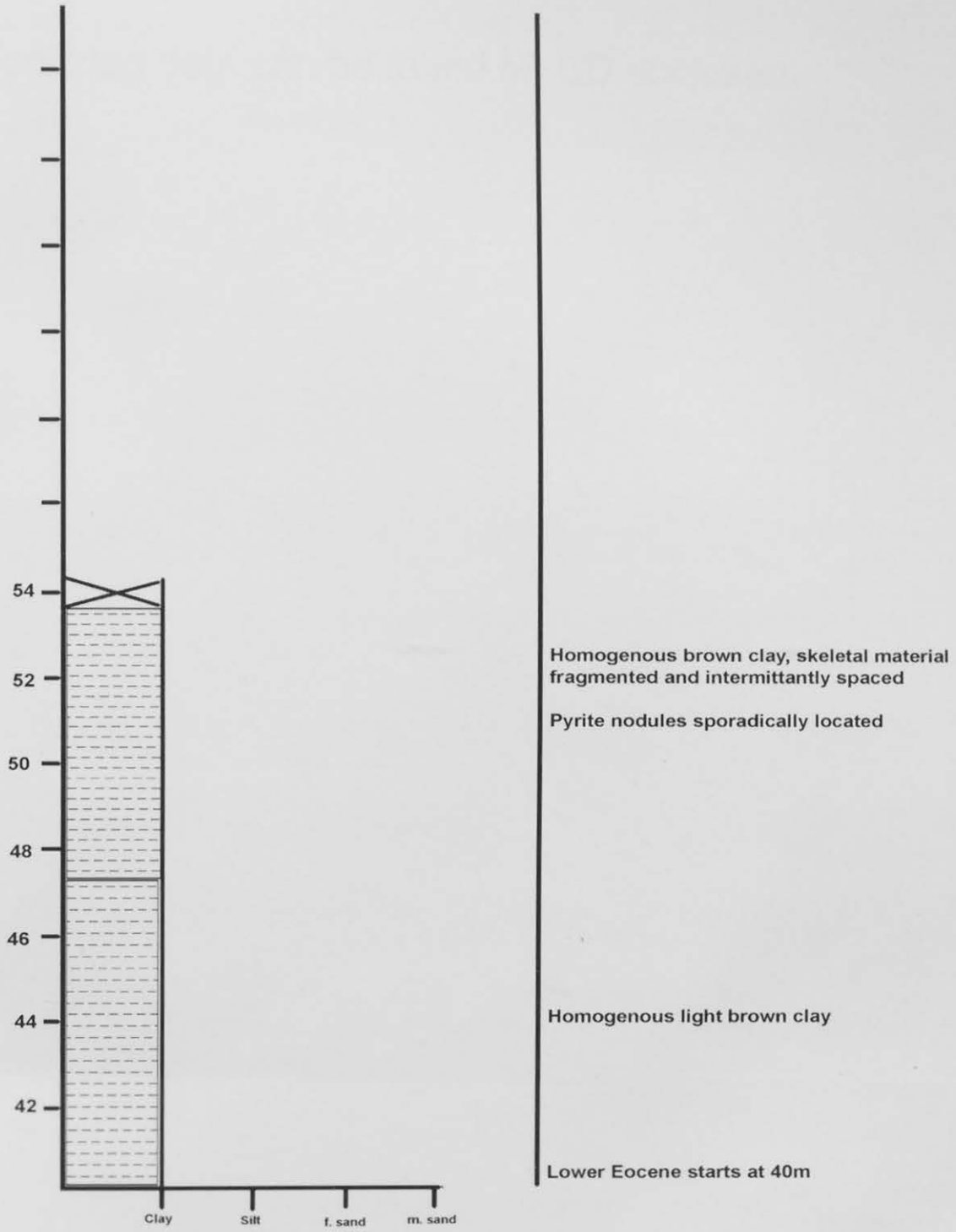

Appendix iii

Sonic log data can be found on CD enclosed.